จุฬาลงกรณ์มหาวิทยาลัย
ทุนวิจัย
กองทุนรัชดาภิเษกสมโภช

รายงานวิจัย

การปรับปรุงสมรรถนะของระบบสื่อสารผ่านเส้นใยแสง โดยการเปลี่ยนอุปกรณ์ทวนสัญญาณแบบอิเลคทรอนิกส์ เป็นอุปกรณ์ขยายสัญญาณทางแสง

โดย

พสุ แก้วปลั่ง

พฤศจิกายน ๒๕๔๗

จุฬาลงกรณ์มหาวิทยาลัย

ทุนวิจัย

กองทุนรัชดาภิเษกสมโภช

รายงานผลการวิจัย

การปรับปรุงสมรรถนะของระบบสื่อสารผ่านเส้นใยแสง

โดยการเปลี่ยนอุปกรณ์ทวนสัญญาณแบบอิเลคทรอนิกส์

เป็นอุปกรณ์ขยายสัญญาณทางแสง

PERFORMANCE IMPROVEMENT OF FIBER-OPTIC TRANSMISSION SYSTEM BY REPLACING ELECTRONIC REPEATERS WITH OPTICAL AMPLIFIERS

โดย

ดร. พสุ แก้วปลั่ง

พฤศจิกายน ๒๕๔๗

ACKNOWLEDGEMENT

At first, I wish to express my utmost gratitude to the office of Thailand submarine cable for giving the information about the Thailand-Malaysia submarince fiber-optic transmission line.

I should thank for my assistances: Mr. Wasis Kasantikul, Mr. Preeda Jarupoom, Mr. Ekkapob Tangdamrongtham, Mr. Thanakorn Ratanasopitkul, and Mr. Noppadon Raopattananon for there helps in running programs, analyzing calculated results, plotting a lot of graphs, working on documentary works and making a number of helpful discussions together with stimulated suggestions to this study.

Finally, I would like to give a special thank with all of my heart to my beloved one for her forbearance and encouragement, my wife, Dr. Orapin Kaewplung and my daughter, Miss Alisara Kaewplung.

ชื่อโครงการวิจัย การปรับปรุงสมรรถนะของระบบสื่อสารผ่านเส้นใยแสงโดยการเปลี่ยนอุปกรณ์ทวนสัญญาณแบบอิเลคทรอนิกส์เป็นอุปกรณ์ขยายสัญญาณทางแสง

ชื่อผู้วิจัย ดร. พสุ แก้วปลั่ง

เดือนและปีที่ทำวิจัยเสร็จ กรกฎาคม ๒๕๔๗

บทคัดย่อ

โครงงานนี้ได้ทำการศึกษาวิธีการ ๔ วิธีคือ การใช้ความยาวคลื่นที่มีการกระจายตามความถี่เป็นศูนย์ในการสื่อสัญญาณ (ZDWL) การจัดการการกระจายตามความถี่ การใช้การสื่อสัญญาณโดยโซลิตอนแสง และการใช้การสังยุคเฟสแสงที่จุดกึ่งกลางระบบ (OPC) ในการพัฒนาสมรรถนะของระบบสื่อสัญญาณผ่านเส้นใยแสงซึ่งใช้อุปกรณ์ทวนสัญญาณแบบอิเลคทรอนิกส์ไปเป็นระบบที่ใช้การขยายสัญญาณทางแสง เราได้เสนอวิธีการออกแบบระบบเพื่อให้ได้อัตราการสื่อข้อมูลสูงสุดในแต่ละวิธีดังกล่าว ระบบสื่อสัญญาณผ่านเส้นใยแสงใต้ทะเลไทย-มาเลเซีย (T-M) ซึ่งมีความยาว ๑,๓๑๘ กิโลเมตรได้ถูกนำมาใช้เป็นต้นแบบในการศึกษา

ในช่วงต้นของรายงาน โครงงานนี้ได้นำเสนอทฤษฎีเกี่ยวกับคุณสมบัติของเส้นใยแสงและผลของคุณสมบัติเหล่านั้นต่อการสื่อสัญญาณ และได้ทบทวนวรรณกรรมเกี่ยวกับหลักการของวิธี ๔ วิธีดังกล่าว หลังจากนั้นโครงงานนี้ทำการจำลองเชิงเลขกับระบบ ZDWL เพื่อศึกษาความผิดเพี้ยนของสัญญาณที่เกิดจากการกระจายตามความถี่อันดับที่ ๓ และปรากฏการณ์เคอร์

เมื่อวิธีสื่อสัญญาณ ZDWL ถูกนำมาประยุกต์ใช้พัฒนาระบบ T-M พร้อมกับวิธีการออกแบบที่นำเสนอโดยโครงงานนี้ พบว่ามีความเป็นได้ที่จะเพิ่มอัตราส่งข้อมูลจาก ๕๖๐ เมกะบิตต่อวินาที ได้ถึง ๘๐ กิกะบิตต่อวินาที สำหรับวิธีการจัดการการกระจายตามความถี่ ผลของการจำลองระบบแสดงให้เห็นว่าเราสามารถเพิ่มอัตราการส่งข้อมูลได้ถึง ๑๐๐ กิกะบิตต่อวินาทีในกรณีช่องสัญญาณเดียว และได้ ๖ ช่องสัญญาณโดยแต่ละช่องสัญญาณมีอัตราส่งช่องละ ๑๐ กิกะบิตต่อวินาทีในกรณีใช้การมัลติเพล็กซ์เชิงความยาวคลื่น อย่างไรก็ตาม เมื่อเรานำวิธีการสื่อสัญญาณโดยโซลิตอนแสงมาใช้เพื่อเพิ่มสมรรถนะของระบบ ผลของการคำนวณเชิงเลขแสดงความเป็นไปได้ในการเพิ่มอัตราส่งข้อมูลได้เพียงแค่ ๒๐ กิกะบิตต่อวินาที เนื่องจากเกิดความผิดเพี้ยนของสัญญาณที่เกิดจากความไม่เป็นเชิงเส้นของเส้นใยแสง อัตราส่งข้อมูลสูงสุดในโครงงานนี้ได้จากการเพิ่มสมรรถนะของระบบโดยใช้วิธี OPC เมื่อดำเนินการออกแบบระบบด้วยวิธีที่เสนอโดยโครงงานนี้ ผลของการจำลองระบบเชิงเลขพบว่ามีความเป็นไปได้ที่จะเพิ่มอัตราส่งข้อมูลได้ถึง ๒๐๐ กิกะบิตต่อวินาที

Project Title Performance improvement of fiber-optic transmission system by replacing electronic repeaters with optical amplifiers

Name of the Investigators Dr. Pasu Kaewplung

Year July 2004

Abstract

We study four methods: the zero-dispersion wavelength (ZDWL) transmission, the dispersion management, the optical soliton transmission, and the midway optical phase conjugation (OPC), for upgrading installed electronic repeater-based optical fiber transmission system to optically amplified system. We derive the optimum design rules for each scheme to achieve the maximum transmission data rate. The 1,318-km-long Thailand-Malaysia (T-M) submarine fiber-optic transmission system is used as the system model.

Firstly, we give the basic knowledge about fiber characteristics and their effects to signal propagation, and review the concepts of four upgrading schemes. Then, the numerical simulation is used for studying the signal distortion induced from the third-order dispersion and the Kerr effect in ZDWL transmission system.

When the ZDWL transmission is employed to upgrade the T-M system with our optimum design guidelines, the possibility of increasing data rate from 560 Mbit/s to 80 Gbit/s is shown. For the dispersion management, the transmission data rate can be extended to 100 Gbit/s for single channel, and to 6x10 Gbit/s for multi-channel wavelength division multiplexing. However, when the soliton scheme is employed to improve the system performance, the numerical result shows the possibility of increasing data rate only to 20 Gbit/s because of nonlinear signal distortions. The highest data rate in this study is obtained from the system upgrading using the midway OPC. By following our design strategies, the possibility of increasing to 200 Gbit/s is numerically shown.

CONTENTS

LIST OF TABLES

LIST OF FIGURES (Continued)

LIST OF FIGURES (Continued)

Figure Page

LIST OF FIGURES (Continued)

Figure Page

LIST OF FIGURES (Continued)

Figure Page

LIST OF FIGURES (Continued)

Figure Page

LIST OF FIGURES (Continued)

Figure Page

LIST OF FIGURES (Continued)

Figure Page

ABBREVIATION LIST

ASE – Amplified Spontaneous Emission Noise

BER – Bit-Error Rate

BPF – Band-Pass Filter

DDF – Dispersion-Decreasing Fiber

DSF – Dispersion-Shifted Fiber

EDFA – Erbium-Doped Fiber Amplifier

FFT – Fast Fourier Transform

FWHM – Full-Width-Half-Maximum

FWM – Four-Wave Mixing

Gbit/s – Giga-Bit per Second

GHz – Giga-Hertz

GVD – Group-Velocity Dispersion

$i = \sqrt{-1}$

km – Kilometer

LPF – Low-Pass Filter

Mbit/s-Mega-Bit per second

MI – Modulation Instability

mW – Milli-Watt

NLSE - Nonlinear Schrodinger Equation

NRZ – Non-Return-to-Zero

OBPF – Optical Band-Pass Filter

OPC – Optical Phase Conjugation

OSNR – Optical Signal-to-Noise Ratio

ps – Pico-Second

RZ – Return-to-Zero

SI – Sideband Instability

SMF – Standard Single-Mode Fiber

SNR – Signal-to-Noise Ratio

SOD – Second-Order Dispersion

SPM – Self Phase Modulation

ABBREVIATION LIST (Continued)

SSFM – Split-Step Fourier Method

TOD – Third-Order Dispersion

Tb/s – Tera-Bit per Second

W - Watt

WDM – Wavelength Division Multiplexing

XPM – Cross Phase Modulation

1. INTRODUCTION

1.1 General Background

Rapid growth on both transmission bit rate and distance in this decade is very remarkable. Transmission of data rate as high as 1 Tbit/s over 10,000 km has been demonstrated [1]. However, at present, there exists many installed fiber systems which still operate with electronic repeaters [2] at very low bit rate.

During the propagation in the transmission fiber, the peak power of the optical signal decreases due to the fiber loss, as well as the signal waveform becomes distort due to the fiber characteristics such as the fiber dispersion, especially the second-order dispersion (SOD), and the fiber nonlinearity, especially the Kerr effect [3]-[10]. The SOD causes the signal pulse broadening while the Kerr effect results in signal spectra broadening during signal transmission in the fiber [3]-[5]. The interaction of the SOD and the Kerr effect will cause severe distortion of both pulse and spectra [4]-[10].

Figure 1.1 shows the configuration of the electronic repeater [2]. In electronic-repeated scheme, after launching to the repeater, the distorted optical signal is converted to electrical signal. The distortion is removed out of signal by mean of electronic signal processing, and then is converted back to optical signal again. By this scheme, the capacity of system is limited by speed of the electronic circuit, which is well-known as " electronic bottle neck ", at the speed of around forty GHz or at the bit rate of 40 Gbit/s [4], [5], [11]. Therefore, to operate the system with bit rate higher than 40 Gbit/s, all optically signal-processed repeater, which uses light processes light, is necessary.

The invention of the Erbium-doped fiber optical amplifier (EDFA) [4], [5], [12]-[15] has significantly opened the possibility of the data transmission at the bit rate higher than 40 Gbit/s. EDFA has many beneficial properties [4], such as polarization independent gain, slow recovery time which prevents the pattern effect, low insertion loss and high saturation output power. The most important thing may be the fact that EDFA is operating in the 1550 nm region where the optical fibers exhibit minimum loss. Moreover, the gain bandwidth of EDFA is sufficiently wide enough so that it realizes a possibility of amplifying the ultra high bit rate signal up to over Tbit/s and a large number of WDM signals. EDFA can also serve as excellent receiver pre-

amplifiers, as they can provide very nearly the theoretical quantum-limited 3-dB noise figure [4]. This is because EDFA can be coupled very efficiently to the single-mode fibers with insertion loss of about 0.1dB, and almost full population inversion can be achieved.

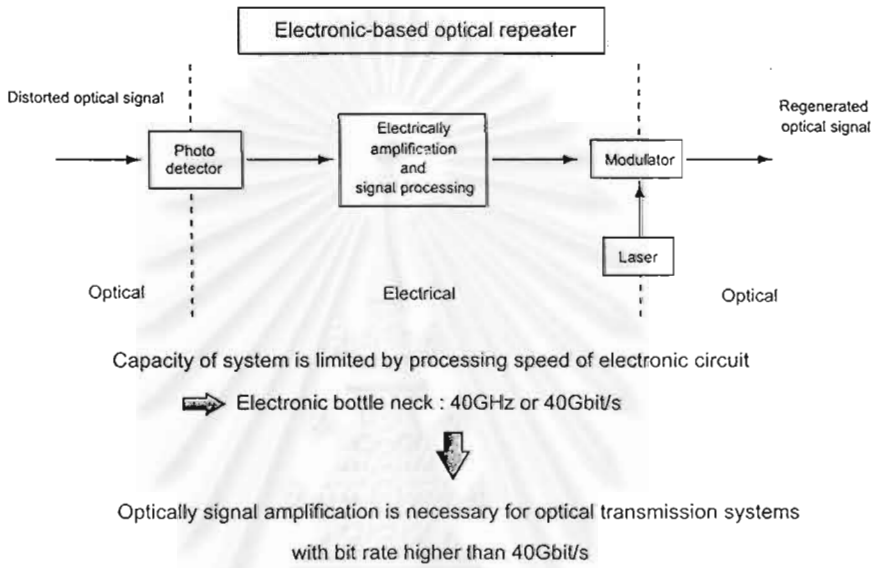

Figure 1.1: Configuration of electronic repeater.

Figure 1.2 shows the configuration of the EDFA, which is commonly used in optically-amplified systems. High output power semiconductor laser diode with operating wavelength 1480 nm or 980 nm is used for stimulating the Stimulated Brillouin scattering effect to occur inside the Er^{3+}-doped optical fiber for coherently amplifying 1550 nm signal input into the fiber. Usually, the EDFA is equipped with two optical isolators. The first is placed at the input in order to eliminate possible disturbances caused by the backward traveling amplified spontaneous emission (ASE) on the upstream span, while the second, at the output, protects the device against possible back reflections from the downstream line. The signal is launched into the active fiber together with the pump radiation through a wavelength division multiplexer (WDM) coupler which minimizes the power losses of both input beams.

The gain bandwidth of EDFA ranges approximately from 1520 nm to 1570 nm so that it is well tuned with the system operating at wavelength near 1550 nm region.

Typical values for the small-signal gain are 30-40dB for pump powers of 50-100 mW. Output powers range from +13dBm up to +20dBm, while the noise is generally very close to the minimum theoretical limit which can be derived from the fundamental laws of physics such as Heisenberg's Uncertainty principle.

However, the EDFA can only amplify the optical signal. Unlike the electronic repeater, the waveform distortion induced from fiber dispersion and fiber nonlinearity can not be removed from the signal at the output of EDFA. Therefore, in order to upgrade the electronic-repeated to the optically-amplified system, the signal distortion induced from the fiber dispersion and nonlinearity must be seriously taken into account.

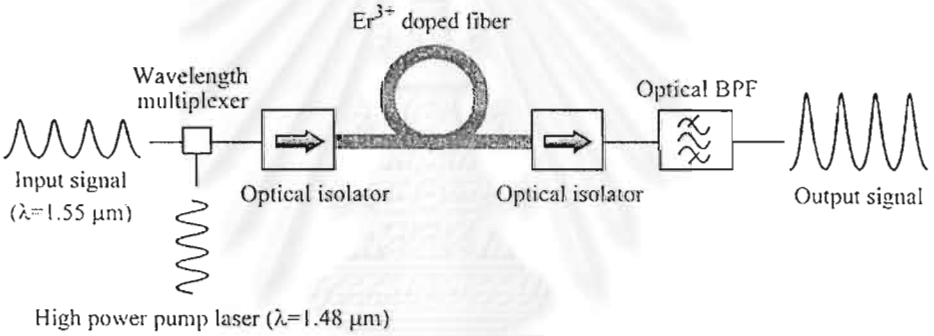

Figure 1.2: Configuration of EDFA.

There are many transmission methods have been proposed in order to overcome the SOD. The zero-dispersion wavelength (ZDWL) transmission [16]-[20] is to set an operation wavelength of the system at zero-dispersion point so that the pulses can propagate without broadening. The dispersion management [21]-[35] is to arrange the various sections of fiber in such a way that none or only very few of them have zero SOD wavelengths that coincide with the carrier wavelength while the total fiber exhibits zero SOD on average. The optical soliton [36]-[47] is to create the signal pulses that can propagate in optical fiber without broadening by balancing the SOD and the self-phase modulation (SPM) effect, which is induced through the Kerr effect, in anomalous dispersion region [4], [5], [36]. Quantitatively, this can be achieved by launching optical pulses with proper input power and width into the fiber. The midway optical phase conjugation [48]-[52] is to perform the optical phase

conjugation (OPC) at the midpoint of system in order to achieve the perfect compensation of both SOD and nonlinear effects if the condition that all of the system characteristics are symmetric with respect to the midway OPC.

Although the SOD is completely compensated, when the ultra-high-bit-rate data is transmitted through an optical fiber, the third-order dispersion (TOD) shows up and influences transmission characteristics. Moreover, the TOD interplays with the SPM, causing severe distortion of both signal waveform and signal spectrum [4].

In the dispersion-managed system where the SOD map is properly designed but the TOD is not compensated, the bit rate of the 10,000-km transmission system is limited only about 10Gbit/s because of the interplay of the TOD with the SPM. It has been shown, by numerical simulations, that when TOD is compensated periodically at the interval quite shorter than the nonlinear scale of the system, the speed limit is possibly raised up over 20Gbit/s [25].

On the other hand, in soliton systems, a recent numerical study shows that the eigen solution to soliton can exist in the transmission line with TOD, and that is stable against the perturbation of TOD [53]. Even without TOD compensation, 40-Gbit/s, 10,000-km transmission has been actually demonstrated by using the dispersion-managed soliton [54].

As an alternative approach for ultrahigh-bit-rate long-haul transmission, midway optical phase conjugation (OPC) is an attractive solution to compensating for the distortion induced from the interplay between the SOD and the SPM [55]. Several recent works have reported the broadband, wavelength-shift-free, and polarization-independent optical phase conjugators [56], [57]. This intensively may bring the OPC systems into a commercial world. However, the ultimate performance of OPC systems is also limited by TOD together with a nonlinear resonance at well-defined signal sideband frequencies induced by periodic amplification process called sideband instability (SI) effect [58].

Taking into account for system model, the longest fiber-optic submarine system that connects Thailand with neighbor country, the Thailand-Malaysia (T-M) fiber-optic submarine transmission system [12], is one of electronic-repeated submarine fiber-optic transmission systems. The system starts from Petchaburi, Thailand, ends at Chugai, Malaysia, with total length of 1,318 km. The fiber is

dispersion-shifted fiber (DSF) [4]. The electronic repeaters are periodically placed at span of 100 km with the last span 118 km. The system operates with single channel with the data rate of only 560 Mbit/s. Such system needs to be upgraded to response the demand for increasing transmission capacity in the future.

1.2 Purpose of this Project

The aim of this project is to present and evaluate the simple and practical approaches, together with optimum design schemes for improving the performance of the electronic repeater-based optical fiber transmission system to achieve maximum performance using the T-M submarine transmission system as the system model. We will replace the electronic repeaters in the system with the optical amplifiers, then employ four SOD compensation methods, the ZDWL transmission method, the dispersion management method, the optical soliton transmission method, and the midway OPC method, for compensation waveform distortion induced from the SOD and the Kerr effect..

1.3 Studying Method

In this project, the computer simulation is used for evaluating the improvement of transmission data rate obtained from each method.

We will start this project by studying four SOD compensation schemes: the ZDWL transmission, the dispersion management, the soliton transmission, and the midway OPC. Study the optimum design rules of each scheme for upgrading the T-M submarine line. Model the T-M submarine line according to each upgrading scheme. The computer simulations will be used to confirm the performance improvement results. In numerical simulations of data transmission in the T-M system, the signal is composed of a 32-bit pseudorandom RZ Gaussian pulse train. The parameters such as fiber loss coefficient, TOD, and nonlinear coefficient will be set at typical values of the dispersion-shifted fiber (DSF). Since we consider in this project only the single channel transmission, the commercially available optical amplifier exhibits sufficiently flat and wide gain bandwidth that can support all bandwidths of the signal used in our simulation. Therefore, in our simulations, the optical amplifier is assumed to be ideal that amplifies the signal by the gain that compensates the optical loss in an

amplifier span. However, each optical amplifier produces ASE noise added to the signal after the signal amplification. In case of the OPC transmission scheme, the optical pulse at the midway of the system will be conjugated by an ideal infinite-bandwidth optical phase conjugator.

The propagation of the optical pulse is calculated by solving the nonlinear Schrodinger equation (NLSE) by the split-step Fourier method (SSFM). The integration step size of the SSFM is always chosen at the value that gives a step size error less than 0.01 %. The system performance is evaluated in terms of the numerical bit-error rate (BER). To calculate the numerical BER of the detected signal, the simulation is repeated 128 times. The numerical Q factor of every bit is then individually calculated at the maximum eye-opening point of the bit period. Based on the assumption of the Gaussian noise distribution, the numerical BER is computed from the bit numerical Q factor and averaged over the entire bits [25]. Commonly, the BER at 10^{-9} is widely set as the system limitation. This means we will not allow the system that yields the BER of the detected signal larger than 10^{-9}.

Finally, the comparison among the results obtained from all schemes, and the discussion of the advantages and the disadvantages of each scheme will be made. Therefore, the research methods for this work are mainly based on the theoretical analysis, and then evaluating their accuracy by the method of computer simulations.

1.4 Studying Steps

1. Study the zero-dispersion wavelength transmission scheme.
2. Use the computer simulation for studying the transmission problems occurring in ZDWL transmission systems
3. Find optimum design rules, and model the T-M system with the ZDWL transmission scheme.
4. Use the numerical simulation to obtain maximum performance upgrading of the T-M system using the ZDWL transmission scheme.
5. Summarize the results, submit the results to international conferences, and present the results in international conferences.
6. Study the dispersion management transmission scheme.

7. Use the computer simulation to confirming the performance improvement comparing to the ZDWL transmission scheme.
8. Theoretically study the design rules of the dispersion management system using the transfer function. Then, apply this design rule to the T-M system.
9. Find optimum design rules, and model the T-M system with the dispersion management transmission scheme.
10. Using numerical simulation to obtain maximum performance upgrading of the T-M system using the dispersion management transmission scheme.
11. Summarize the results, submit the results to international conferences.
12. Studying the soliton transmission scheme, finding optimum design rules, and modeling the T-M system with the soliton transmission scheme.
13. Using numerical simulation to obtain maximum performance upgrading of the T-M system using the soliton transmission scheme.
14. Summarize the results, submit the results to international conferences.
15. Studying the midway OPC scheme, finding optimum design rules, and modeling the T-M system with the midway optical phase conjugation scheme.
16. Using numerical simulation to obtain maximum performance upgrading of the T-M system using the midway OPC scheme.
17. Summarizing the results, making the comparison among the results obtained from several schemes, making the discussion about the advantages and the disadvantages of each upgrading scheme, writing a final report, and presenting the work in international conferences or publishing the work in periodical journal.

1.5 Organization of this Report

This paper is organized as follows. Chapter 2 gives the basic knowledge about fiber characteristics and their effects to signal propagation and the concepts of four SOD compensation schemes. Also in this chapter, the SSFM, which is the main numerical method used in this project is also noted. Chapter 3 is devoted to the numerical study of the problems induced from the TOD and the Kerr effect that limit the signal propagation at ZDWL. In chapter 4, we study the performance improvement of the T-M system, when the ZDWL transmission is employed to upgrade the system to

optically amplified system. We also discuss about the optimum design rules for the ZDWL transmission.

Chapter 5 shows the significant improvement in signal transmission by using the dispersion management method instead of the ZDWL transmission. We also provide the design guidelines for achieving the maximum performance. The numerical results based on the T-M system demonstrate the success of increasing data rate beyond the ZDWL transmission. Chapter 6 involves the numerical simulations of the soliton transmission in upgrading the T-M system. We also provide the design strategies for the soliton system. In chapter 7, the OPC are considered for improving the transmission data rate of the T-M system. By following our system design rules, we demonstrate that the OPC provides possible higher data rate transmission than other methods. The computer simulation realizes the data rate as high as 200 Gbit/s in the T-M system. Finally, we summarize this report and make the comparison among the upgrading schemes in chapter 8.

2. SIGNAL TRANSMISSION IN OPTICAL FIBER

In this chapter, we will describe about the fiber characteristics and their effects on signal propagating in optical fiber. Next, the concepts of four second-order dispersion (SOD) compensation methods focused in this project is also be discussed

Optical fibers are always considered as the lossless mediums because of their extremely small value of a loss coefficient (minimum 0.2 dB/km at an operation wavelength 1.55 μ m) [4], [5]. This will lead to the extension of repeater spacing for more than 100 km while in the systems employing coaxial cables whose repeater spacing is limited to a few kilometers. Furthermore, according to the fact that optical fibers are made of SiO_2 glass, so optical fibers will have robustness against the disturbances from the surrounding circumstance more than those systems that use metal wires as transmission mediums. The above reasons make the fiber-optic systems the most expectable systems for nowadays and also, future telecommunication.

The behavior of optical signal when propagating in single-mode optical fiber is mainly determined by three main effects: fiber loss, fiber dispersion, and fiber nonlinearity. The fiber loss causes the exponentially decrease of signal power during the propagation, which is necessary to be compensated by repeater for long distance transmission. The dispersion, especially the SOD, results a broadening of optical pulse, while the fiber nonlinearity, especially the Kerr effect, yields a broadening of signal spectrum. In fact, the dispersion and nonlinearity interplay with each other, resulting in the distortion of both signal and its spectrum.

2.1 Fiber Loss

Let P_i is the power launched at the input of a fiber length L, the transmitted power: P_T is given by

$$P_T = P_i \exp(-\alpha L), \tag{2-1}$$

where α is the attenuation constant, commonly referred to as the fiber loss. It is customary to express the fiber loss in units of dB/km by using the relation

$$\alpha_{dB} = -\frac{10}{L}\log\left(\frac{P_T}{P_i}\right) = 4.343\alpha\,, \qquad (2\text{-}2)$$

where α_{dB} is the attenuation constant in dB/km expression. The fiber loss depends on the wavelength of light. Figure 2.1 shows the optical loss characteristic of single-mode fibers as a function of the operation wavelength.

The factors that are mainly contributed to the fiber loss are material absorption induced by OH ion and Rayleigh scattering [4], [5]. Other factors that causes additional loss is bending losses and boundary losses (due to scattering at the core-cladding boundary). The total loss of a fiber link on optical communication systems also includes the splice loss that occurs when two fiber pieces are joined together. The fiber loss causes the exponential decrease of optical signal power without giving rise to any change in signal shape also its spectrum.

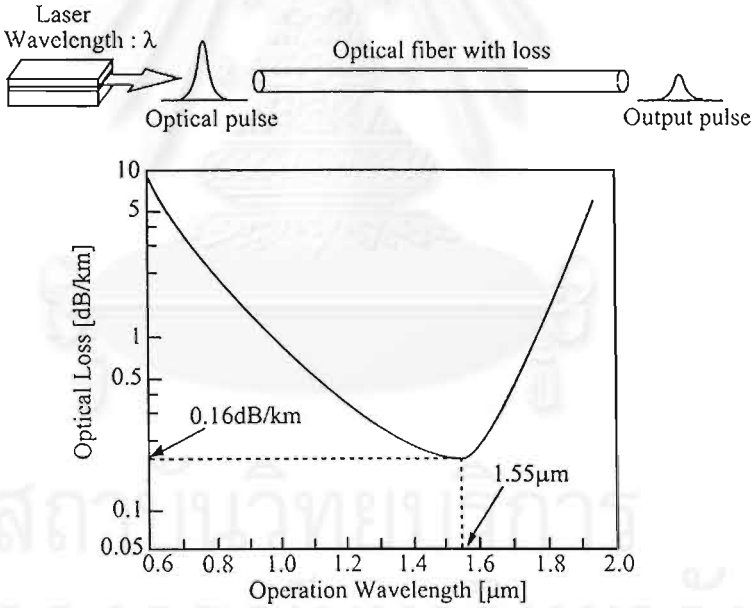

Figure 2.1: Optical loss characteristic of single-mode fibers.

2.2 Chromatic Dispersion

When an optical pulse is launched to the fiber, its different frequency components associated with the pulse travel at different speeds. It will lead to the pulse broadening induced by the delay of transit time of each frequency component.

This effect is well known as the chromatic dispersion, which may be one important limitation of a bit-rate or a distance in fiber-optic communication systems.

In the case if we consider optical fiber as a medium, dispersion play a critical role in propagation of short optical pulses since different spectral components associated with the pulse travel at different speeds given by $c/n\omega$ and the shorter pulses will have broader spectrum width.

Mathematically, the effects of fiber dispersion are accounted for by expanding the signal propagation constant β in a Taylor series about the lightwave carrier frequency ω_0.

$$\beta(\omega) = \beta_0 + \beta_1(\omega - \omega_0) + \frac{1}{2}\beta_2(\omega - \omega_0)^2 + \frac{1}{6}\beta_3(\omega - \omega_0)^3 \ldots, \qquad (2\text{-}3)$$

where β_1 in Eq. (2-3) refers to the inverse of group-velocity of the pulse envelope and also be known as first-order group-velocity dispersion (GVD) parameter. The second-order GVD parameter β_2 is responsible for pulse broadening, which relates to the SOD, and the third-order GVD β_3, which relates to the TOD, causes signal waveform distortion in ultra-high bit rate signal transmission.

The SOD: D is also commonly used in the fiber-optics literature in place of β_2. It is related to β_2 by the relation

$$D = -\frac{2\pi c}{\lambda^2}\beta_2. \qquad (2\text{-}4)$$

Figure 2.2 shows schematically the variation of β_2 and D with wavelength λ for optical fibers. The most notable feature in Fig. 4 is that β_2 and D vanishes at a wavelength λ_D. λ_D is often referred to as zero-dispersion wavelength which is about 1.3 μm in the case of standard single-mode fibers (SMF) and becomes 1.55 μm where the fiber loss is minimum in dispersion-shifted fibers (DSF).

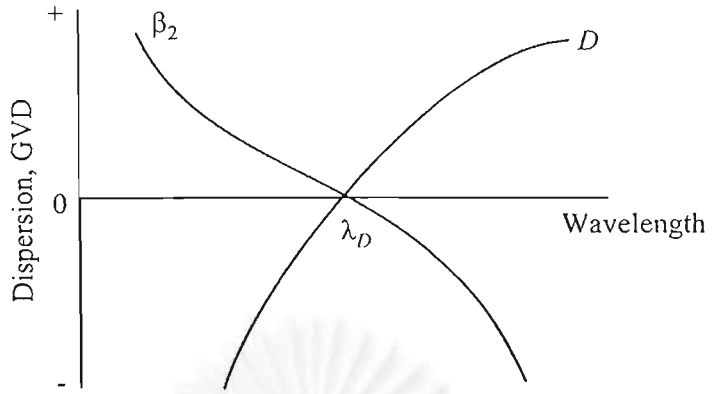

Figure 2.2: Dispersion characteristics of single-mode fibers.

The pulse can propagate without broadening in the zero-dispersion wavelength (ZDWL) region, and the systems which operate at the ZDWL are known as ZDWL transmission systems which are expected to achieve high bit-rate and long transmission distance since the performance of the systems no longer limited by the dispersion-induced broadening. However, it should be noted that dispersion does not vanish at λ_D. Pulse propagation near λ_D requires the inclusion of the TOD. Their inclusion is however necessary only when the pulse wavelength approaches λ_D to within a few nanometers.

According to Fig. 2.2, for wavelength such that $\lambda < \lambda_D$, $\beta_2 > 0$, the fiber is said to exhibit normal dispersion. In the normal-dispersion regime, the higher frequency (blue-shifted) components of an optical pulse travel slower than the lower frequency (red-shifted) components. By contrast, the opposite occurs in the so-called anomalous-dispersion regime in which $\lambda > \lambda_D$, $\beta_2 < 0$. The anomalous-dispersion regime gives an interest for the study of nonlinear effects because it is in this regime that optical fibers can support nonlinear optical pulse soliton through a balance between the dispersive and nonlinear effects.

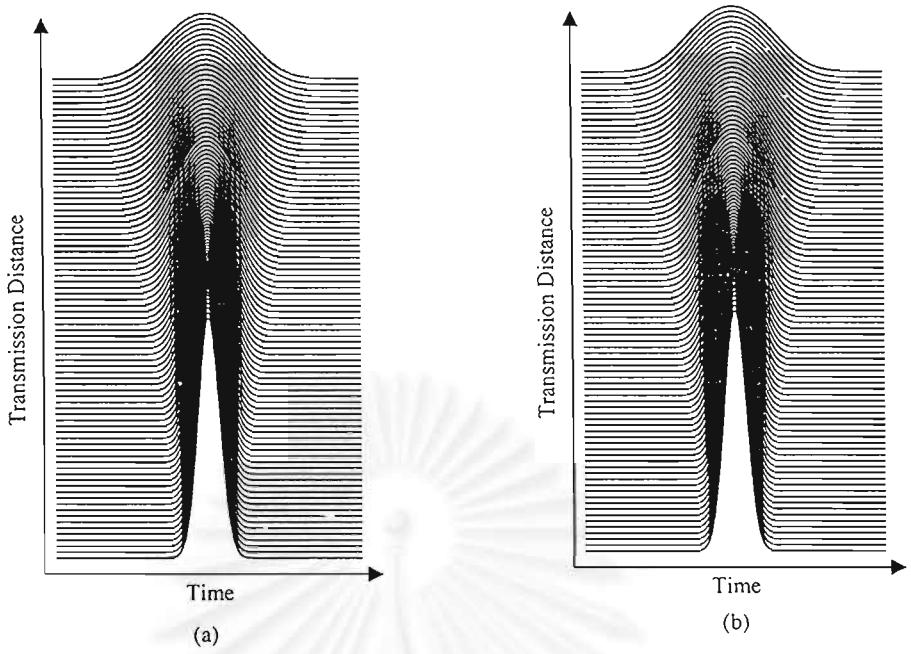

Figure 2.3: Evolution of single optical pulse in single-mode fiber with the effect of dispersion, (a) in normal dispersion regime ($\beta_2 > 0$), (b) in anomalous dispersion regime ($\beta_2 < 0$).

It should be noted here that the dispersion-induced pulse broadening does not depend on the signs of β_2. Different signs but same values of β_2 will lead to the same magnitude of broadening. Moreover, even though β_2 results in pulse broadening, it does not cause the change in the spectrum of the pulse. Figure 2.3 shows the propagation of single optical pulse propagates along the optical fiber in the presence of the effect of β_2.

In general the extent of broadening is governed by the SOD length by

$$T_{out} = T_0 \left(1 + \left(\frac{z}{L_D}\right)^2\right)^{\frac{1}{2}}, \tag{2-5}$$

where T_{out} denotes the transmitted pulse width. The SOD length L_D is defined as

$$L_{d2} = \frac{T_0^2}{|\beta_2|}. \tag{2-6}$$

The SOD length L_D is the parameter which determines the length scale over which the SOD becomes important for pulse evolution along a fiber length L when $L_{d2} < L$.

The difference between propagation of a pulse in normal-dispersion region and in anomalous-dispersion region is the sign of linear phase modulation of the transmitted pulse. This linear phase modulation can be express as the time dependence of the optical phase $\phi(z,T)$ caused by the effect of β_2.

$$\phi(z,T) = -\frac{\mathrm{sgn}(\beta_2)(z/L_{d2})T^2}{1+(z/L_{d2})^2 T_0^2} + \tan^{-1}\left(\frac{z}{L_{d2}}\right), \tag{2-7}$$

where $\mathrm{sgn}(\beta_2) = \pm 1$ depending on the sign of β_2. The time dependence of the phase $\phi(z,T)$ implies that the instantaneous frequency differs across the pulse from the central frequency ω_0. The difference $\Delta\omega$ is just the time derivative $-\partial\phi/\partial T$ and is given by

$$\Delta\omega = -\frac{\partial\phi}{\partial T} = \frac{2\,\mathrm{sgn}(\beta_2)(z/L_D)T}{1+(z/L_D)^2 T_0^2}. \tag{2-8}$$

The phenomenon that frequency changes across the pulse is generally known as the frequency chirp. Although the incident pulse is unchirped but after propagating in dispersive fiber the pulse will be chirped. The chirp $\Delta\omega$ depends on the sign of β_2. Figure 2.4 shows the difference between frequency chirp in normal-dispersion regime and anomalous-dispersion regime.

In the normal-dispersion regime, $\Delta\omega$ is negative at the leading edge $T < 0$ and increases linearly across the pulse. The opposite occurs in the anomalous-dispersion regime.

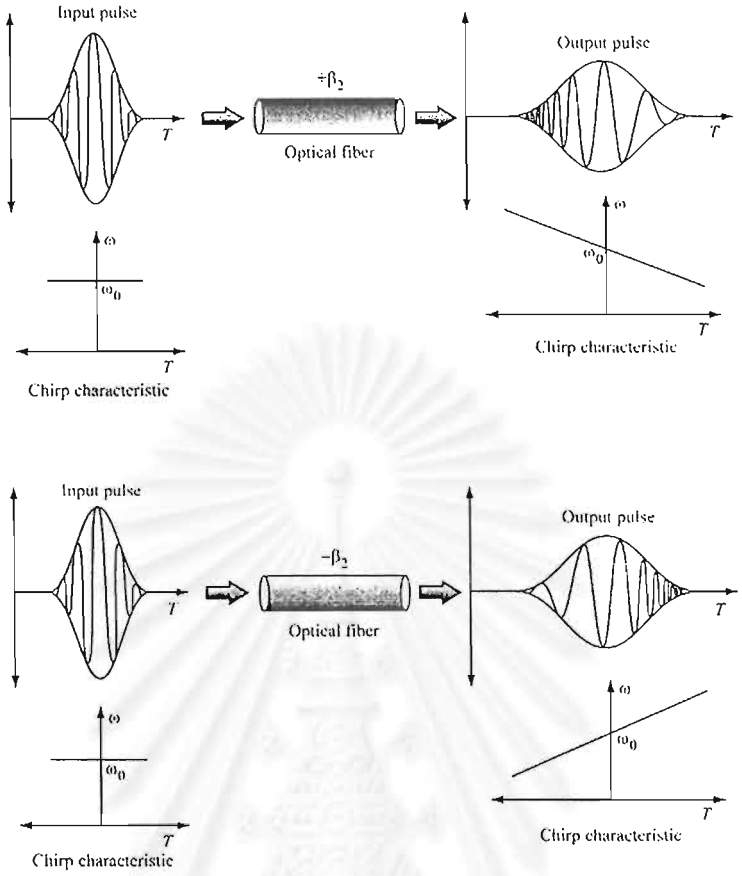

Figure 2.4: Linear frequency chirps induced by fiber SOD, (a)in normal dispersion regime (+ β_2), (b) in anomalous dispersion regime (- β_2).

2.3 Third-order Dispersion [4], [18]

The SOD-induced pulse broadening discussed above is due to the second-order GVD term proportional to β_2 in the expansion (3). Although the contribution of this term dominates in most cases of practical interest, it is sometimes necessary to include the higher-order term proportional to β_3 in this expansion.

Since β_3 is the derivative of β_2 by the frequency ω: $\beta_3 = d\beta_2/d\omega$. The effect of β_3 can be explained in term of the effect of the SOD slope or, for convenience, the dispersion slope. As shown in Fig. 2.5, for broadband optical signal such as ultrashort pulses or OTDM signal [17], different the signal spectral component will experiences different SOD values due to the slope of the SOD curve. Therefore, it is often necessary to include β_3 for such signal.

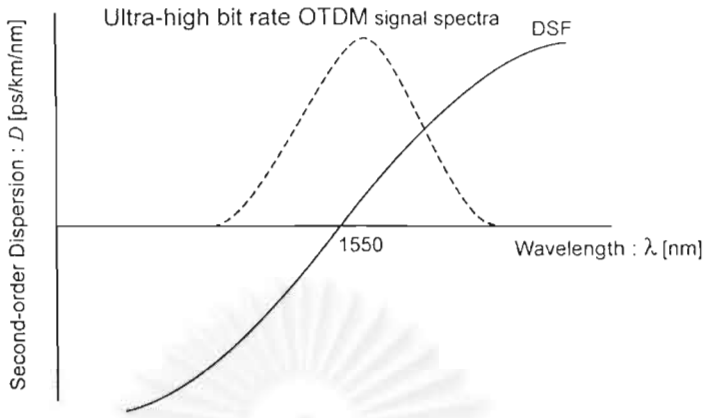

Figure 2.5: Broadband optical signal on fiber SOD band.

The important parameter widely used representing the effect of β_3 is the TOD, which is defined by the derivative of the SOD: D by wavelength λ, therefore: TOD = $dD/d\lambda$. Typically, near ZDWL of DSF, $\beta_3 \approx 0.2\text{ps}^3/\text{km}$ and TOD = 0.06 ps/km/nm^2.

In order to compare the relative importance of the SOD and the TOD terms, it is useful to introduce the TOD length defined as

$$L_{d3} = \frac{T^3}{|\beta_3|}. \tag{2-9}$$

The TOD will play a significant role only if $L_{d3} \leq L_{d2}$.

Figure 2.6(a) shows the single optical pulse propagates along the optical fiber with the effect of positive TOD and Fig. 2.6(b) and (c) shows the initial pulse shape and the output pulse, respectively. The output optical pulse is distorted such that it becomes asymmetry with an oscillatory structure near one of its edges. It should be noted that the dispersive effect does not cause any change in the output spectrum. For the case of positive TOD shown in Fig. 2.6, the oscillation appears near the trailing edge of the pulse.

For the case of $D = 0$, oscillations are deep with intensity dropping to zero between successive oscillations. However, these oscillations damp significantly even for the relatively small values of D.

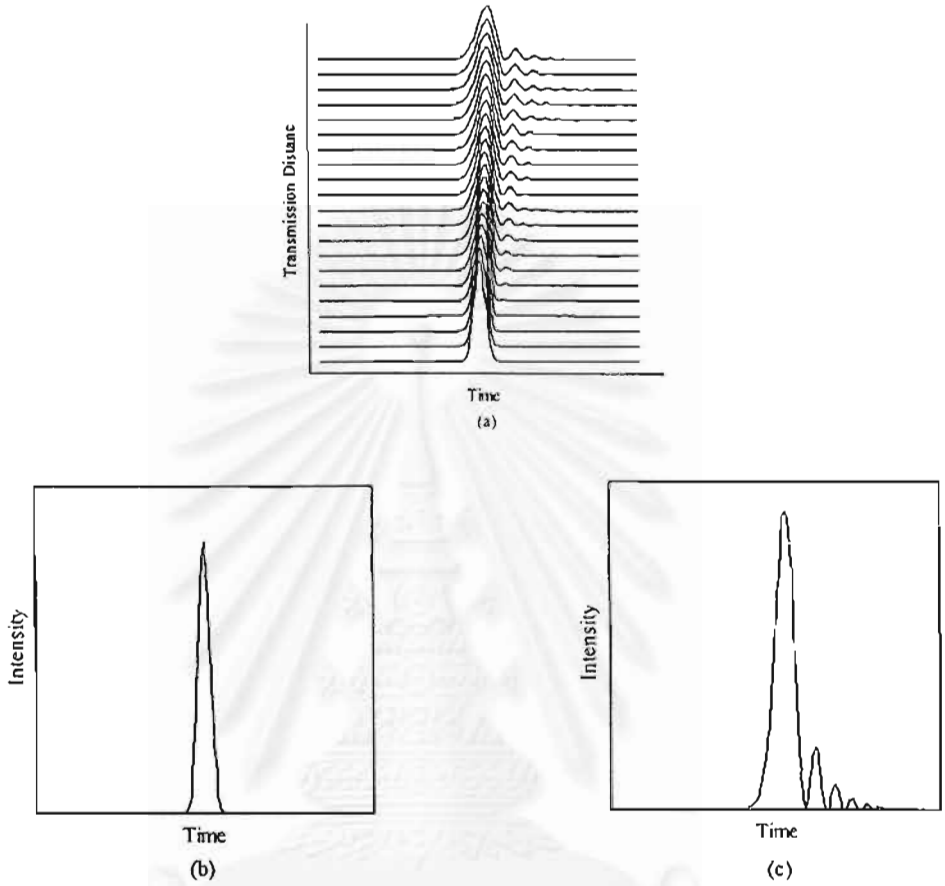

Figure 2.6: Transmission of an optical pulse and in single-mode fiber with the effect of TOD, (a) pulse evolution, (b) initial pulse shape, (c) pulse at output end of fiber.

2.4 Fiber Nonlinearity

Most of the nonlinear effects in optical fibers originate from the Kerr effect, which induced through the nonlinear refraction. The nonlinear refraction is a phenomena that refers to the intensity dependence of the refractive index. The expression of the refractive index, which includes the term of light intensity dependence, becomes

$$\bar{n}\left(\omega,|A|^2\right)=n(\omega)+n_2|A|^2 \tag{2-10}$$

where $n(\omega)$ is the linear part. $|A|^2$ is the optical signal intensity inside the fiber, and n_2 is the nonlinear-index coefficient.

The intensity dependence of the refractive index, or the Kerr effect, leads to a large number of interesting nonlinear effects. The one most widely studied are self-phase modulation (SPM) [4]. SPM refers to the self-induced phase shift experienced by optical field during its propagation in optical fibers. Its magnitude can be obtained by changes of the phase of an optical field by

$$\phi = \bar{n}k_0 L = \left(n(\omega) + n_2|A|^2\right)k_0 L \ , \tag{2-11}$$

where $k_0 = 2\pi/\lambda$ and L is the fiber length. The intensity-dependent nonlinear phase shift caused by SPM is

$$\phi_{nl} = \bar{n}k_0 L|A|^2 \ . \tag{2-12}$$

The SPM is responsible for spectral broadening of optical pulses. When the SPM interacts with the SOD in the normal-dispersion regime, it will lead to the breaking of the optical pulse. By contrast, if the SPM balances with the SOD in anomalous-dispersion regime, this will lead to the existence of optical solitons.

If we considers the pulse propagation in lossless optical fibers, $U(z,t)$ now represents the normalized envelope function of the optical pulses, Eq. (2-12) should be modulated to time-distance-depended equation which fits to the description of pulse propagation in fiber,

$$\phi_{nl}(z,t) = |U(z,t)|^2 z / L_{nl} \ , \tag{2-13}$$

where the nonlinear length L_{NL} which represents the length of fiber at which the SPM becomes the dominant effect is defined as

$$L_{nl} = \frac{1}{\gamma P_0} \ , \tag{2-14}$$

where P_0 denotes the input peak power of the pulse and γ is the nonlinear coefficient which is proportional to the nonlinear refractive index n_2. $U(z,t)$ appearing in Eq. (2-13) is the optical field normalized by peak power.

Equation (2-13) shows that SPM gives rise to an intensity-dependent phase shift while the pulse shape governed by $|U(z,t)|^2$ remains unchanged. The

nonlinear phase shift $\phi_{nl}(z,t)$ given by Eq. (2-12) increases with the propagated distance z. SPM-induced spectral broadening is a consequence of the time dependence of $\phi_{nl}(z,t)$. This can be understood by nothing that a temporally varying phase implies that the instantaneous optical frequency differ across the pulse from its central value ω_0. The difference $\Delta\omega$ is given by

$$\Delta\omega = -\frac{\partial\phi_{NL}}{\partial t} = -\frac{\partial|U(z,t)|^2}{\partial t}\frac{z}{L_{nl}}, \qquad (2\text{-}15)$$

and the frequency of the pulse now becomes time-depend function. Figure 2.7 shows the modulation of optical carrier frequency of the pulse obtained from Eq. (2-15).

The modulation of frequency or the time dependence of $\Delta\omega$ can be viewed as a frequency chirp. The chirp is induced by SPM and increases in magnitude with the propagated distance. The temporal variation of the SPM-induced chirp in $\Delta\omega$ in Fig. 2.7 has two interesting features. First, $\Delta\omega$ is negative near the leading edge (red shift) and becomes positive near the trailing edge (blue shift). Second, the chirp is linear and positive (up-chirp) over the large central region. Since the characteristic of the SPM-induced frequency chirp is similar to the linear up-chirp, we should call this chirp the nonlinear up-chirp.

Figure 2.8 shows the spectrum of single optical pulse propagating along the optical fiber with only the effect of SPM. The most notable feature of Fig. 2.8 is that SPM-induced spectral broadening is accompanied by an oscillatory structure covering the entire frequency range. In general, the spectrum consists of many peaks and the outermost peaks are the most intense.

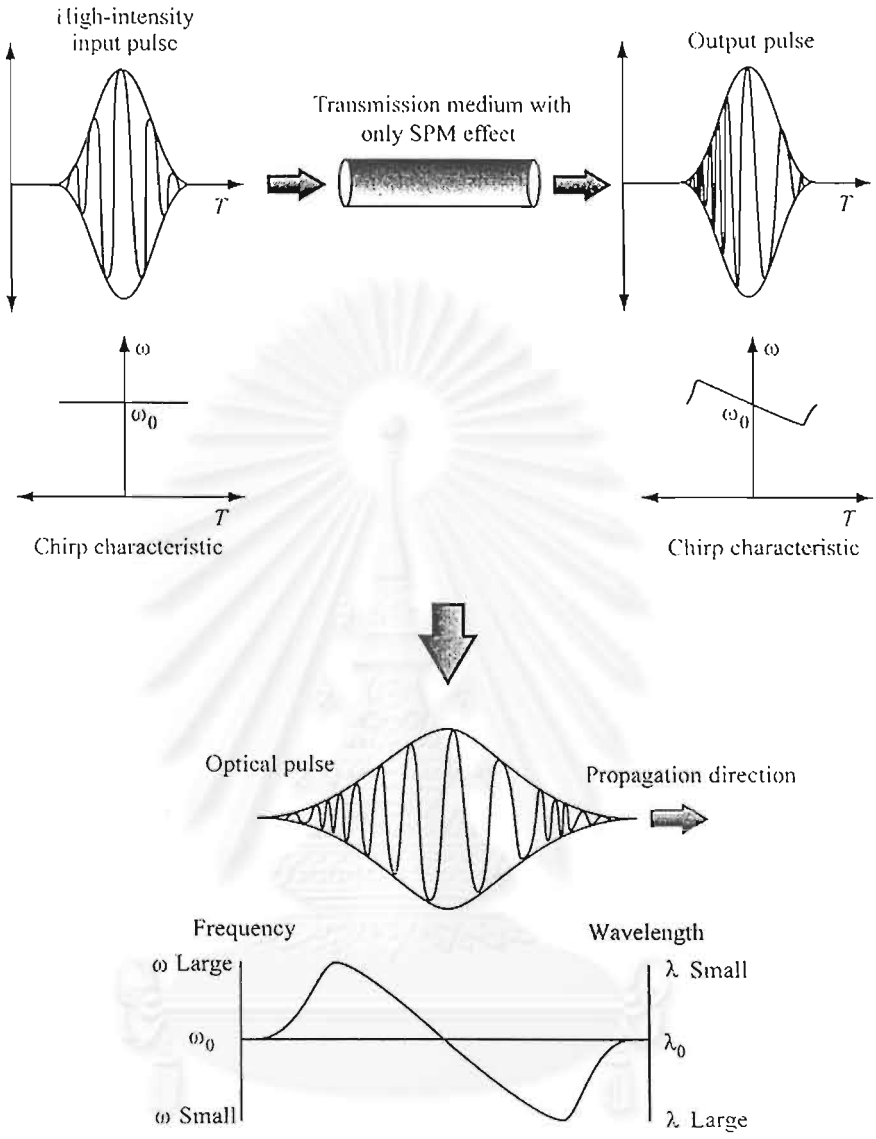

Figure 2.7: Modulation of optical frequency inside the pulse due to SPM.

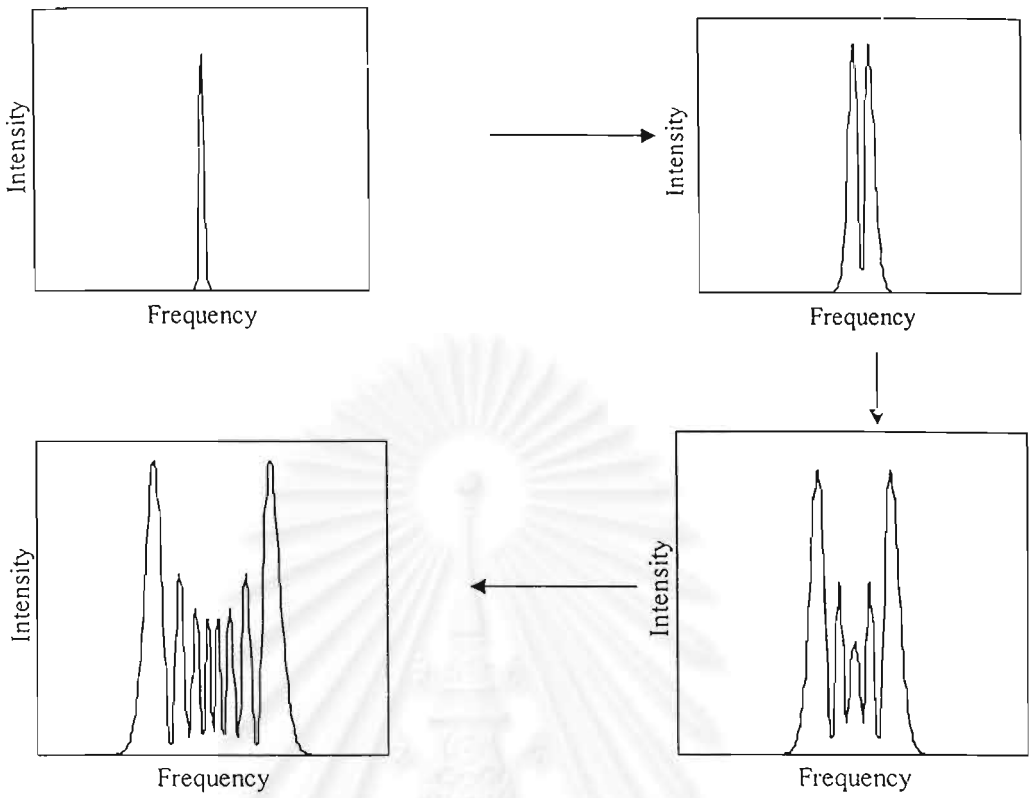

Figure 2.8: Evolution of optical spectrum in the presence of SPM.

2.5 Nonlinear Schrodinger Equation and Split-Step Fourier Method

The propagation of signal pulses in optical fiber is governed by the nonlinear Schrodinger equation (NLSE) [4]

$$\frac{\partial A}{\partial z} = -\frac{\alpha}{2}A - \frac{i}{2}\beta_2 \frac{\partial^2 A}{\partial T^2} + \frac{1}{6}\beta_3 \frac{\partial^3 A}{\partial T^3} + i\gamma |A|^2 A, \qquad (2\text{-}16)$$

where A denotes the complex amplitude of the signal, z the propagation distance, α the attenuation coefficient, β_2 the second-order GVD coefficient, β_3 the third-order GVD coefficient, γ the fiber nonlinearity coefficient, and $T = t - z/v_g$ the time measured in a frame of reference moving with the pulse at the group velocity v_g.

However, NLSE generally does not have the analytic solutions except for some specific cases. Because of this reason, a numerical method is therefore necessary for solving this equation. In this project, we will use the numerical

method called split-step Fourier method (SSFM) [4] which has been extensively used to solve the nonlinear equation. As shown in Fig. 2.9, by this method, a fiber length is divided into a large number of small segments δ of width where each segment is assumed to have the effects of nonlinearlity N or the dispersive effect $D(i\omega)$ only. Then the Fourier transform based on fast-Fourier transform (FFT) algorithm is utilized to solve the propagation of the pulse that is disturbed only by the effects of dispersions and the effects of nonlinearities separately.

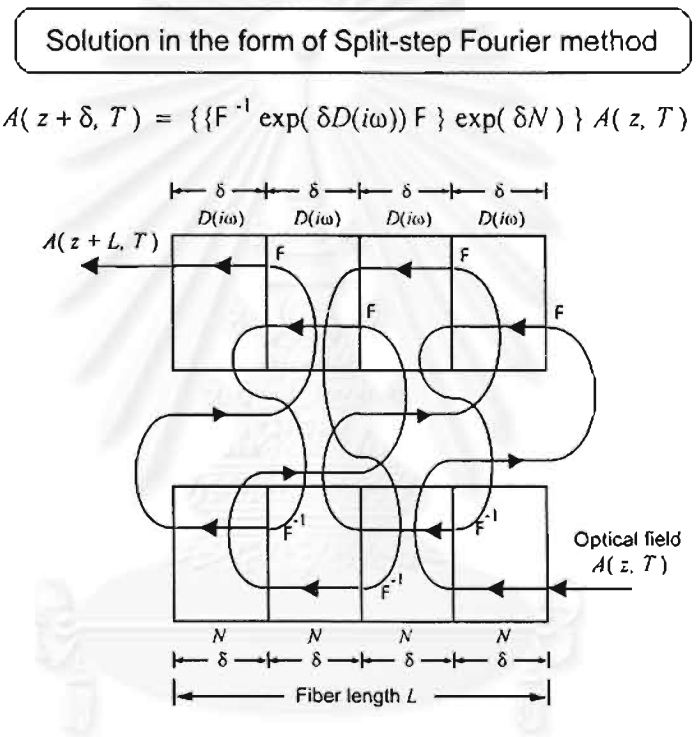

Figure 2.9: Split-step Fourier algorithm for calculating signal propagation in optical fibers.

2.6 Second-order Dispersion Compensation Schemes

The problem which plays critical role in a limitation of optical fiber system performance is considerably originated from fiber SOD that causes the broadening of the signal pulses during propagation inside the fiber. There are 4 main schemes have been proposed in order to overcome the SOD effect.

2.6.1 Zero-dispersion wavelength transmission [18]-[21]

According to the dispersion characteristic of optical fibers shown in Fig. 2.2, the GVD parameter β_2 and the dispersion parameter D vanish at the wavelength of λ_D which is referred to 1.55 μm for the DSF. The idea of this kind of system is simple: setting an operation wavelength of the system at zero-dispersion point so that the pulses can propagate without broadening. The advantages of the zero-dispersion systems arise from their simple construction and the avoidance from dispersion-limited performance. However, it is considerably difficult to set the operation wavelength exactly at the zero-dispersion point.

The problems of the zero-dispersion systems, as discussed above, grow up from the TOD resulting in pulse distortion and broadening [4], [18]. When the input power of the signal becomes intense, the nonlinearity of the fiber mainly causes the problems in zero-dispersion transmission. The two main problems in zero-dispersion transmission induced from fiber nonlinearity are the interaction between SPM and TOD and the enhancement of optical amplifier noise due to SPM [19]-[21]. The above two problems seriously result the signal waveform distortion and the rapid spreading of signal spectra.

2.6.2 Dispersion management [22]-[35]

As discussed above, fiber systems whose operation wavelength is located directly at the ZDWL point encounter problems mainly induced by the Kerr effect. Since the SOD length defined by Eq. (2-6) becomes infinity and no longer is compared to the nonlinear length at ZDWL point, the Kerr effect becomes stronger and pays important role in limiting the system performance. In order to avoid the problems, a very slight displacement of a carrier wavelength from ZDWL may be one way to alleviate the problems [22]-[35].

Furthermore, the more sufficient method is to arrange the various sections of fiber in such a way that none or only very few of them have ZDWL that coincide with the carrier wavelength while the total fiber exhibits zero SOD on average. A method for construction a fiber system which consists of fiber sections that are arranged such that the SOD of each amplifiers span is zero at the operation wavelength are generally called dispersion management.

The idea of dispersion management comes from the completely cancellation of the frequency chirp resulting in the recovery of the pulse shape. If we consider the fiber section consisting of two pieces of fibers with the same value of SOD but different symbols (+ and -) shown in Fig. 2.10. This section of fiber exhibits the zero SOD on average. An optical pulse launched to this fiber will be frequency-chirped induced by the SOD. The pulse will be broadened due to the SOD-induced pulse broadening. However, when the pulse is entered to the fiber which exhibits the opposite SOD symbol, the frequency-chirping occurs in the opposite direction so that it will cancel the chirp induced by the first fiber resulting in pulse compression.

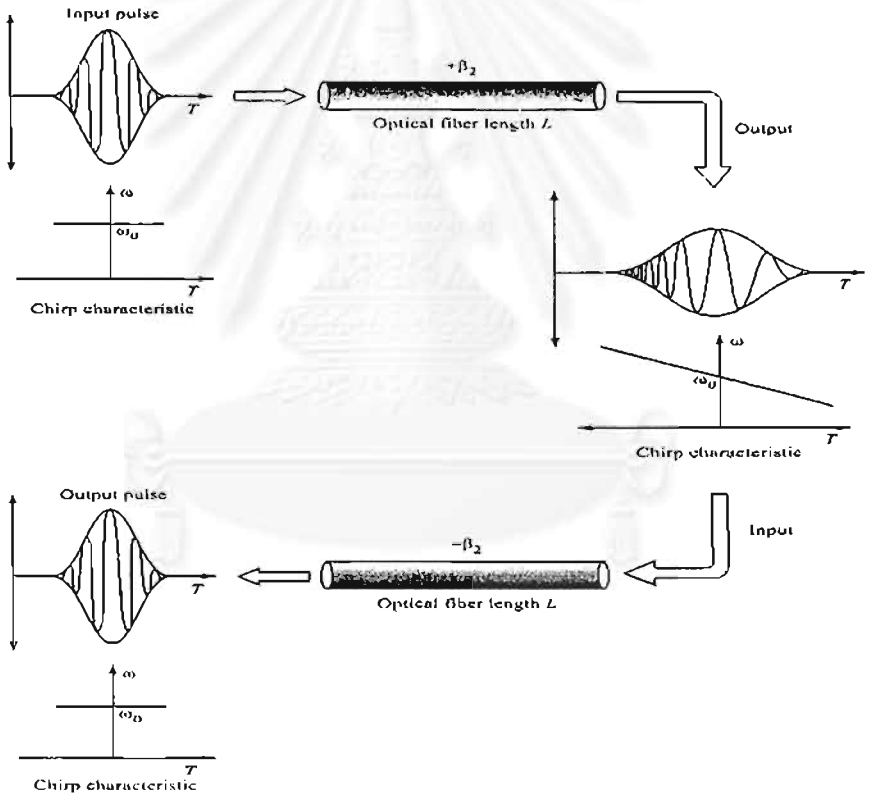

Figure 2.10: Concept of dispersion management method.

2.6.3 Optical soliton [36]-[47]

Soliton refers to special kind of waves that can propagate undistorted over long distances and remain unaffected after collision with each other. Optical solitons in optical fibers are conformed by balancing the SOD and the SPM in anomalous dispersion region [4], [5], [36]. Quantitatively, this can be achieved by launching optical pulses with proper input power and width into the fiber. The most attractive characteristic of optical solitons is that they can propagate in optical fibers without pulse shape distortion over a long distance if the fiber loss is negligible. There are other several other reasons why solitons are attractive for optical communication systems generally and therefore why they should be considered as a possible route for system upgrades. In particular, solitons are compatible with all optical switching and routing technologies [11]. The ability to optically process signal is essential if the bottleneck problems encountered at switching nodes are to be overcome for the high data rates.

The generation of optical soliton in optical fibers based on the idea of dispersion compensation which is achieved by the frequency-chirp cancellation occurring by transmitting optical pulses in two pieces of optical fibers whose symbols of SOD are opposite. In the case of nonlinear effect, if we launch an intense optical pulse to the fiber with operating wavelength situating at anomalous dispersion region, the nonlinear up-chirp will occur through the SPM and at the same time the linear down-chirp will be induced by the anomalous dispersion. Since the chirp induced by SPM and chirp induced by SOD exhibit opposite symbols, they will cancel each other during propagation inside resulting in pulse compression or broadening depending on the input power of the pulse. If we enter the optical pulse to the fiber with an appropriated power which is related to the value of β_2 and pulse width, the nonlinear up-chirp and linear down-chirp will cancel each other in such a way that no pulse compression and pulse broadening during propagation. Such the optical pulse which can travel inside the fibers with no change in pulse shape and spectrum by balancing the effect of SPM and SOD refers to the optical soliton.

Figure 2.11 illustrates how the soliton can maintain its shape during the propagation by the balance of frequency chirp by SPM and chirp by fiber SOD in

anomalous dispersion region. Qualitatively, in the absence of fiber loss, such sotiton phenomena can be met at the balance point of SOD and SPM via the condition: $L_{nl} = L_{d2}$, which yields the input power P_0 required for conforming the soliton for given β_2 and pulse width T.

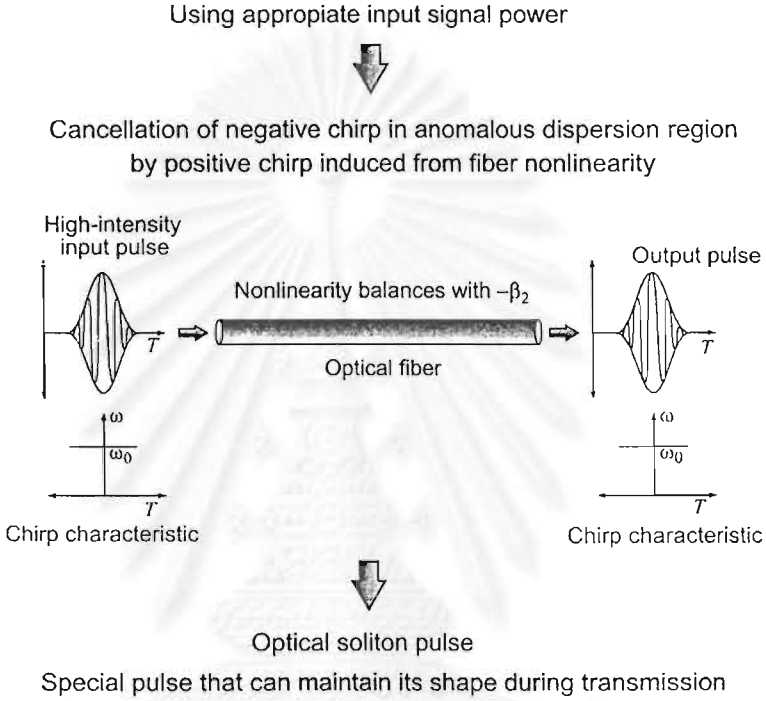

Figure 2.11: Soliton generated by the balance of SPM and SOD in anomalous dispersion region.

The problems in soliton transmission systems are roughly classified into the following three problems: the fiber loss, [4], [5], [42]-[44] the mutual interaction between adjacent solitons [4], [45], and the Gordon-Haus effect [46], [47]. To transmit soliton pulses through actual optical fibers, especially for a long distance, it is necessary to consider the fiber loss. The fiber loss results in exponentially increase of soliton width and decrease of soliton peak. It is necessary to amplify the soliton periodically to maintain its power. With the EDFA, the soliton power is amplified to amplitude larger than that required for forming the fundamental soliton (the soliton in lossless fibers) so that its average power along the fiber is still the fundamental soliton power. Such a soliton called

the guiding-center soliton [42] or average soliton [43], which is stable when the ratio of the amplifier spacing and the soliton period is much less than unity [44].

In addition to the stability requirement, there are two other effects limiting the capacity of soliton transmission. When the solitons are closely spaced, the mutual interaction changes the velocity of the solitons and causes the soliton to move out of the detection window [4], [45]. On the other hand, the noise introduced by the optical amplifier randomly modulates the carrier frequency of the soliton, and the group velocity varies. This effect leads to the timing jitter and is known as the Gordon-Haus effect [46], [47].

In order to increase the transmission data rate of the T-M system with soliton scheme, such as the power of soliton, the soliton separation, and the bandwidth of the optical bandpass filter must be carefully designed to lower these two effects.

2.6.4 Midway optical phase conjugation [48]-[52]

This kind of system performs optical phase conjugation (OPC) at the midpoint of system in order to compensate both dispersive and nonlinear effects. Figure 2.12 shows schematically the midway OPC system. The optical phase conjugator is placed at the midpoint of the system. Under the condition that all of the system characteristics are symmetric with respect to the midway OPC, generating the conjugate signal of the first-half-transmitted signal at the midway of the system, all of the phase distortions induced in the first half are completely compensated via the self-recovery effect of the conjugate signal when transmitting through the second half of the system. However, in real transmission, three problems including one from an asymmetric system characteristic occur and limit a performance of OPC systems.

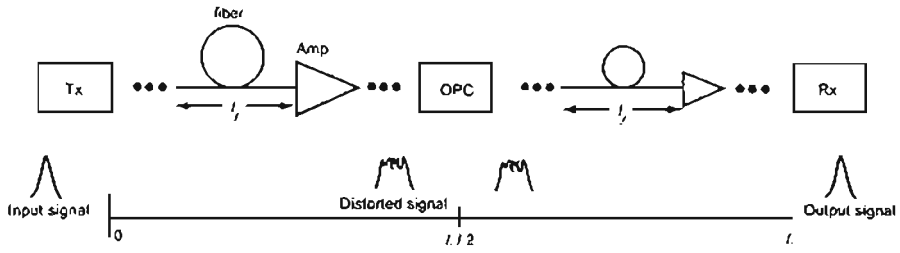

Figure 2.12: Midway OPC system.

According to the nonlinear Schrodinger equation (NLSE) (Eq. (2-16)) which governs the propagation of signal pulses in an optical fiber, taking the complex conjugation of NLSE, we obtain

$$-\frac{\partial A^*}{\partial z} = +\frac{\alpha}{2}A^* - \frac{i}{2}\beta_2\frac{\partial^2 A^*}{\partial T^2} - \frac{1}{6}\beta_3\frac{\partial^3 A^*}{\partial T^3} + i\gamma\left|A^*\right|^2 A^*, \qquad (2\text{-}17)$$

where * denotes the complex conjugate operation. Eq. (2-17) describes the complex conjugate amplitude of the signal A propagating in backward direction through the fiber which exhibit reverse sign of α and β_3. According to Eq. (2-16) and (2-17) indicates that if we generate the complex conjugate of the distorted pulses at the midway of a transmission link and let them travel through the second half of the link, we will obtain the complex conjugate of the undistorted input pulses at the output end. The nonlinear waveform distortion caused by the Kerr effect and the SOD is thus perfectly compensated at the output end. However, to achieve the perfect compensation two conditions are needed. First, the transmission fiber of the second half must have negative β_3 while its β_2 still keeps the same sign as that of first half. Second, the propagation of signal through the second half requires a distributed gain instead of distributed loss since the sign of α must be reversed.

According to the first requirement, the widely-used transmission fibers such as the conventional single-mode fiber (SMF) and the dispersion-shifted fiber (DSF) both exhibit positive TOD. Therefore, similar to other systems, the TOD in OPC systems cannot be compensated by OPC but it just accumulates along the system length and will also cause the signal waveform distortion [48], [49]. On the other hand, the second condition can be satisfied only in an ideal lossless medium. In real system with long distance transmission, a periodic lumped amplification must be used for maintain signal power in order to obtain good

signal-to-noise ratio (SNR) at receiver. The fiber loss and this periodic amplification forms a periodic signal power distribution along the system length and at the same time produces a periodic variation of fiber refractive index through the Kerr effect of an optical fiber. By this process, it seems like a grating is virtually constructed in the transmission fiber. As shown in Fig. 2.13, a resonance between the virtual grating and the signal will occur at the signal sideband component whose wave vector matches the wave vector of this virtual grating resulting in exponential growth of that component with transmission length. This phenomenon is known as the sideband instability (SI), which causes signal waveform distortion if SI arises at frequency inside the signal bandwidth, which cannot be eliminated by using optical bandpass filter [50]-[52].

Qualitatively, SI can be considered as four-wave mixing (FWM) effect [4] which is quasi-phase-matched by the assistance of the periodic power variation induced virtual grating as the condition

$$k_{+} + k_{-} = 2k_0 + k_f . \tag{2-18}$$

In Eq. (2-18), k_0 denote the wave number of the signal which acts as a pump, $k_{\pm}$ the sideband wave numbers, and k_f the wave number of the virtual grating which is given as

$$k_f = \frac{2\pi n}{l_f}, \tag{2-19}$$

where $n = 0,\pm1,\pm2,...$, and l_f is the amplifier spacing. The sideband frequency ω_n shifted from the carrier frequency, at which SI arises is obtained from Eq. (2-18) and (2-19) as

$$\omega_n = \pm\sqrt{\frac{1}{|\beta_2|}\left(k_f n - 2\,\mathrm{sgn}(\beta_2)\overline{P}\right)}. \tag{2-20}$$

where $\overline{P}$ is the path-averaged signal power. The power gain $\lambda(\omega_n)$ of SI at each n-order resonance frequency is

$$\lambda(\omega_n) = 2P_0|F_n|, \tag{2-21}$$

where P_0 denotes the signal input power and F_n the n-order of the Fourier series coefficient of the periodic function $\alpha(z)$ whose period is equal to l_f.

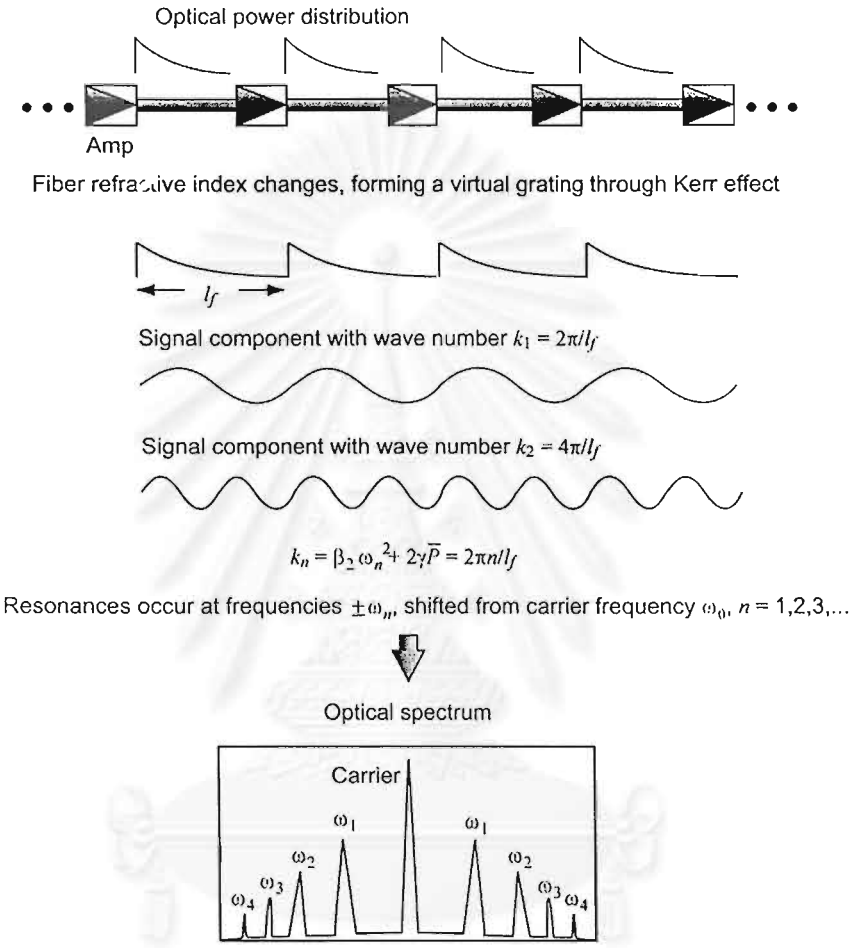

Figure 2.13: The occurrence of SI in chain of periodic amplification.

In the absence of fiber nonlinearity, it is not necessary to install the optical phase conjugator at the exact midpoint of the system. The position to place the optical phase conjugator theoretically can be moved to anywhere on the system. The optical signal can restore its shape at the output end of fiber by adjusting the accumulated dispersion at the end of system. However, in the presence of fiber nonlinearity, when the optical conjugator is moved out from the midpoint,

optimum design strategies that can used for reducing the fiber nonlinearity must be derived.

3. INVESTIGATION OF PROBLEMS IN ZERO-DISPERSION WAVELENGTH TRANSMISSION BY COMPUTER SIMULATIONS

By using optical amplifiers to compensate for fiber loss and setting signal carrier wavelength at zero-dispersion wavelength (ZDWL) of the transmission fiber, the loss and the second-order dispersion (SOD)-limited transmission distance can be overcome. However, unlike present electronic repeater based systems where the pulses are regenerative at each repeater, in optically amplified systems the accumulation of higher-order dispersion, especially the third-order dispersion (TOD) and the amplifier ASE noise become limiting factors in transmission distance or bit rate. Furthermore, it is well known that optical fibers show nonlinear behavior under conditions of high power and long interaction length. In ZDWL region, the relevant power-distance products for optically amplified systems can be so large as to make fiber nonlinearity a dominant factor in determining the design of long distance systems.

Understanding how system performance is degraded by the TOD and the ASE in the presence of fiber nonlinearity is crucial for designing this kind of system. In this section, the problems encountered in the design of ZDWL transmission systems are discussed. Section 3.1 discusses about the accumulation of amplifier noise. In section 3.2, we consider and demonstrate the problems induced from nonlinear interaction between the Kerr effect and TOD. Section 3.3 is devoted to the nonlinear interaction between the Kerr effect and amplifier noise.

3.1 Accumulation of Optical-Amplifier Noise

Accumulated ASE noise is by far the most important source of noise in the receiver. As a result, a minimum optical power level will be required along the line so as to obtain a sufficient signal-to-noise ratio (SNR) required for achieving good transmission quality. Assuming that the amplifier gain exactly compensates the total loss between successive amplifiers, for n_{amp} amplifier, the accumulated power of ASE noise N_{total} at

the output end is given by Eq. (3-1).

$$N_{total} = N_{sp} n_{amp} hf (G-1) B_{opt} . \tag{3-1}$$

where N_{sp} is the spontaneous emission factor, h is Planck's constant, f is the carrier frequency of the signal, G is the gain of the optical amplifier, and B_{opt} is the bandwidth of the optical bandpass filter. Now, if we use the fact that the amplifier gain G must offset the line loss between amplifiers, we find that $\alpha L_a = \ln(G)$, where L_a is the amplifier spacing. Thus we can replace n_{amp} by $\alpha L/\ln(G)$, to obtain

$$S_{ASE}(f) = hf_0 \alpha H(G) N_{sp} L , \tag{3-2}$$

where

$$H(G) = \frac{G-1}{\ln(G)}, \tag{3-3}$$

and L is total system length. The above equations show the rapid increase of the ASE noise as the amplifier spacing, and hence their needed gain, increases.

Here we use the split-step Fourier method (SSFM) for calculating pulses evolution with the accommodation of ASE noise. The system is assumed to be zero SOD system. The initial pulse train is a pseudo-random 16-bit NRZ signal. For investigating only the accumulation of ASE noise, we neglect all the nonlinear effects and the dispersive effects and no filter is employed to this system.

Figure 3.1 shows the result of the simulation with each curve represents the pulse shape after propagating for every 5 amplifier. This is clearly seen that the ASE noise is accumulated and increases linearly with the increment of the number of amplifier. The accumulation of ASE noise will result in degradation of SNR ratio, and hence the bit-error rate of the system, since the average power of the signal will be maintained constant along the system length by the amplifiers but the ASE noise increases according to Eq. (3-1).

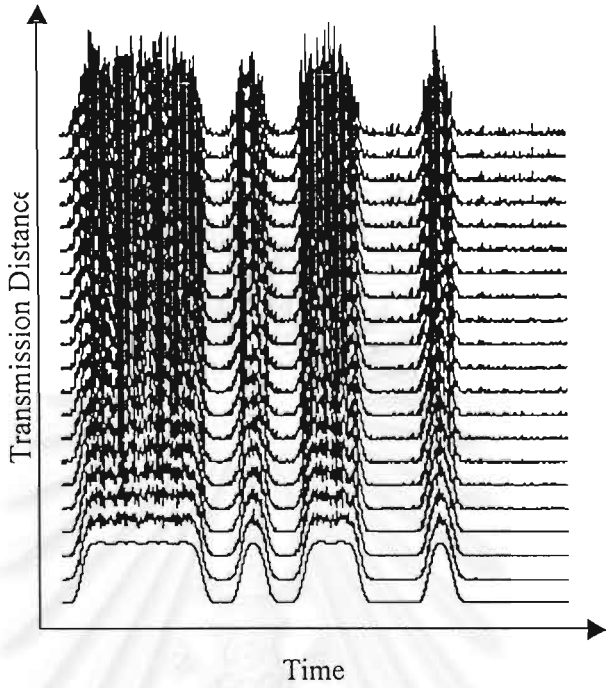

Figure 3.1: Accumulation of amplifier noise on pulse evolution.

3.2 Pulse Distortion by Interaction between self-phase modulation effect and third-order dispersion

Propagation of short, intense optical pulses through single-mode fibers is of considerable importance because of the current interest in high-capacity, long haul, optical transmission systems. As pulses get shorter and more intense, both dispersive and nonlinear effects become increasingly more important. Commonly one has attempted to avoid the SOD-induced pulse broadening by operating the system at the ZDWL at which the fiber has the same group velocity for all frequencies associated with the pulse. The chromatic dispersion, however, does not vanish entirely at the ZDWL, and the higher-order dispersion, especially the TOD should be considered for an appropriate modeling of the propagation characteristics of single-mode fibers.

Even when the nonlinear effects are negligible, the TOD can distort and broaden the optical pulses. The situation can change dramatically when the nonlinear

effects become important and need to be considered together with the higher-order dispersion. Agrawal has classified this problem into three categories [50] by using the ratio R between the scales of nonlinear length and TOD length,

$$R = \frac{L_{d3}}{L_{NL}} = \frac{\gamma P_0 T_0^3}{\beta_3}, \tag{3-4}$$

where L_{d3} denotes the TOD length and L_{NL} is the nonlinear length. γ is the nonlinear coefficient, P_0 is the power of the signal, T_0 is the signal pulsewidth, and β_3 is the TOD parameter. These two scales have been discussed in [4]. The three categories of the problem are thus identified as follows.

- When $R \gg 1$, the SPM dominates over TOD.
- When $R \ll 1$, the TOD dominates over the SPM.
- When $R \approx 1$, the two effects are equally important.

To evaluate the characteristic of the problem in each propagation regime, we perform the numerical calculation based on the SSFM. The parameters used for the calculation are listed as follows. The optical fiber is the DSF with ZDWL at 1,550 nm. $\beta_3 = 0.2$ ps^2/km and $\gamma = 3.6$ W^{-1}km^{-1}. The optical signal is a single Gaussian pulse with input signal power of 20 mW. It should be noted that the peak power using for calculation may be higher than practical system and the fiber loss is neglected. This is because we set such parameters for emphasizing the problem. With these parameters, the ratio R is calculated to be

$$R = 0.26 T_0^3. \tag{3-5}$$

If we set $R = 1$, the corresponded pulse width T_c will be

$$T_c = \left(\frac{1}{0.26}\right)^{\frac{1}{3}} = 1.57 \text{ ps}. \tag{3-6}$$

A. Dominant Nonlinearity

This section considers the case of relatively broad pulses compared to the characteristic width $T_c (T_0 \gg T_c)$ propagating in the fiber. We show the pulse evolution and its spectrum evolution in Fig. 3.2 with each waveform is recorded after propagating every 10 km. The initial pulse width $T_0 = 25$ ps and its spectrum using for

simulation are shown in Fig. 3.3 (a) and (b). Figure 3.3 (c) and (d) shows the results after propagating for 200 km. We note that the pulse shape is hardly changed whereas the pulse spectrum has broadened considerably with an oscillatory structure. The spectral broadening is a consequence of the SPM induced by the Kerr effect. The effect of TOD is to introduce an asymmetry, seen clearly in the pulse spectrum of Fig. 3.3 (c). This is, however, a minor effect in the regime where the nonlinearity is dominant.

B. Dominant TOD

In this section we consider the case of ultrashort pulses with width $T_0 \ll T_c$. The pulse evolution and its spectrum evolution are shown in Fig. 3.4 with each waveform is recorded after propagating every 20 cm. The initial pulsewidth $T_0 = 50$ fs and its spectrum using for simulation are shown in Fig. 3.5 (a), and (b). Figure 3.5 (c), and (d) shows the intensity and spectral profiles of the initial pulse at the output end of a fiber of length 4 m. In contrast to Fig. 3.5 (b), the spectral profile is almost identical to the initial profile. On the other hand, the pulse acquires significant structure on the trailing edge appearing in the form of subpulses of decreasing amplitudes as T increases.

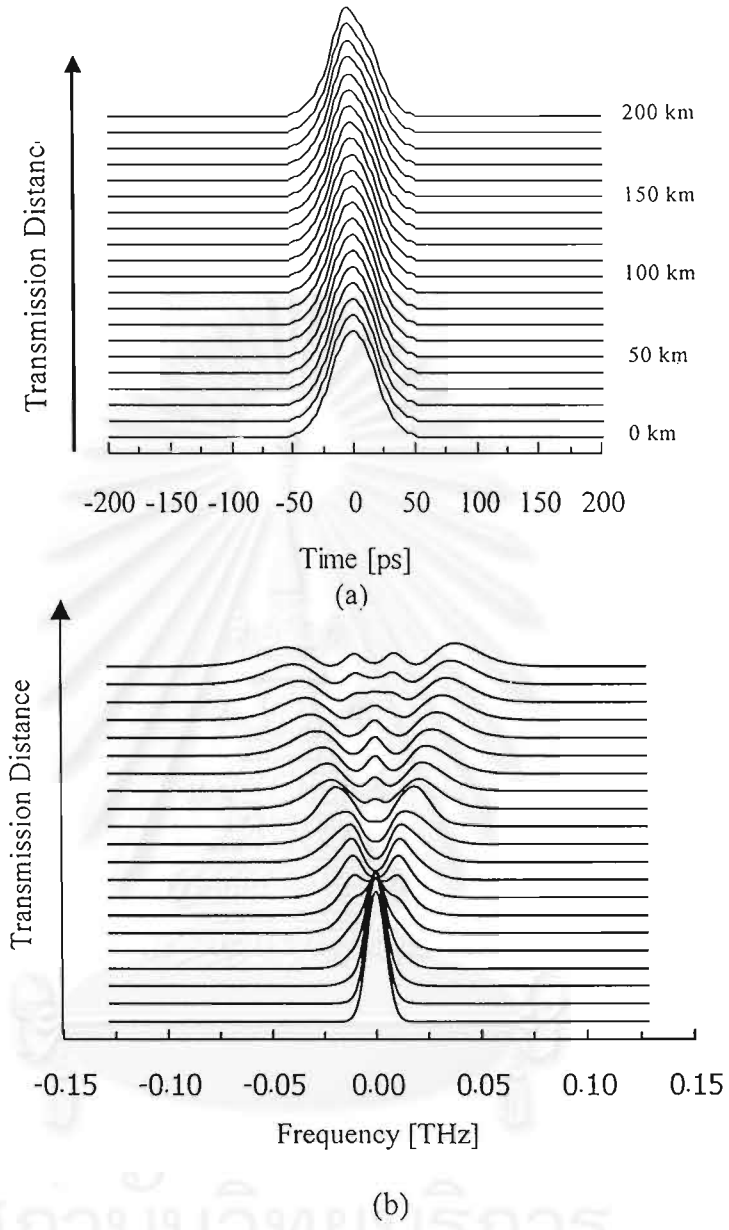

Figure 3.2: Optical pulse and its spectrum evolution where the fiber nonlinearity is dominant, (a) pulse evolution, (b) spectral evolution.

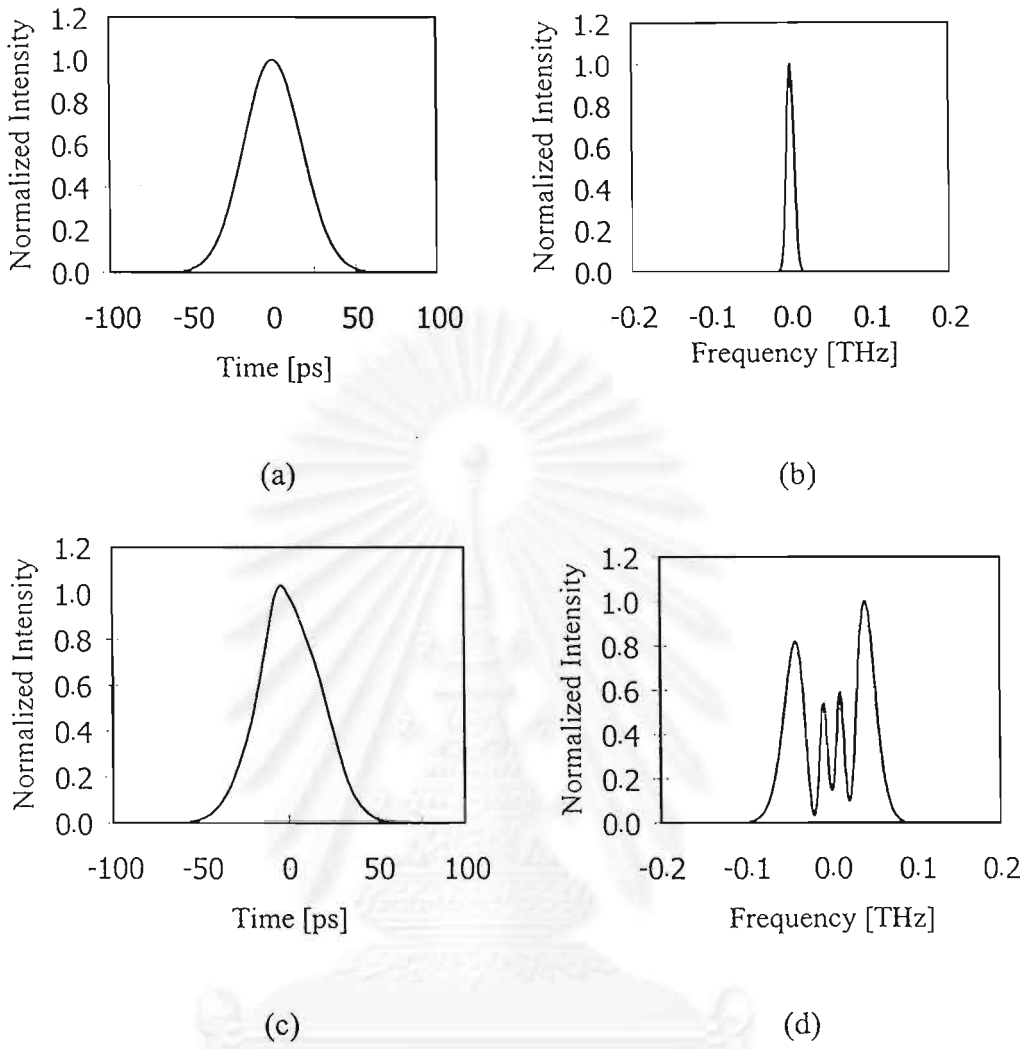

Figure 3.3: Optical pulse before and after propagation according to Fig. 3.2, (a) initial pulse, (b) initial spectrum, (c) 200-km propagated pulse, (d) 200-km propagated spectrum.

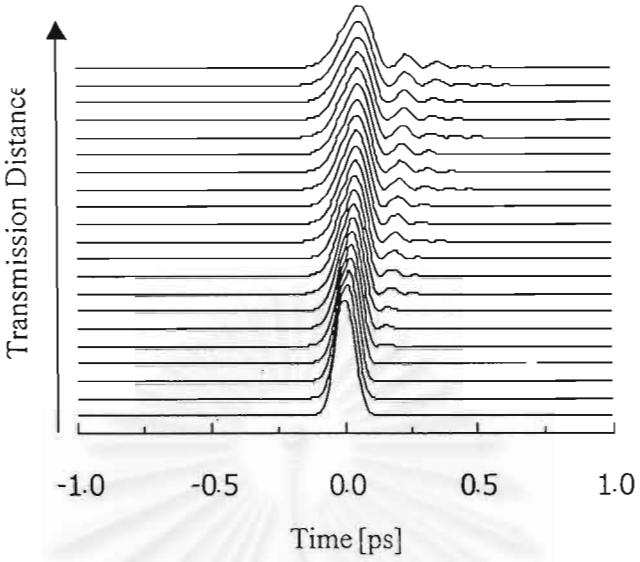

(a)

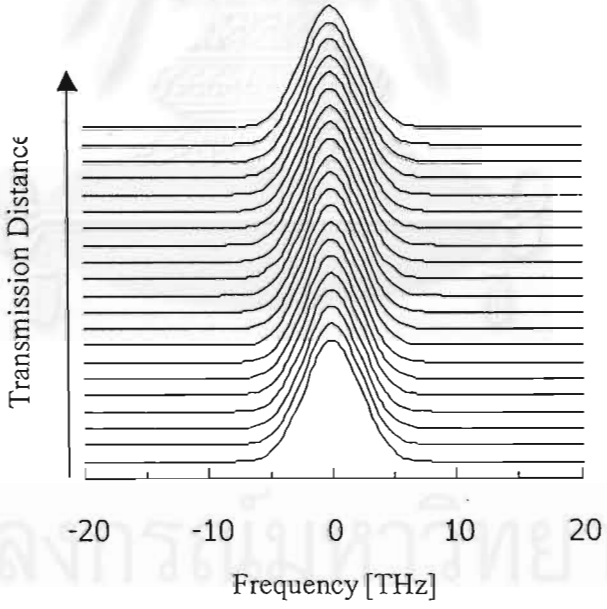

(b)

Figure 3.4: Ultrashort pulse and its spectrum evolution where the TOD is dominant, (a) pulse evolution, (b) spectral evolution.

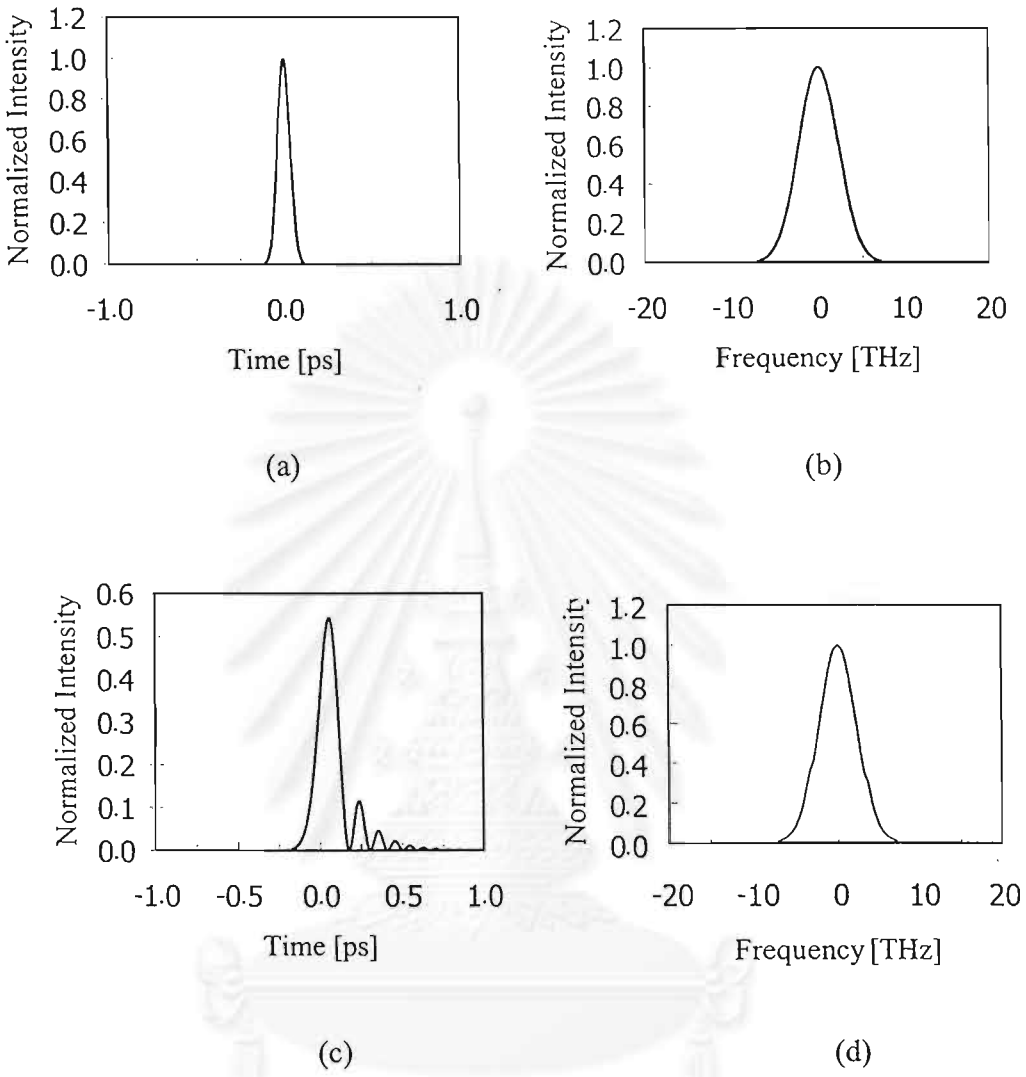

Figure 3.5: Ultrashort pulse before and after propagation according to Fig. 3.4, (a) initial pulse, (b) initial spectrum, (c) 4-m propagated pulse, (d) 4-m propagated spectrum.

It should be noted that the TOD-induced subpulses appear on the leading edge when β_3 is negative. Since the nonlinearity does not play a significant role in the TOD-dominant regime, the qualitative behavior can be reasonably well understood by neglecting the nonlinear term in the NLSE and obtaining the approximated solution using Airy function [17]. The location of subpulses varies with distance. Further, their widths at a given distance are not the same and decrease slowly as their number

increases.

C. TOD and SPM Comparable

The preceding results have shown that depending on whether the SPM, or the TOD dominates either the pulse spectrum or the pulse shape is mainly affected during propagation. In this section we consider the important intermediate region wherein the TOD and the SPM are comparable. As a result of interplay between the TOD and the SPM, none of the analytic results are applicable.

We simulate again with an input Gaussian pulse with $T_0 = 4$ ps which is comparable to the characteristic time $T_c = 1.57$ ps. The pulse evolution and spectrum evolution for distances 200 km are shown in Fig. 3.6 with each waveform represents the pulse after propagating every 20 km. Figure 3.6 looks difficult to understand the feature of the problem. We again show the pulse shape and its spectrum after propagating 75 km, 125 km, 150 km, 175 km, and 200 km in Fig. 3.7 and Fig. 3.8, respectively. According to Fig. 3.7 and Fig. 3.8, both the shape and spectrum are affected during propagation.

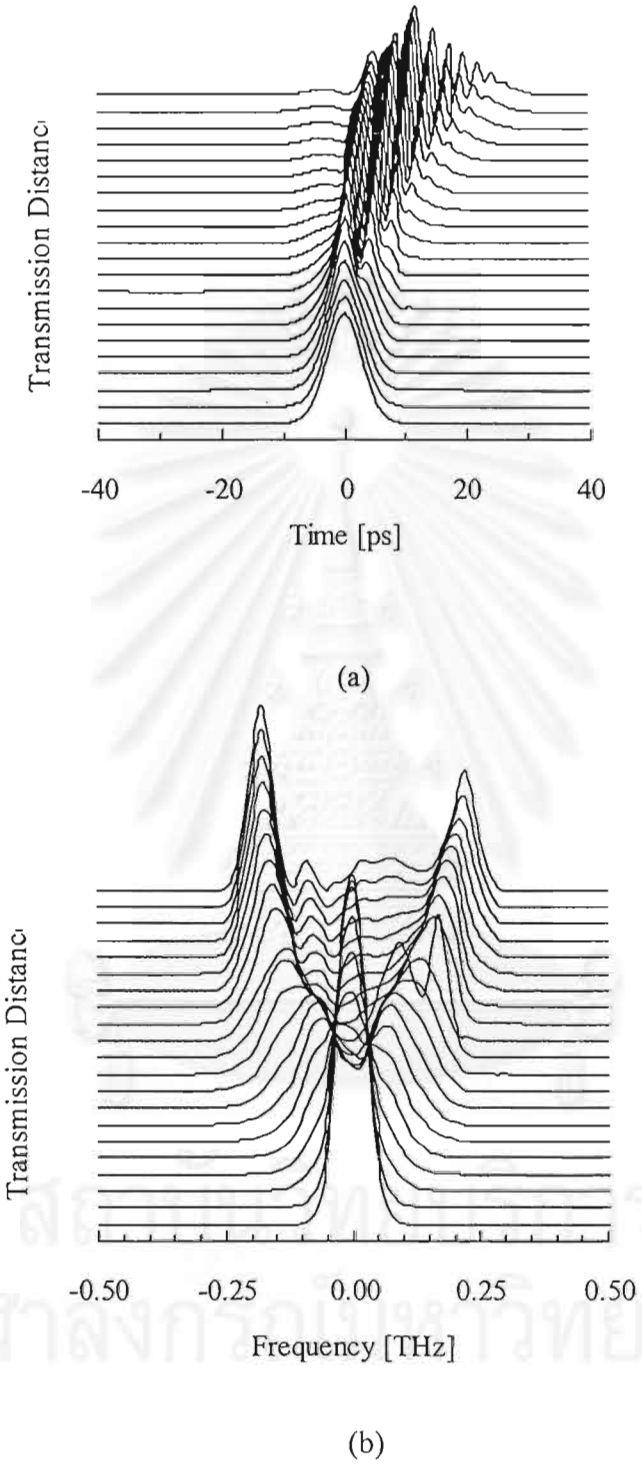

Figure 3.6: Optical pulse and its spectrum evolution when the TOD and the SPM are comparable, (a) pulse evolution, (b) spectral evolution.

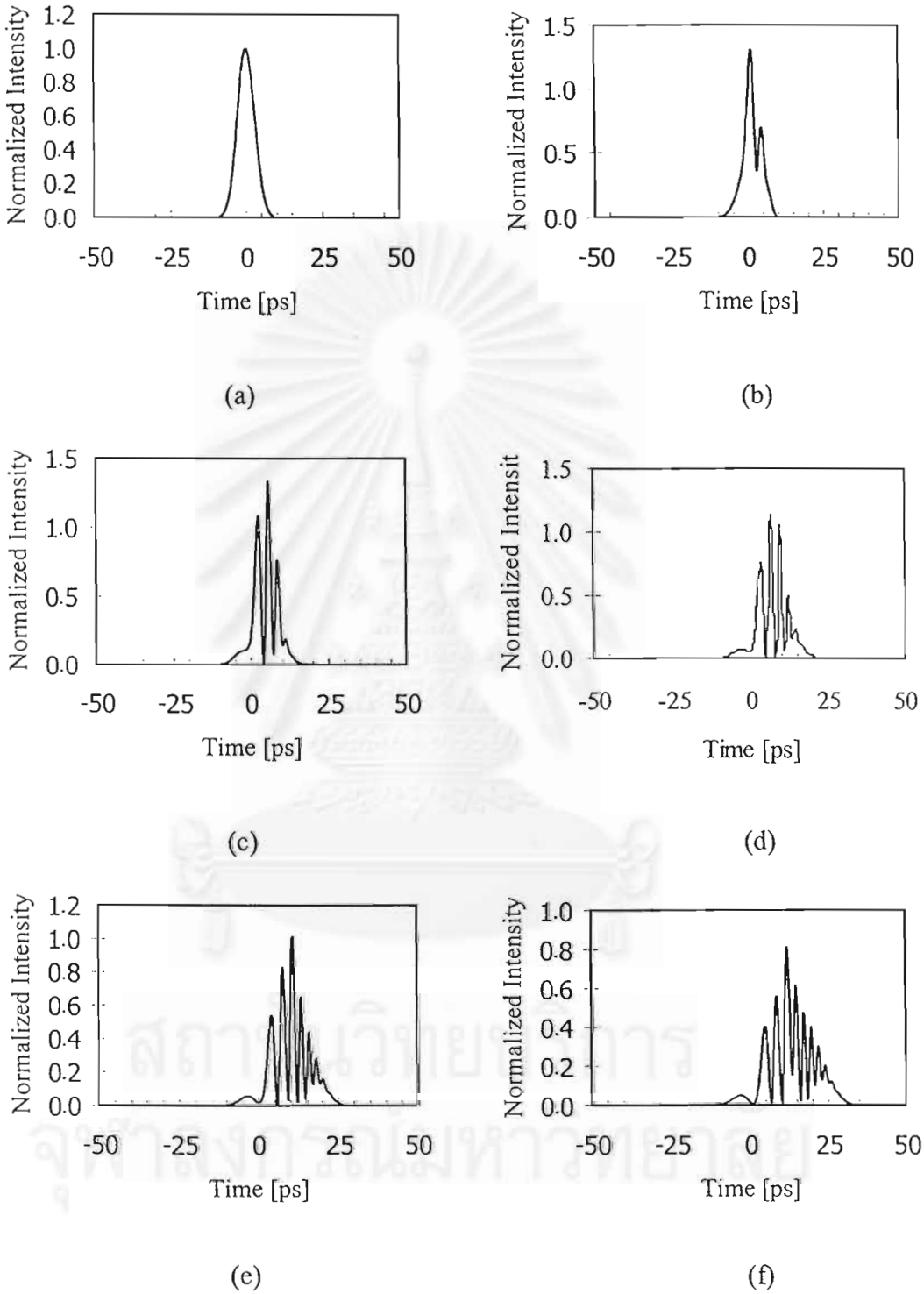

Figure 3.7: Optical pulse at several distances according to Fig. 3.6, (a) initial pulse, (b) 75 km, (c) 125 km, (d) 150 km, (e) 175 km, and (f) 200 km.

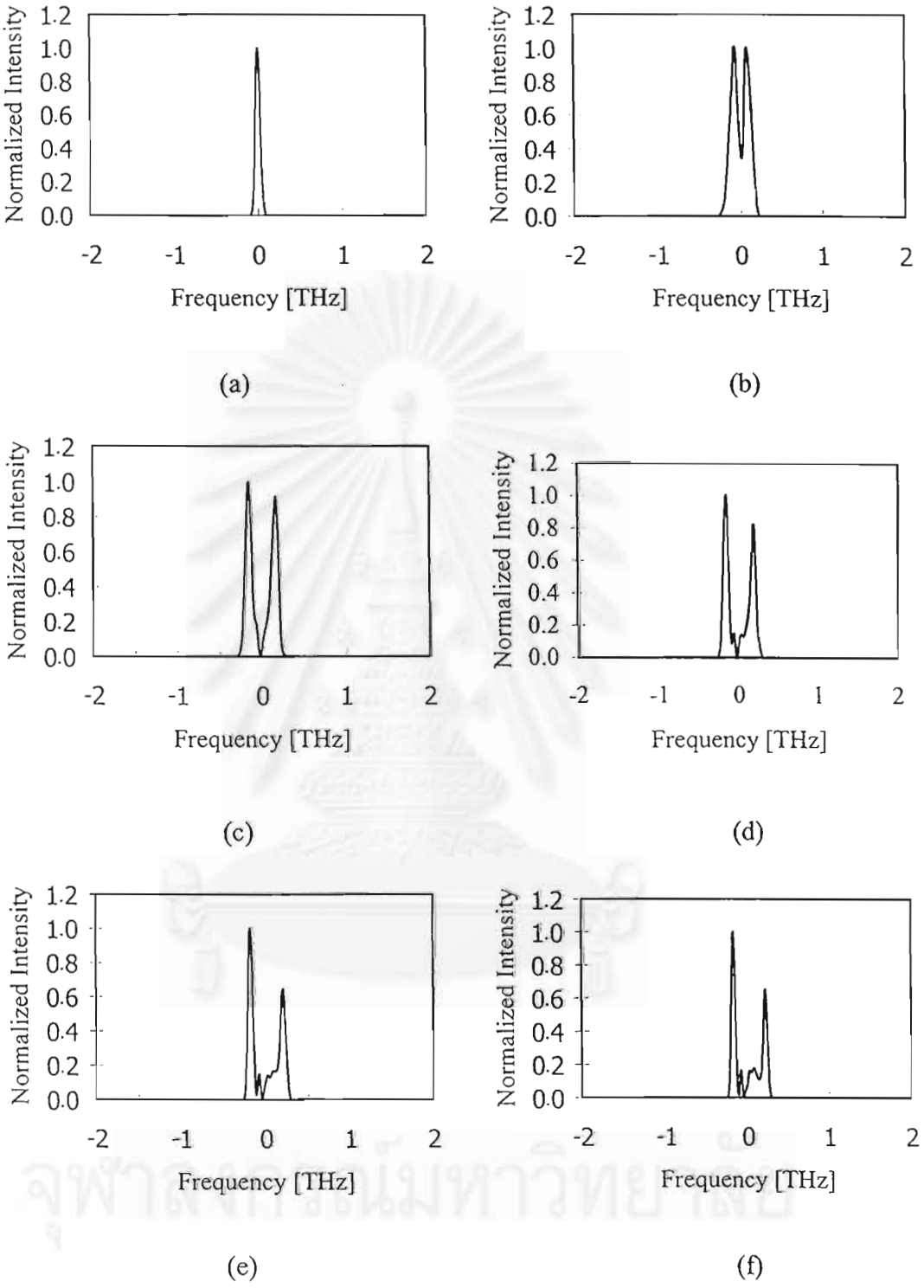

Figure 3.8: Optical spectrum at several distances according to Fig. 3.6, (a) initial spectrum, (b) 75 km, (c) 125 km, (d) 150 km, (e) 175 km, and (f) 200 km.

In particular, the dispersive effect governed by β_3 introduces oscillatory structure in the pulse shape. However, in contrast to the result shown in Fig. 3.7, the modulation in not complete, i.e., the intensity minimum does not go to zero. The number of subpulses rapidly increases with the transmission distance due to the effect of TOD. After 200 km, the pulse exhibits a large number of TOD-generated subpulses. A remarkable feature is that the first subpulse is no longer the most intense one. This can be explained that the SPM is shifting the power distribution among various subpulses.

Back to the optical spectrum evolution shown in Fig. 3.8, the optical spectrum is dominated by two asymmetric peaks of the optical frequency. This double-peak superstructure is the direct consequence of the SPM-induced spectral broadening of the pulse propagating inside the fiber. The asymmetry is a result of the TOD. These peaks are a manifestation of the periodic structure of subpulses in the pulse shape and their frequency is approximately given by the repetition rate of subpulses. The additional side peaks at twice the fundamental frequency also occur since the subpulse structure is not exactly periodic.

In practical, the ZDWL system is operating with pulse width of over 10 ps. This means that the system situates at the nonlinear regime. However, even the system length becomes longer than the TOD length, the situation is finally changed to the regime where the TOD and nonlinearity is comparable. This feature can also be observed by extending the propagation distance of the simulation in this section.

To evaluate this problem encounting the real system we simulate the zero-dispersion system by the initial 16-bit NRZ super Gaussian pulses instead of a single pulse. A fiber loss and EDFA are also included to the calculation to make the simulation similar to the real system as much as possible. The parameters used in the simulation are the same as the above simulation setting. The fiber loss of 0.2 dB/km is also added to the simulation with the periodic amplification for compensating this loss at every 50 km. The input signal is a 16-bit NRZ super Gaussian pulse with one-bit time slot of 100 ps. Therefore, the bit rate of this signal is 10 Gbit/s. The input power is 5 mW. The pulse evolution and spectrum evolution for distances 5000 km are shown in Fig. 3.9 with each waveform represents the pulse shape after traveling every

250 km. We again show the pulse shape and its spectrum after propagating 1,250 km, 2,500 km, 3,250 km, and 3,750 km, and 5,000 km in Fig. 3.10 and Fig. 3.11, respectively.

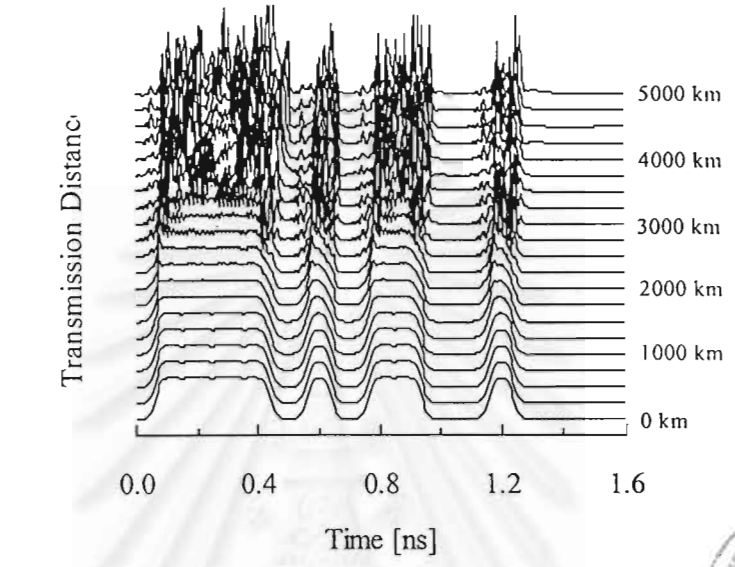

(a)

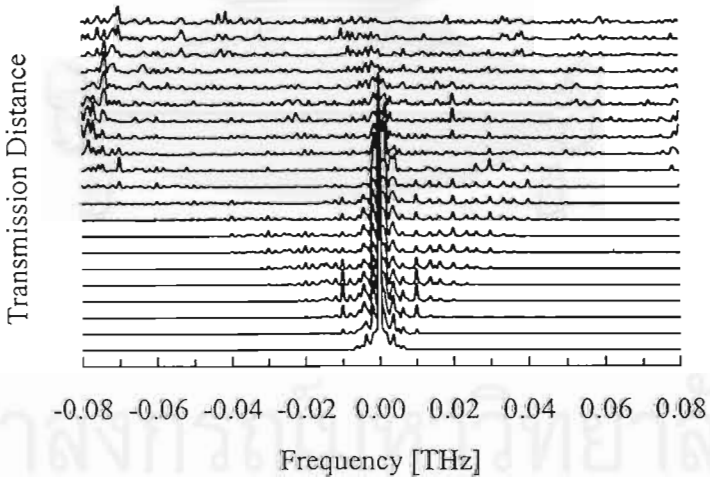

(b)

Figure 3.9: 16-bit NRZ optical signal and its spectrum evolution at ZDWL when the effects of TOD and SPM are comparable, (a) signal evolution, (b) spectral evolution.

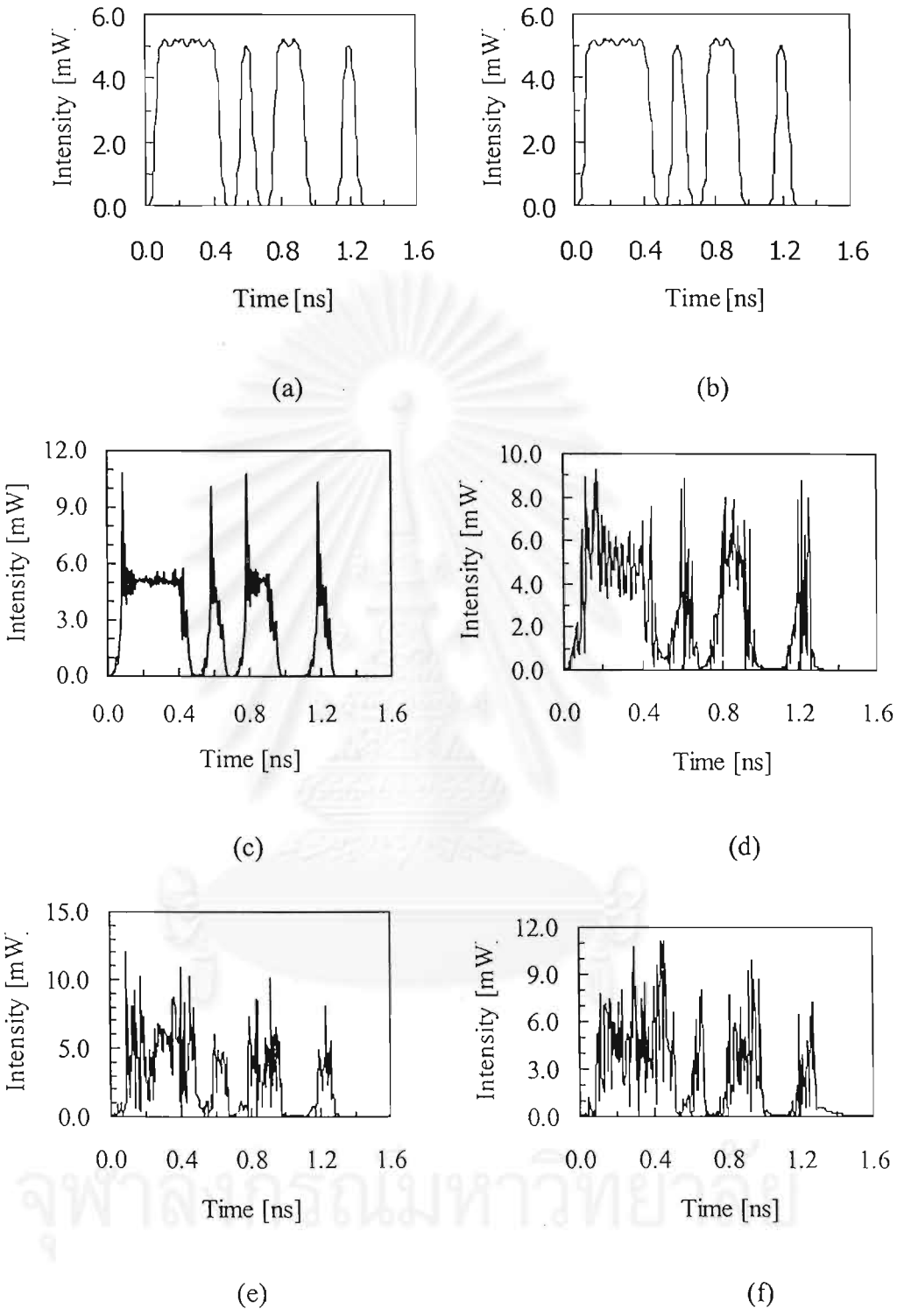

Figure 3.10: Optical signal at several distances according to Fig. 3.9, (a) initial pulse, (b) 1,250 km, (c) 2,500 km, (d) 3,250 km, (e) 3,750 km, (f) 5,000 km.

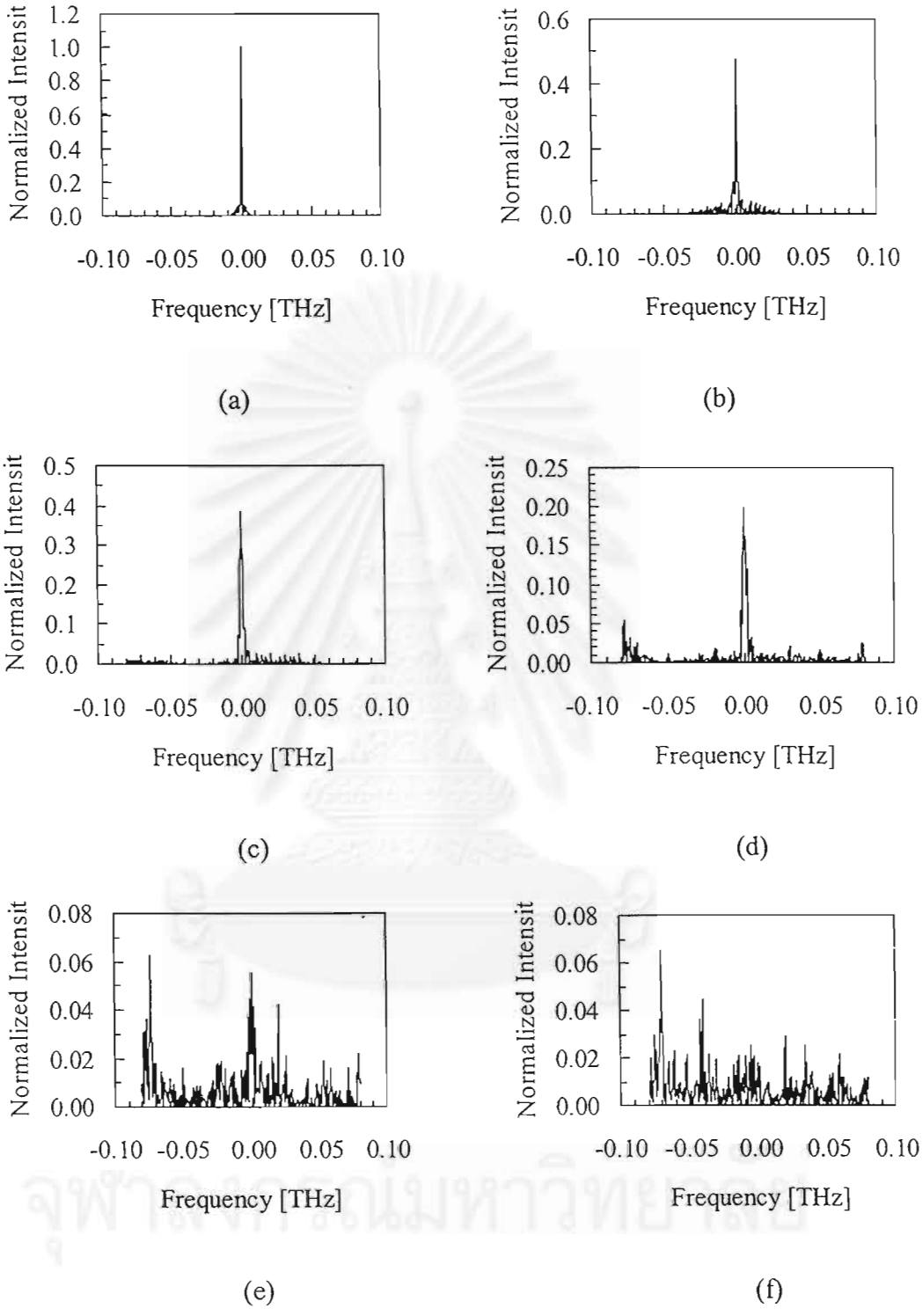

Figure 3.11: Optical spectrum at several distances according to Fig. 3.9, (a) initial spectrum, (b) 1,250 km, (c) 2,500 km, (d) 3,250 km, (e) 3,750 km, (f) 5,000 km.

According to the pulse width the system is clearly operating in the nonlinear regime. As a result, the NRZ pulses remain unchanged at a distance of 1,250 km while their optical spectrum is gradually broadening due to the SPM-induced spectrum broadening. When the spectrum is broad enough for creating the frequency components which satisfy the phase matching of a four-wave mixing (FWM) process, new more frequency components are created and the center spectrum will act as a pump which transfers its energy to the new components. This can be seen in Fig. 3.11 where the peak power of the spectrum decreases and the side-band new frequency components rise up. After traveling 2,500 km where the dispersion length becomes comparable the pulses start to break and have the oscillatory structure. The corresponding spectrum in Fig. 3.11 (c), as one would expect, shows the increase of side-band frequency components and the decrease of center spectrum peak resulting from the process of FWM.

For a distance over 2,500 km as shown in Fig. 3.11 (d), (e), and (f) the new frequency components whose number increases rapidly with the distance become more intense and comparable with the center frequency. They will lead to the large pulse distortion as shown in Fig. 3.10 (d), (e) and (f). Since the generation of the new components almost occurs randomly, the distortion in pulse shape is unexpected. At the distance of 5,000 km (Fig. 3.11 (f)), the center frequency completely transfer its energy to the side band. Some frequency components grow up rapidly and become the most intense than others. The whole spectrum exhibits a noise-like shape and spreads all over the background spectrum bandwidth. The corresponded distorted pulse shape shown in Fig. 3.10 (f) also becomes noise-like as the pulses break into subpulses whose intensity are randomly changed with a distance.

3.3 Enhancement of Optical Amplifier Noise by Kerr Effect through Process of Four-Wave Mixing

In a system using optical amplifiers, the ASE noise form each amplifier is accumulated. The total ASE power at the output end of a fiber has been shown and discussed in Eq. (3-1). However, the interplay between the nonlinear refractive index or the Kerr effect

and the SOD of optical fibers enhances the ASE noise more than the amount shown in Eq. (3-1).

Gordon and Mollenauer discussed the enhancement of the phase noise due to the nonlinear refractive index [59], and Ryu observed such effect experimentally [60], [61]. On the other hand, Marcuse pointed out that the parametric gain originated from the FWM effect induces the excess amplifier noise near the ZDWL [62], [63]. Ryu found that the transmitted signal is contaminated by the amplifier noise more seriously in the negative dispersion region than in the positive SOD region [64]. Kikuchi first showed the analytical treatment of this effect and his result confirmed Ryu's work that the positive SOD is favorable for suppressing the enhancement of the ASE noise [65], [66].

Kikuchi has classified the operating state of lightwave systems employing in-line optical amplifiers into the three categories [65], [66]:

1. Normal state, where $\frac{1}{2}|\beta_2|(2\pi f_m)^2 \gg 2\gamma P_0$, where f_m is the modulated frequency, the amplitude noise component and the phase noise component transfer their powers with each other during propagation along the fiber. However, in one repeater separation, the total ASE power is simply reduced by the optical loss, and no excess noise is generated. The ASE noise power at the output end is just the linear accumulation of the ASE power generated from each amplifier given by Eq. (3-1).

2. Phase noise state, where $\beta_2 > 0$ and $\frac{1}{2}|\beta_2|(2\pi f_m)^2 \ll 2\gamma P_0$, only the phase noise component is enhanced by the Kerr effect resulting in the excess phase noise. In the special case of ZDWL transmission, the bandwidth of the excess phase-noise spectrum is extending indefinitely. It can also be interpreted that a FWM process between the signal light and the ASE noise is phase-matched by the Kerr effect resulting in the growth up of ASE noise. As a result, the signal spectrum spreads to many times larger than its initial width, so that the signal power will be lost by the optical filter employed in the system. The enhancement of the ASE noise through the FWM process is shown in Fig. 3.12. Although the use of large bandwidth optical filter may be one choice to solve

the problem, the SNR at a receiver will be degraded unavoidably by the large amount of ASE noise which passes through the wide bandwidth optical filter. The excess phase-noise severely degrades the performance of coherent detection systems. However, in intensity-modulated-direct-detection (IM/DD) systems, phase-noise is canceled at the receiver, which detects only the absolute value of the square of the signal. The degradation of the IM/DD systems only arises from the impossibility of filtering the noise inside the bandwidth of the signal, saying in other word the signal-noise beat, since this will reduce the detected signal power and degrade the SNR.

3. Modulation instability state, where $\beta_2 < 0$ and $\frac{1}{2}|\beta_2|(2\pi f_m)^2 \ll 2\gamma P_0$, both amplitude noise component and phase noise component grow up exponentially. This effect is nothing but the modulation instability [4]. It can well be explained that the phase noise component converted from the amplitude noise component through the Kerr effect is constructively positive feedback by the anomalous dispersion resulting in the exponential growth of both components with the increase of transmission distance.

To confirm the above-mentioned theory, we perform computer simulations of the noise enhancement effect on the ZDWL transmission. The parameters used for setting up the simulation is listed as follows. The optical signal is the 16-bit NRZ super Gaussian pulse train whose one-bit time slot 100 ps. The peak power of the signal is 5 mW. The system length is 5,000 km. The tramsmission fiber is DSF with typical parameters used in above calculations. The optical amplifiers are used with amplifier spacing of 50 km. After amplification, the optical amplifier adds noise to the signal with the spontaneous emission factor N_{sp} of 1.6. The ASE noise is added to the simulation by generating spectral components whose real and imaginary parts are zero-mean independent Gaussian random variables whose variance is chosen to produce an average noise power per amplifier of

$$N_i = N_{sp} hf (G-1)\frac{1}{T}, \tag{3-7}$$

where $1/T$ is the bandwidth occupied by one Fourier component of the discrete Fourier spectrum whose time base of T = 1.6 ns contains the 16-bit pulse train. A complex Gaussian random variable of this kind is added to each Fourier component of the spectrum after each amplifier. The TOD is neglected here because we intend to concentrate only to the problem induced by the interplay between the ASE noise and the Kerr effect. An optical band-pass filter is not applied to the simulation for avoiding an undesirable loss caused by the filter, which occurs in relative-long distance zero-dispersion system.

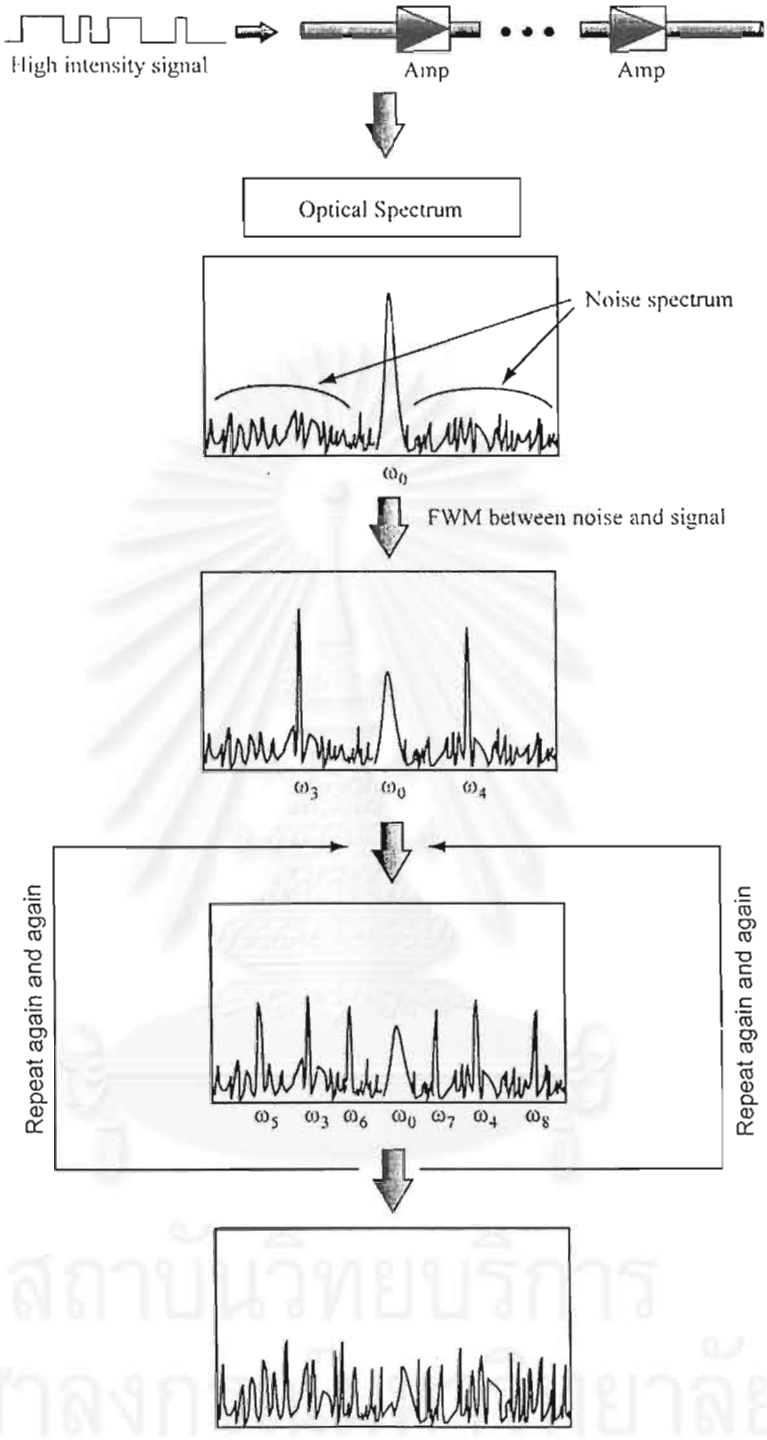

Figure 3.12: Four-wave mixing arising from ASE noise.

Figure 3.13 shows the results of the simulation in context of pulse train evolution and its spectrum evolution. The pulse shape and its spectrum at distance 0 km (input end), 1,000 km, 2,000 km, 3,000 km, 4,000 km, and 5,000 km are shown in

Fig 3.14 and Fig. 3.15, respectively.

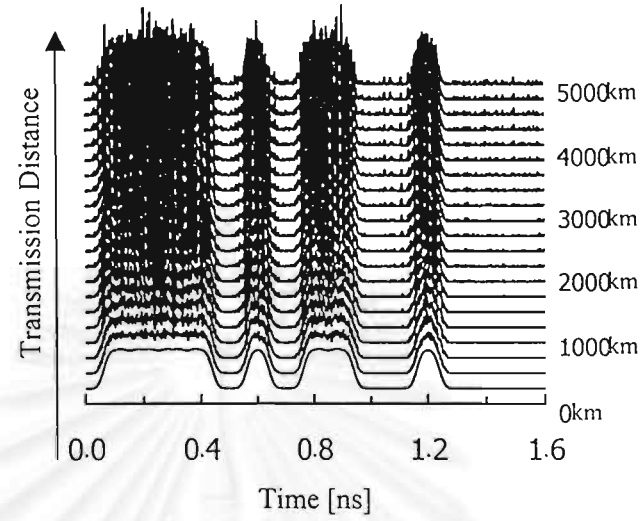

(a)

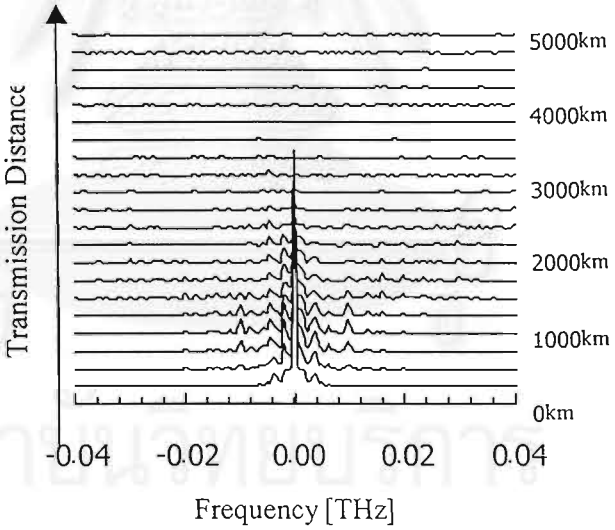

(b)

Figure 3.13: 16-bit NRZ signal and its spectrum evolution at ZDWL in the presence of nonlinear interaction between Kerr effect and amplifier noise, (a) signal evolution, (b) spectral evolution.

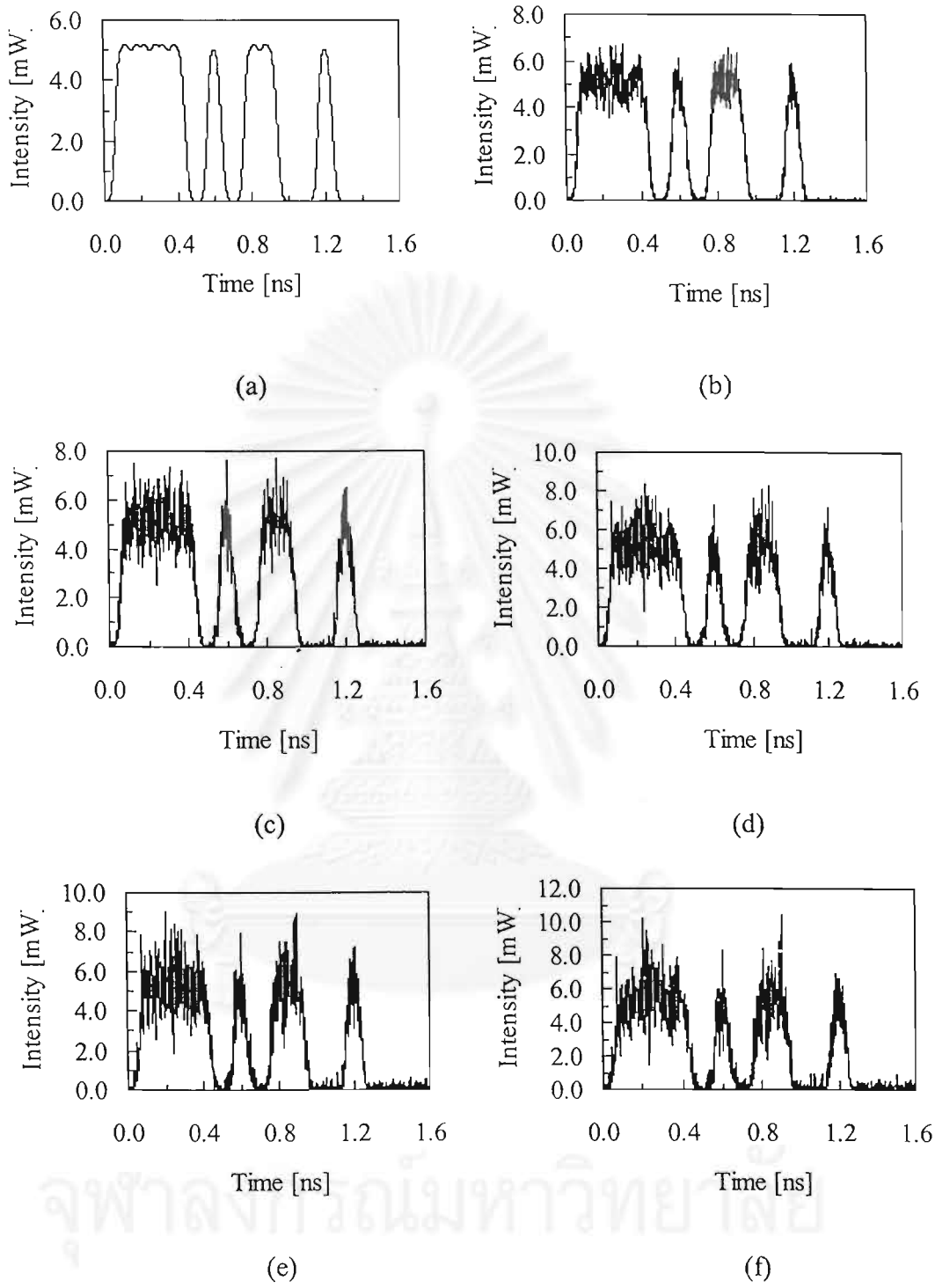

Figure 3.14: Optical signal shape at several distances according to Fig. 3.13, (a) input end, (b) 1,000 km, (c) 2,000 km, (d) 3,000 km, (e) 4,000 km, (f) 5,000 km.

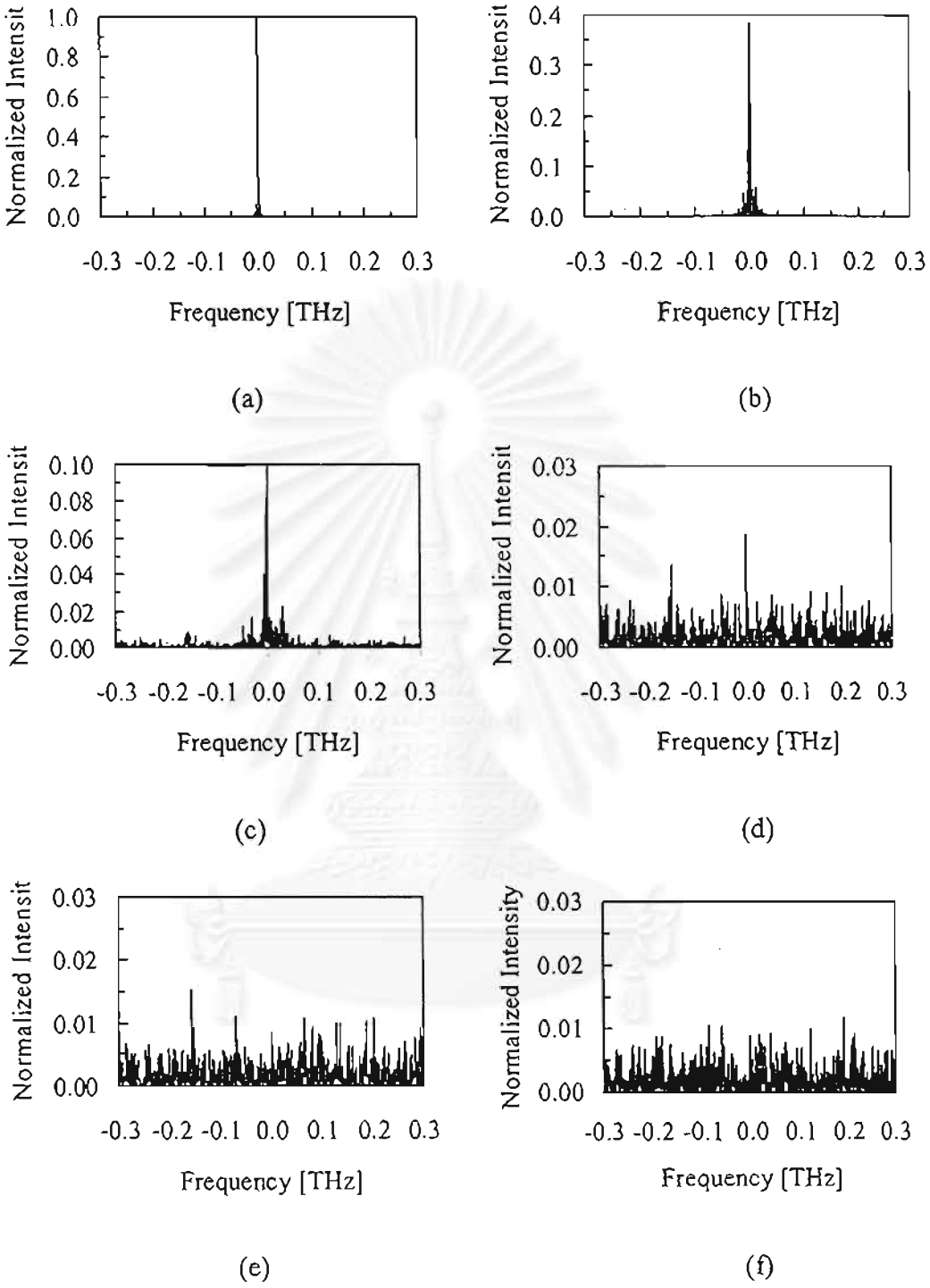

Figure 3.15: Optical spectrum at several distances according to Fig. 3.14, (a) input end, (b) 1,000 km, (c) 2,000 km, (d) 3,000 km, (e) 4,000 km, (f) 5,000 km.

As appearing in signal and spectral evolution in Fig. 3.13, the amount of noise on the signal is accumulated and is increasing with the increase of distance while its spectrum spreads rapidly over the whole spectrum bandwidth and finally becomes noise-like. According to the above-mentioned, it should be noted here that the accumulation of the noise on the signal shape is the linear accumulation since the system is operating at the phase noise state where only the phase noise will be enhanced by the Kerr effect so that the enhancement factor of the amplitude noise is still unity. Moreover, at the square-law detector, which only detects the power and the power fluctuation of the signal caused by the amplitude noise, phase-noise is canceled. By this reason, the accumulation of the ASE noise in ZDWL systems is linear.

However, the excess phase-noise results in the indefinite-spreading of the optical spectrum by the FWM process between the signal and the ASE noise, as discussed above. As a result, in order to maintain the signal power, the optical band-pass filter applied to this kind of systems must have a wide bandwidth. This will lead to the degradation of the signal-to-noise ratio at a receiver by the large amount of ASE noise, which passes through the wide bandwidth optical filter.

To understand how the nonlinear interaction of signal and noise has influenced the signal transmission, we perform the simulation again by ignoring the Kerr effect, leaving other parameter unchanged. The results in signal evolution and its spectrum evolution are shown in Fig. 3.16. The signal and its spectrum at distance 5,000 km are shown in Fig. 3.17.

By neglecting the Kerr effect, the operating state of the system is approximately situated in normal state and all of the enhancement factors become unity. Thus, it is obvious that the accumulation of ASE noise is linear. The result from Fig. 3.16 makes clear that the noise accumulation in ZDWL system is also linear since the signal in Fig. 3.16 are almost the same as that of ZDWL which is shown in Fig. 3.13. The spectrum in Fig. 3.17 (d) is almost indistinguishable from the input spectrum; the ASE noise contributed by the amplifiers is not visible on the scale of this linear plot. This result accounts for the different characteristic between the linear systems and the nonlinear zero-dispersion system or, in other words, the different operating state of the systems.

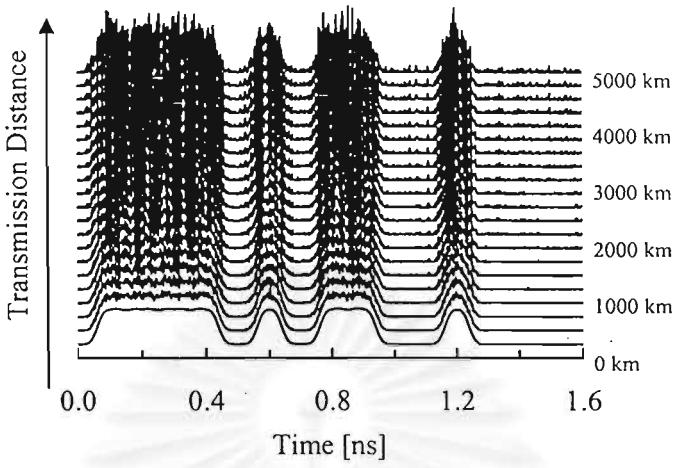

(a)

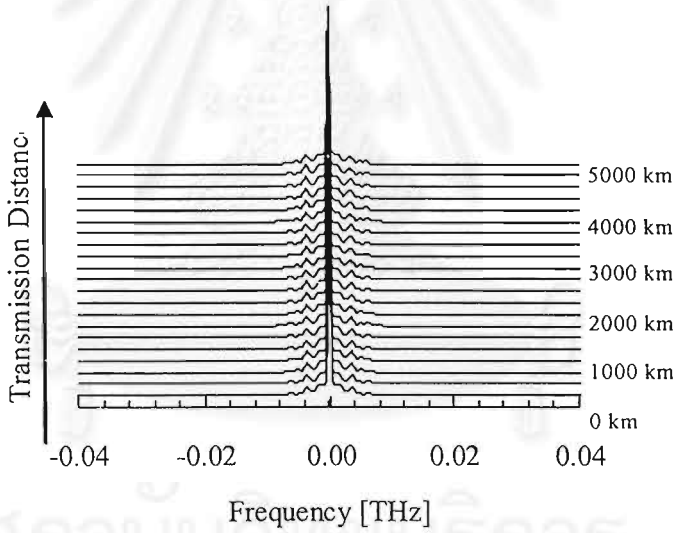

(b)

Figure 3.16: 16-bit NRZ signal and its spectrum evolution at ZDWL in absence of the Kerr effect (normal state of noise), (a) signal evolution, (b) spectral evolution.

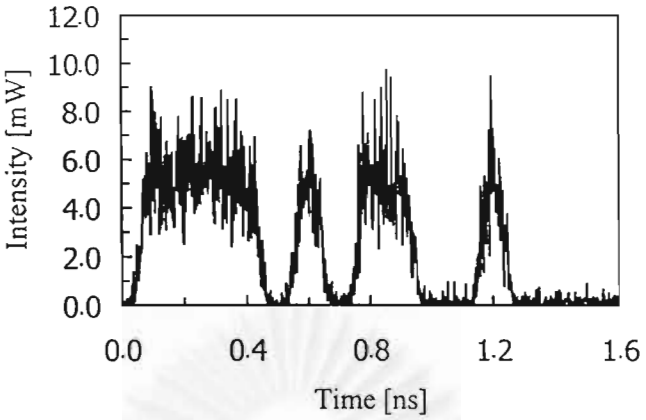

(a)

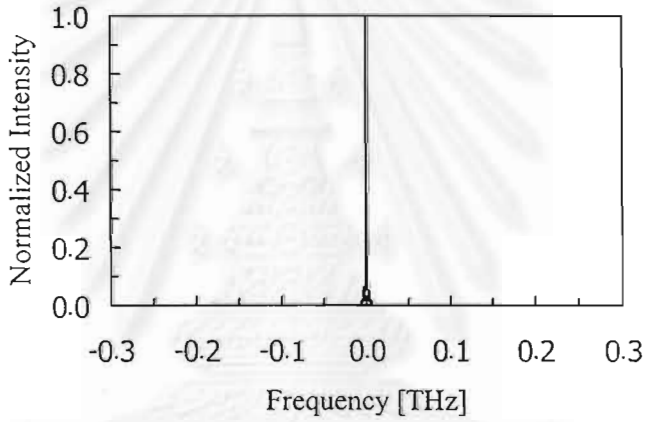

(b)

Figure 3.17: Optical signal and spectrum according to Fig. 3.16, (a) signal at 5,000 km, (b) spectrum at 5,000 km.

To explore the problem further, we repeat the simulation of the same single wavelength channel in the presence of the Kerr effect and ASE noise, but this time we place the operating wavelength slightly off the zero-dispersion point. This can be done by assuming that $\beta_2 = 0.2$ ps^2/km. This means that we are operating in the same state as the zero-dispersion (phase-noise state) but, however, in the presence of SOD. How this slight shift in operating wavelength affects the signal transmission is shown in Fig. 3.18 by the signal and its spectrum evolutions. The signal and its spectrum after 5,000 km are also shown in Fig. 3.19.

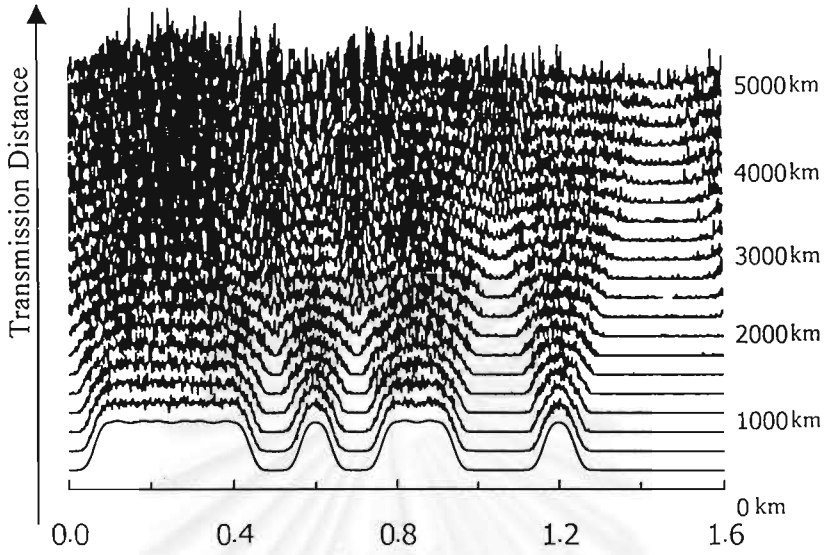

(a)

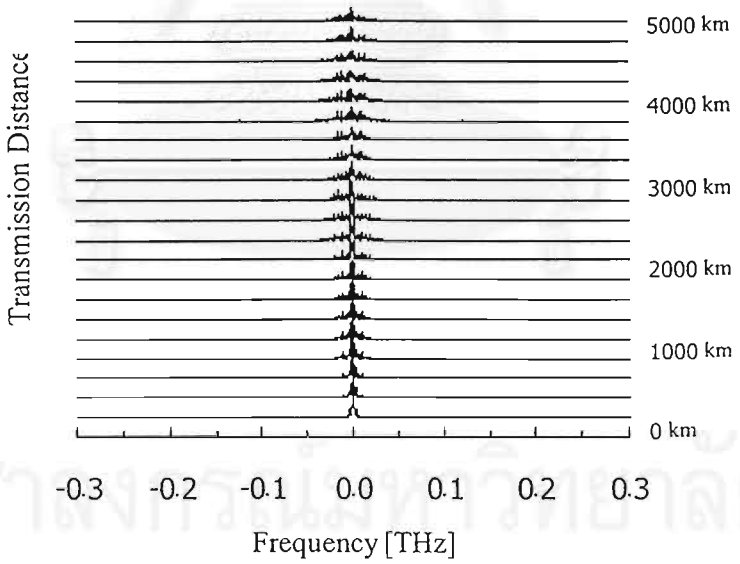

(b)

Figure 3.18: 16-bit NRZ signal and its spectrum evolution in phase noise state, (a) signal evolution, (b) spectral evolution.

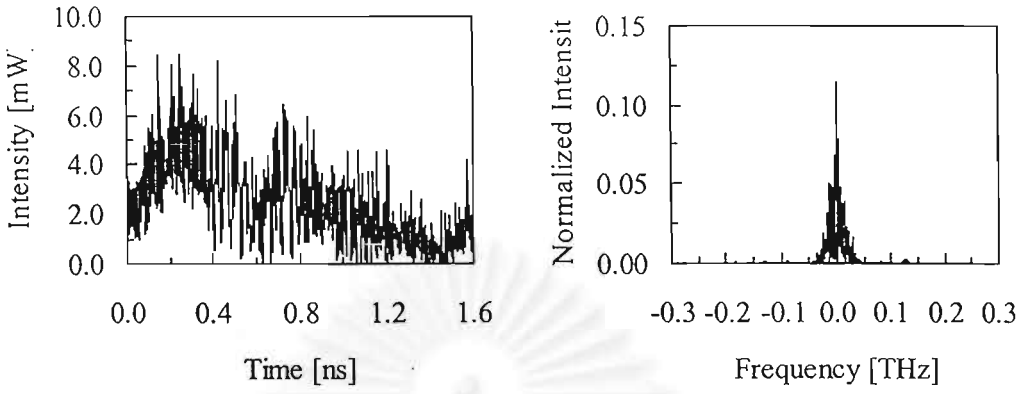

(a) (b)

Figure 3.19: Optical signal and spectrum according to Fig. 3.18, (a) signal at 5,000 km, (b) spectrum at 5,000 km.

Due to the SOD induced pulse broadening, the pulses are gradually broadening with the increase of distance. After 2,000 km the pulses broaden over each other and become undistinguishable whether ZERO or ONE. Since the operation wavelength is placed very near the ZDWL point, the spectrum are also gradually broadening but by the slower rate than that of zero-dispersion.

Next, we perform the further simulation of signal transmission in modulation instability state by placing the operating wavelength at the anomalous dispersion region. This is done by changing the sign of β_2 $\left(\beta_2 = -0.2\text{ps}^2/\text{km}\right)$ and leave other parameters unchanged. The signal and its spectrum evolutions are shown in Fig. 3.20. The signal and its spectrum after 5,000 km are also shown in Fig. 3.21.

After 1,000 km the signal start to break itself into subpulses which exhibit very shape spikes. This is resulted from the modulation instability generated subpulses occurring from the nonlinear interaction between ASE noise and signal as discussed above. As the result, the output spectrum, as shown in Fig. 3.21 (d), is broader than those of Fig. 3.17 (d) and Fig. 3.19 (d), however, narrower than that of zero-dispersion.

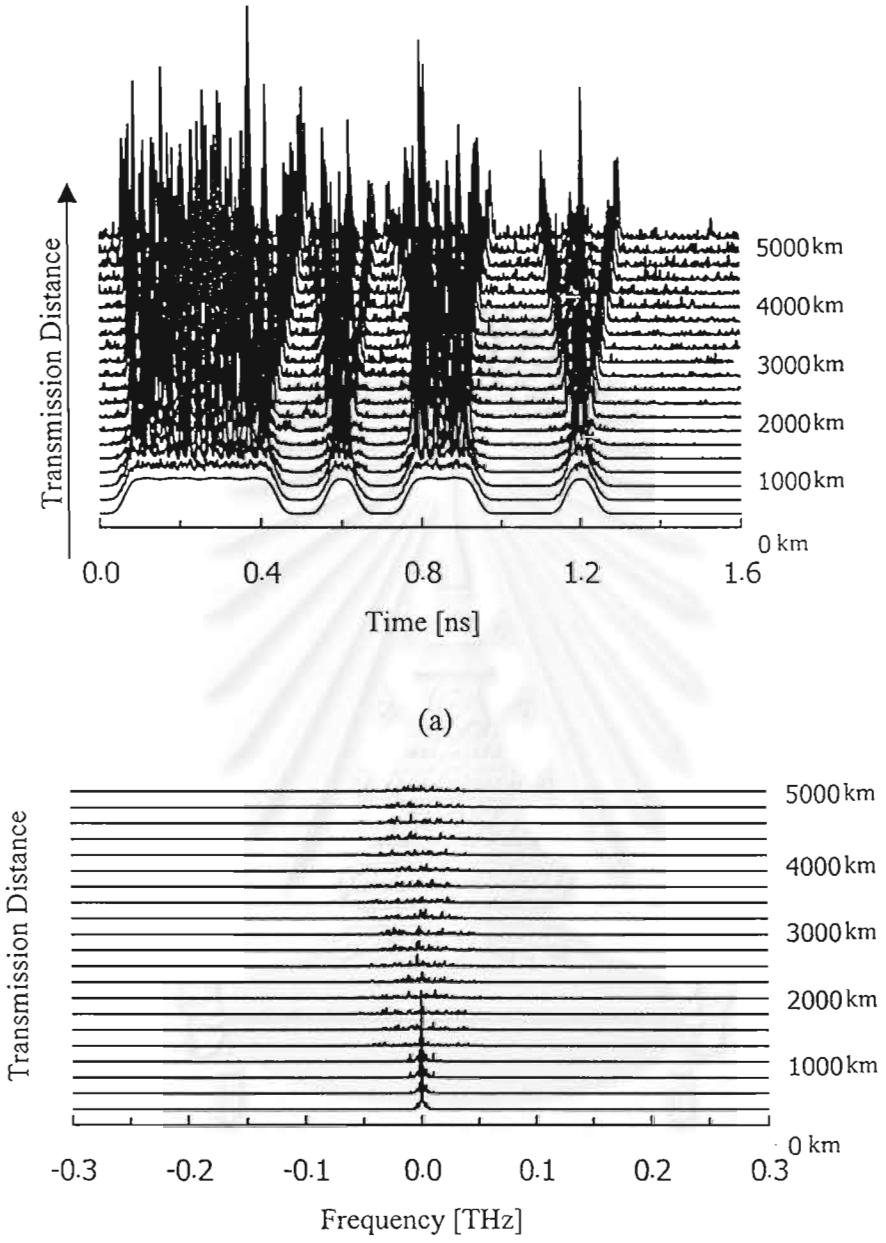

Figure 3.20: 16-bit NRZ signal and its spectrum evolution in modulation instability state, (a) signal evolution, (b) spectral evolution.

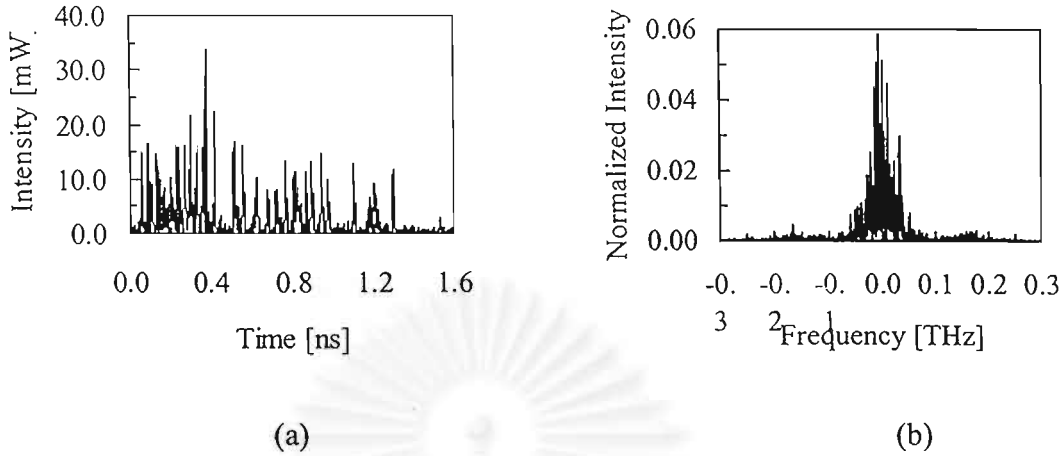

Figure 3.21: Optical signal and spectrum at several distances according to Fig. 3.20, (a) input pulses, (b) input spectrum, (c) signal at 5,000 km, (d) spectrum at 5,000 km.

3.4 Nonlinear Signal Transmission at ZDWL in the Presence of TOD and ASE Noise

In real system, we cannot consider the two problems discussed above separately as the TOD and ASE noise exist and interplay with the signal through the processes of nonlinear effects during the transmission. To evaluate the problem that occurs in the presence of TOD and ASE noise, we perform the computer simulation without neglecting these two parameters. The system parameters set for the simulation are the same as used in the previous section and β_3 is 0.2 ps^3/km.

Figure 3.22 shows the results of the simulation by signal evolution and its spectrum evolution. The pulse shape and its spectrum at distance 0 km (input end), 1,000 km, 2,000 km, 3,000 km, 4,000 km, and 5,000 km are shown in Fig. 3.23 and Fig. 3.24, respectively. Comparing distance by distance to the results of the simulations when we consider only the nonlinear interplay between signal and the TOD or the signal and ASE noise, the signal distortion in Fig. 3.23 is more severe and the pulses exhibit a complicated shape. During the transmission, the pulses have a slight broadening and a small time-shifted in their trailing directions, which increase with the distance. These appearances are mainly caused by the interplay between the

Kerr effect and the TOD.

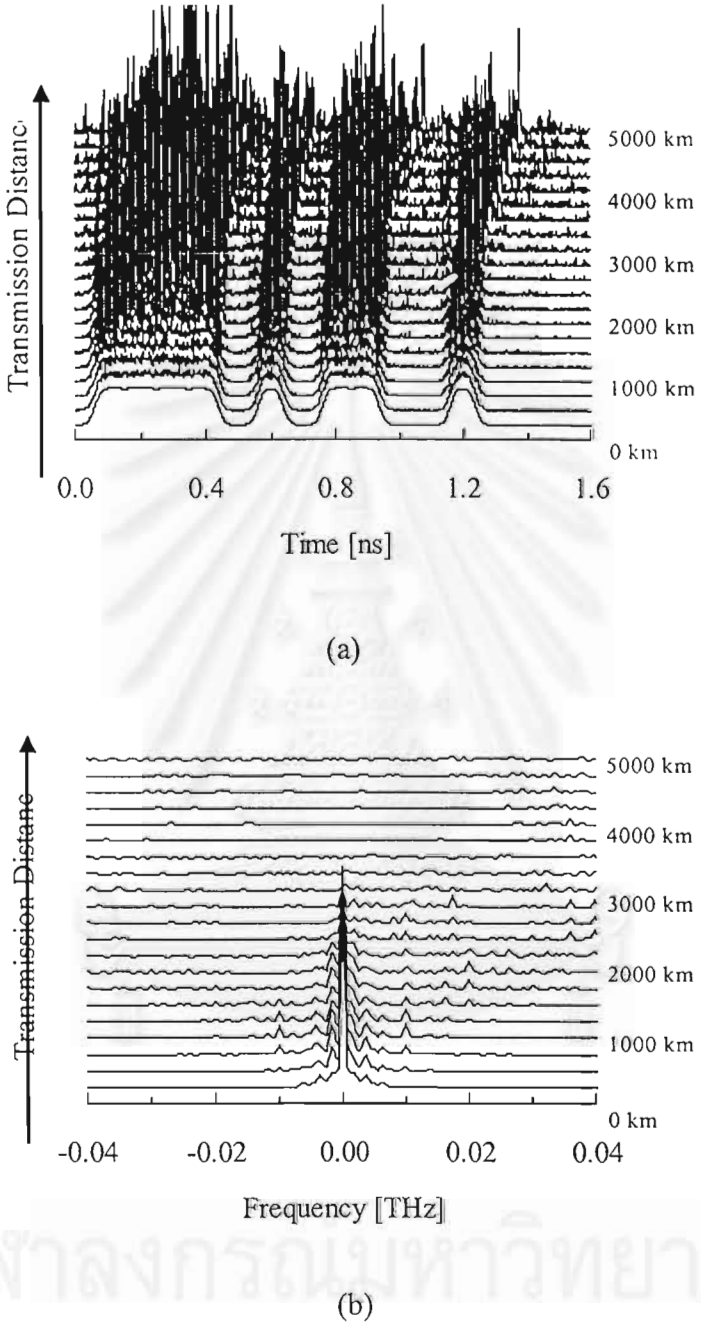

Figure 3.22: 16-bit NRZ signal and its spectrum evolution in the presence of both TOD and ASE noise, (a) signal evolution, (b) spectral evolution.

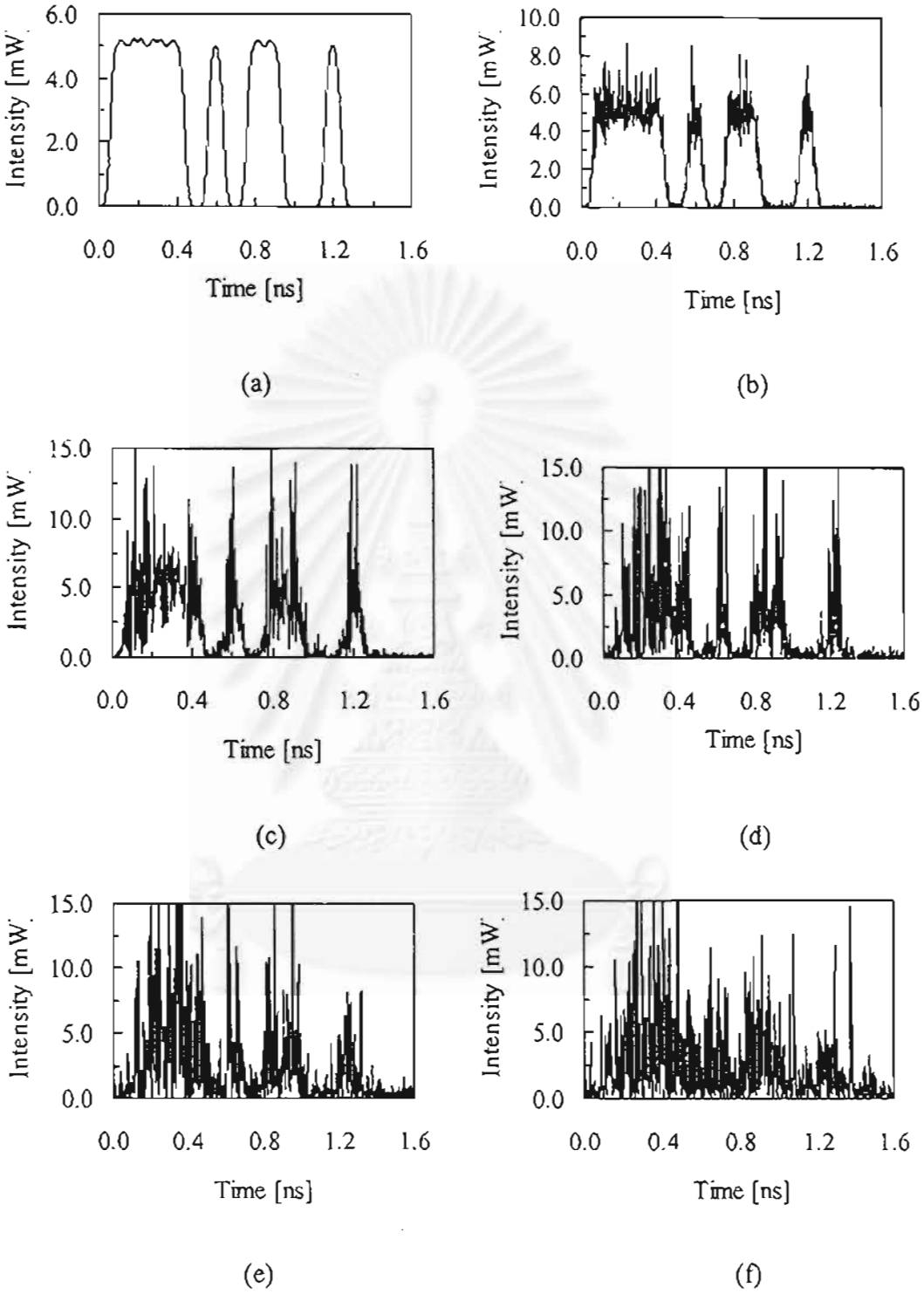

Figure 3.23: Optical signal shape at several distances according to Fig. 3.22, (a) initial pulse, (b) 1,000 km, (c) 2,000 km, (d) 3,000 km, (e) 4,000 km, (f) 5,000 km.

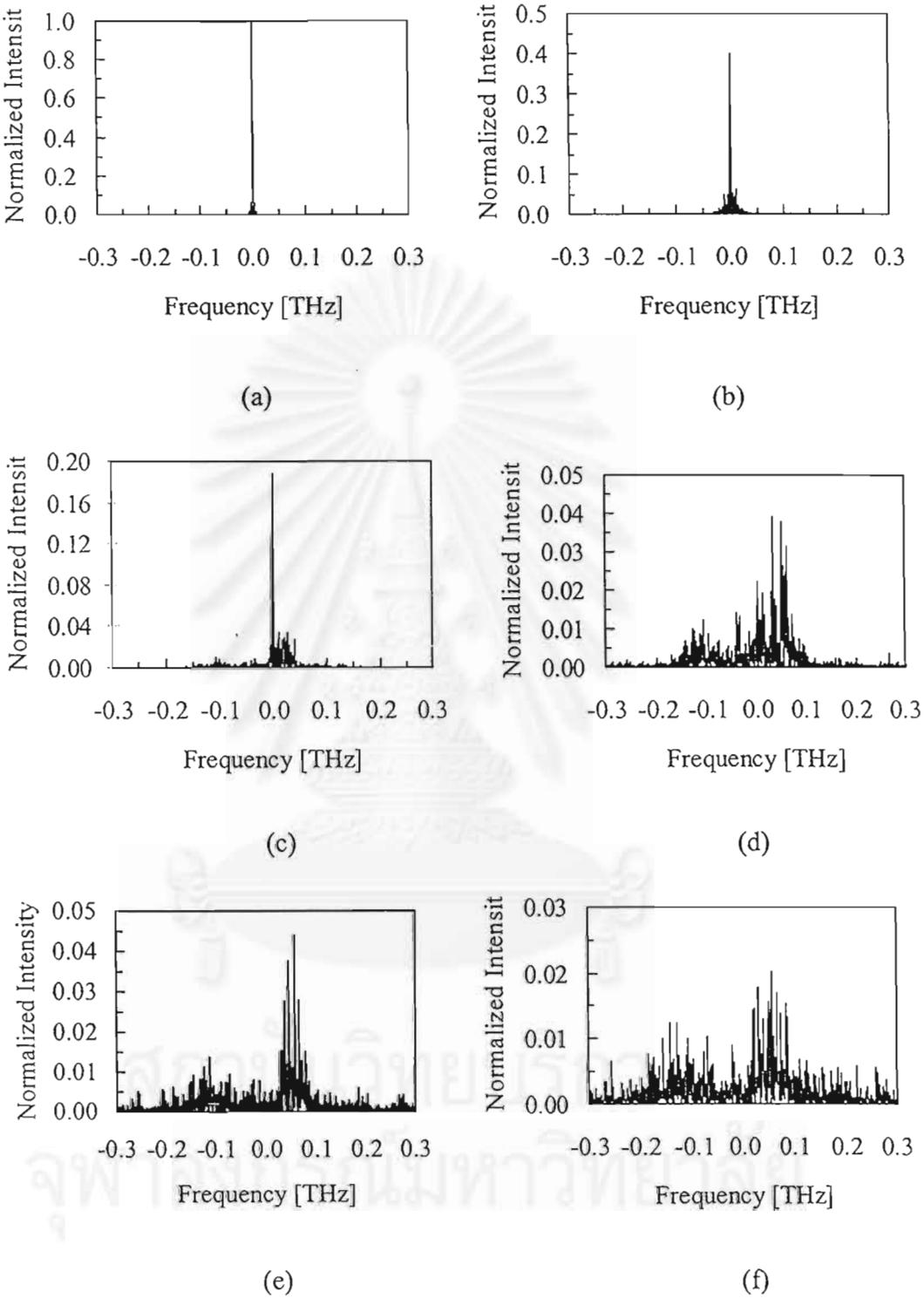

Figure 3.24: Optical spectrum at several distances according to Fig. 3.22, (a) initial pulse, (b) 1,000 km, (c) 2,000 km, (d) 3,000 km, (e) 4,000 km, (f) 5,000 km.

The spectrums of the signal shown in Fig. 3.24 appear in broadened structures. However, the spectrum here seems to have a slower rate of broadening and the most intense peak still situates near the center of a spectrum bandwidth. Furthermore, the spectrum in Fig. 3.24 (f) exhibits two-peak structure. This may be resulted from the TOD. However, the main degradation of system performance, as one would expect, still arises from the degradation of SNR ratio resulted from large amount of noise which enters a receiver through wide bandwidth optical filter used for maintaining the signal power.

For conclusion, even though the distortion of the signal and the spreading out of its spectrum are induced to occur by the nonlinear interplay, it is not difficult to understand that the pulses may still be recognized in the time domain. In region where there is no signal there is also no interaction, so that in a spatial and temporal description there is no nonlinear interaction at the position of a logical ZERO. The interaction deforming the logical ONEs travels at the same velocity as the pulses, since we operate at the point of zero dispersion. Thus, although the pulses become deformed, they do not lose their identity and can still be recognized. The main degradation of the system performance is due to the fact that the spectrum would have been constrained by the inline-optical filters which cause not only a loss of energy but also additional pulse distortion. However, even though the pulses may still be recoverable if given sufficiently wide filters, the spreading of the spectrum is intolerable since it forces us to admit too much undesirable noise to the receiver, degrading the SNR.

4. PERFORMANCE IMPROVEMENT OF THAILAND-MALAYSIA SUBMARINE FIBER-OPTIC SYSTEM USING OPTIMIZED ZERO-DISPERSION TRANSMISSION

In this chapter, we present simple and practical approaches, together with design schemes for achieving the maximum performance, using the zero-dispersion wavelength (ZDWL) transmission and the optical amplification. To our knowledge, this is the first time that the design guideline for the ZDWL transmission is presented. Following our guidance, the possibility of increasing data rate in the 1,318-km-long Thailand-Malaysia (T-M) submarine system from 560 Mbit/s to 80 Gbit/s is numerically shown.

4.1 Design for Achieving Maximum Performance in ZDWL Transmission

The advantage of the ZDWL system to other types of systems mainly originates from its simplicity of system configuration. By only placing the carrier wavelength at zero-dispersion wavelength of optical fiber, the limitation of the system performance due to the fiber second-order dispersion (SOD) is easily overcome. However, for long-haul high-speed transmission, strong Kerr effect, as well as the third-order dispersion (TOD) at ZDWL cause serious problems to the signal transmission, resulting in poorer performance compared to other non-zero-SOD systems. Nevertheless, we present here that the ZDWL transmission using optical amplifiers with optimum design is very simple and very cost-performance scheme for sufficiently increasing the data rate of the installed fiber systems.

In order to break through the electronic bottle-neck, the first step of upgrading is to replace the electronic repeaters with the optical amplifiers. Then, the second step is to find the optimum input signal power and the optimum bandwidth of an optical bandpass filter (OBPF) which gives the maximum performance of the system. The increase in input signal power improves the SNR at a receiver, at the same time, results in the system penalty due to the Kerr effect. The optimum power will exist at the balance point of these improvement and degradation. On the other hand, since the self-phase modulation (SPM) via the Kerr effect causes rapid spectrum broadening at ZDWL, the maximum system

performance will be reached when we use the OBPF with an appropriate bandwidth that collects all signal spectra with the least amount of noise.

For overcoming the signal distortion induced from the TOD, the third step is to calculate the TOD length (L_{d3}) and the nonlinear length of the system (L_{nl}), which are defined in [4]. These characteristic lengths can be interpreted as the distance where those effects become significant. When L_{d3} is longer than system length, no TOD compensator is needed. On the other hand, if L_{d3} is shorter than the system length, we have to install the TOD compensators periodically at the length shorter than L_{nl} to avoid the interplay between the TOD and the Kerr effect. To further increase the data rate, the span should be shortened in order to obtain good SNR with the use of low input signal power. Then, the Kerr effect is consequently reduced.

4.2 Computer Simulations

To demonstrate the efficiency of our proposed upgrading scheme, we consider the T-M submarine system as the simulation model. The system starts from Petchburi, Thailand, ends at Chugai, Malaysia, with total length of 1,318 km. The fiber is the DSF. The electronic repeaters are periodically placed at a span of 100 km with the last span of 118 km. The system operates with single channel with the data rate of only 560 Mbit/s.

In the simulations, the optical signal is composed of a 32-bit pseudorandom RZ Gaussian pulse train with a duty cycle of 0.5. The fiber loss coefficient, the TOD, and the fiber nonlinear coefficient of dispersion-shifted fiber (DSF), respectively, are typical values of 0.2 dB, 0.06 ps/km/nm, and 2.6 $W^{-1}km^{-1}$. The SOD is assumed to randomly fluctuate around ZDWL point every 2 km with a varience of 0.5 ps/km/nm. The optical amplifier produces ASE noise in process of amplification with a noise figure of 5.3 dB. At the end of system, the bandwidth adjustable OBPF is placed. The TOD compensator is an ideal device that multiplies the signal with negative amount of linearly accumulated phase shift caused by TOD.

The propagation of the optical pulse is calculated by solving the nonlinear Schrodinger equation by the split-step Fourier method (SSFM) [4]. The

integration step size of SSFM is always chosen at the value that gives a step size error less than 0.01 %. The receiver is modeled by a sixth-order Bessel-Thompson low-pass filter, followed by a bit-error rate (BER) detector. The system performance is evaluated in terms of the numerical BER. The bandwidth of the OBPF is always adjusted to obtain the minimum BER. To calculate the numerical BER of the detected signal, the simulation is repeated 128 times. The numerical Q factor of every bit is then individually calculated at the maximum eye-opening point of the bit period. Based on the assumption of the Gaussian noise distribution, the numerical BER is computed from the bit numerical Q factor and is averaged over the entire bits.

A. 40-Gbit/s Data Transmission

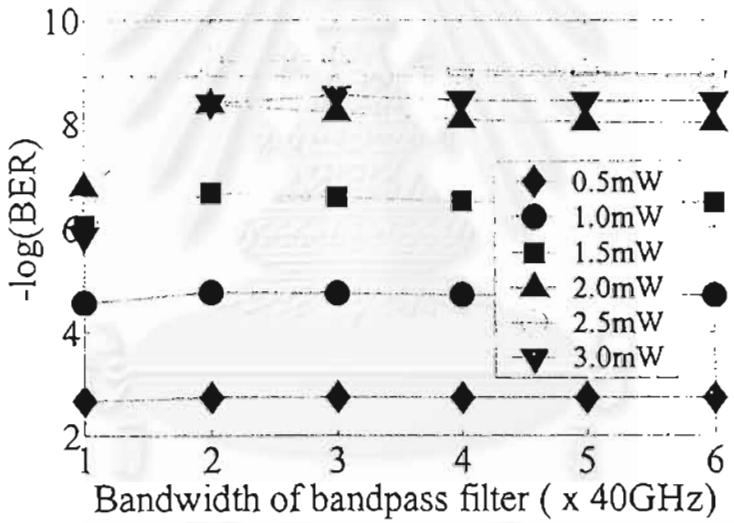

Figure 4.1: Numerical BER of the transmitted 40-Gbit/s signal as a function of OBPF bandwidth for several input signal powers.

We start the simulation with the data rate of 40 Gbit/s, which is the bottle-neck speed of the electronic repeaters. Figure 4.1 shows the numerical BER of the transmitted 40-Gbit/s signal as a function of OBPF bandwidth for several input signal powers. The minimum BER is obtained with the optimum power of 2.5 mW (shown by spaced circles) and the OBPF bandwidth of 80 GHz. In Figure 28, the BER are obtained without using TOD compensator. With defining BER = 10^{-}

[9], which is commonly used for the limitation in lightwave systems, as the system limitation, the T-M system can be upgraded for 40-Gbit/s data transmission by only using ZDWL and replacing electronic repeaters with optical amplifiers.

Figure 4.2 (b) shows the 40-Gbit/s signal using the input power of 2.5 mW and the bandwidth of the OBPF of 80 GHz, compared with its input waveform shown in Fig. 4.2 (a). The signal which is composed of a 32-bit pseudorandom RZ Gaussian pulse train with a full-width at the half maximum (FWHM) of 12.5 ps (duty cycle = 0.5). From Fig. 4.2, sufficiently good output signal waveform is observed.

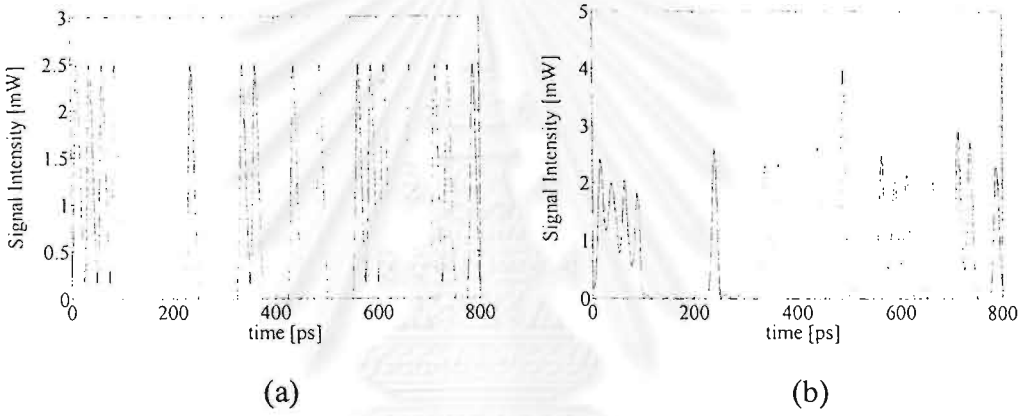

Figure 4.2: (b) Output waveform of this 40-Gbit/s signal using the input power of 2.5 mW and the bandwidth of the OBPF of 80 GHz, compared with (a) its input waveform. The signal is composed of a 32-bit pseudorandom RZ Gaussian pulse train with a full-width at the half maximum (FWHM) of 12.5 ps (duty cycle = 0.5).

For this 40 Gbit/s data transmission, the employment of TOD compensator may not give significant improvement of the BER since L_{d3} (=,4,430 km) is much longer than the system length. Therefore, in this case, the TOD still does not appear to affect the signal propagation. Figure 30 shows the BER of the transmitted 40-Gbit/s signal with the input power of 2.5 mW, as a function of OBPF bandwidth when the TOD compensators are used in several schemes, compared with the SNR-limited BER (shown by spaced circles), the BER where the TOD is neglected (shown by squares), and the BER without the TOD

compensation (shown by reversed triangles). It should be noted that the SNR-limited BER is calculated by neglecting the nonlinear coefficient of the DSF and performing the TOD compensation at the end of the system. As predicted, the use of 13 TOD compensators placed periodically at the output of every amplifier (shown by diamonds) or the use of only one TOD compensator at the end of the system (shown by triangles) can only slightly improve BER. This result mentions that the TOD compensation is still not necessary at this speed of data transmission.

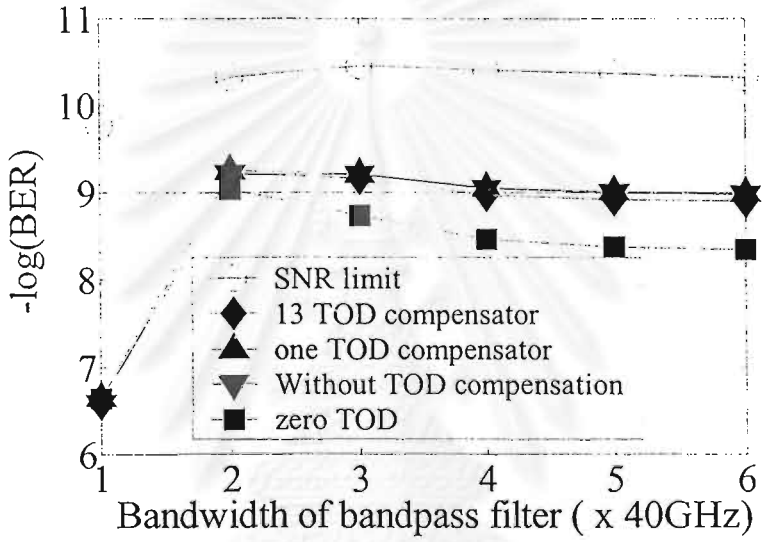

Figure 4.3: BER of the transmitted 40-Gbit/s signal with the input power of 2.5 mW, as a function of OBPF bandwidth when the TOD compensators are used in several schemes, compared with the SNR-limited BER, the BER where the TOD is neglected, and the BER without TOD compensation.

When the TOD is completely neglected (shown by squares), the BER becomes the worst because the TOD intrinsically causes the decrease of optical signal peak power and the asymmetrical broadening of optical signal pulse, therefore, the existence of TOD along the transmission can help reducing the nonlinear waveform distortion caused by the Kerr effect which is very strong in the zero-dispersion wavelength transmission scheme. Also, the difference in BER between the SNR-limited BER and the TOD-compensated BER originates from the signal waveform distortion induced by the Kerr effect.

B. 80-Gbit/s Data Ttransmission

To explore whether the system is capable for higher transmission rate, we perform the computer simulation based on the signal with a data rate of 80 Gbit/s. Figure 4.4 shows the numerical BER of the 80-Gbit/s signal after transmission, as a function of OBPF bandwidth for several input signal powers. The BER less than 10^{-9} cannot be obtained for all input powers and all OBPF bandwidth values. This is due to large amount of noise is generated through the very high amplifier gain in order to compensate the fiber loss in relatively long amplifier spacing (100 km). The noise will be strongly enhanced by the Kerr effect induced the conversion of amplitude noise components to phase noise components along the transmission in ZDWL [2]-[4]. This results in rapid signal spectral broadening and consequently brings large amount of noise entering the receiver.

In order to achieve the BER less than 10^{-9} for the transmission of this data rate, the first strategy is to reduce the amplifier span to 50 km with last span of 68 km. This will require the use of the optical amplifiers double in number. Figure 4.5 shows the results of the 80-Gbit/s data transmission using the 50-km span for several input signal power as a function of the bandwidth of the OBPF. From Fig. 4.5, the optimum power is 1 mW and the optimum OBPF bandwidth is 80 GHz. It should be noted that the optimum power of this data rate is lower than that of the data rate of 40 Gbit/s because the improvement in the SNR due to the use of shorter span. However we cannot achieve BER < 10^{-9} with these optimum parameters. This is mainly resulted from the TOD because L_{d3} (= 554 km) becomes shorter than the system length.

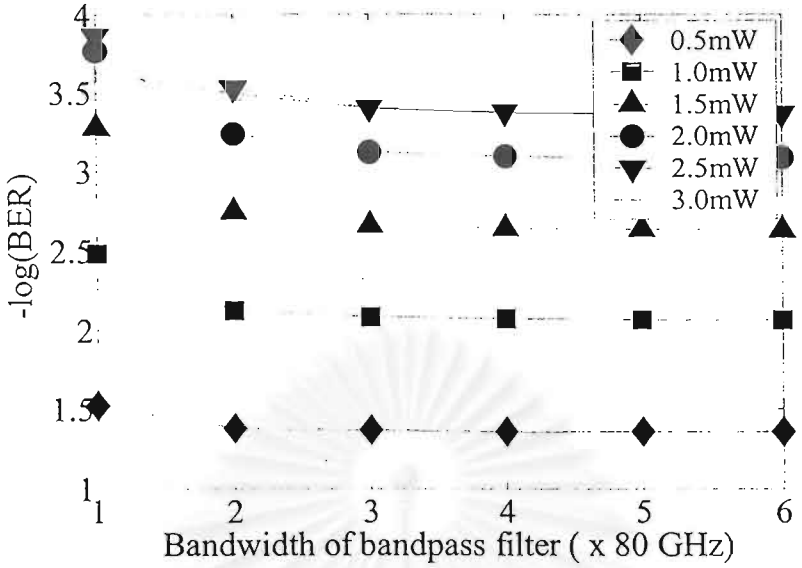

Figure 4.4: Numerical BER of the 80-Gbit/s signal after transmission, as a function of OBPF bandwidth for several input signal powers.

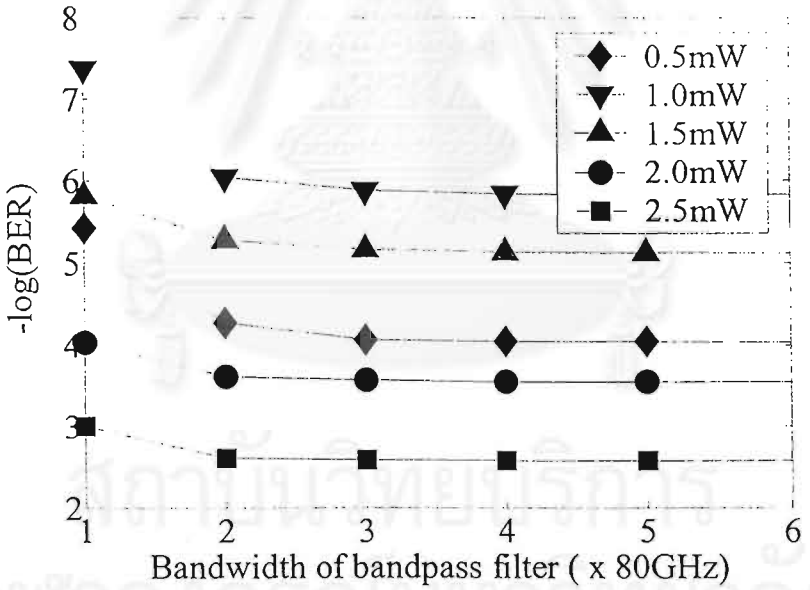

Figure 4.5: Numerical BER of the 80-Gbit/s signal after transmission with the amplifier span is reduced to 50 km, as a function of OBPF bandwidth for several input signal powers.

In order to improve the BER characteristic of the data transmission at bit rate of 80 Gbit/s, we investigate the transmission performance of the system when the TOD is compensated. Figure 4.5 shows the BER of the transmitted 80-Gbit/s

signal with the input power of 1.0 mW and the span of 50 km as a function of OBPF bandwidth when the TOD compensators are used in several schemes, compared with the SNR-limited BER (shown by reversed triangles), the BER where the TOD is neglected (shown by circles), and the BER without the TOD compensation (shown by diamonds).

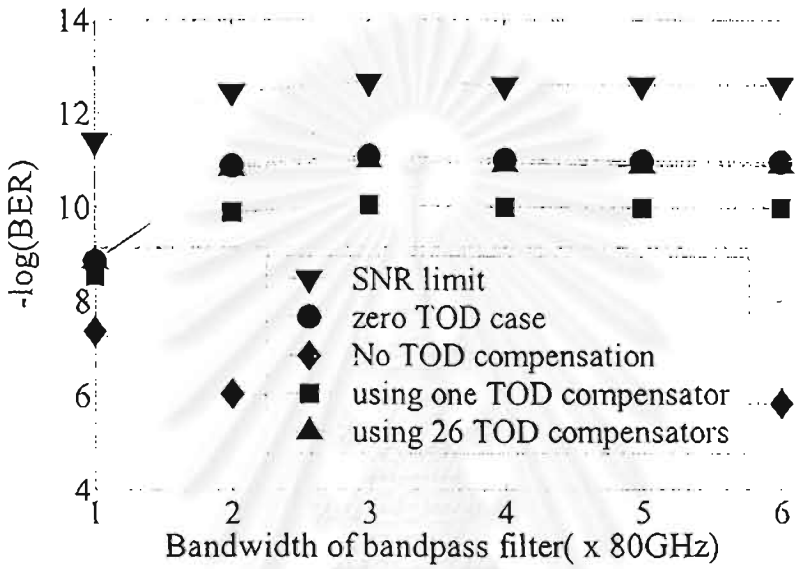

Figure 4.6: BER of the transmitted 80-Gbit/s signal with the input power of 1.0 mW and the amplifier span of 50 km, as a function of OBPF bandwidth when the TOD compensators are used in several schemes, compared with the SNR-limited BER, the BER where the TOD is neglected, and the BER without TOD compensation.

From the results in Fig. 4.6, the use of only one TOD compensator placed at the end of system (shown by squares) can significantly improve the BER to be lower than 10^{-9}. The minimum BER for this case obtained by setting the bandwidth of the OBPF at 240 GHz. Since L_{nl} for the 1-mW input power is 980 km, the placement of TOD compensators at the output end of each amplifier (shown by triangles) yields better BER because the accumulated the TOD is reset before turning to interplay with the Kerr effect. However, when the use of only one TOD compensator gives the BER less than 10^{-9}, we should use only one TOD

compensator in order to help reducing the system cost. The output of the signal with the data rate of 80 Gbit/s using the input power of 1 mW, the bandwidth of OBPF of 240 GHz, the 50-km amplifier span with one TOD compensator placed at the end of system is shown in Fig. 4.7.

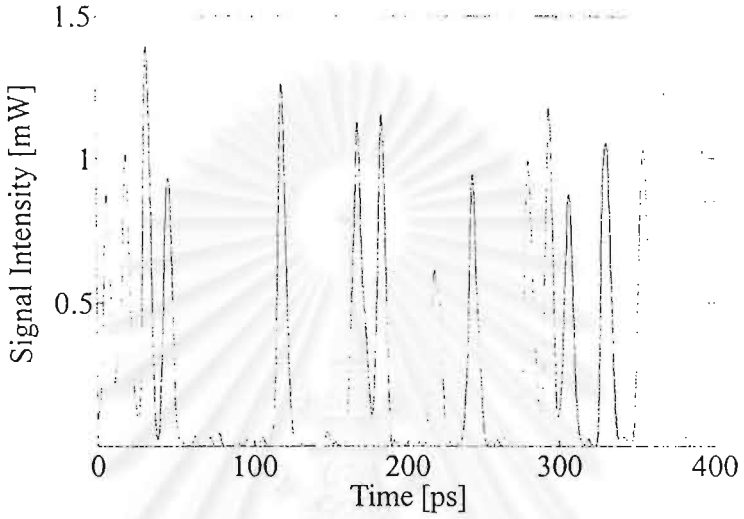

Figure 4.7: Output of the signal with data rate of 80 Gbit/s using the input power of 1 mW, the bandwidth of OBPF of 240 GHz, the 50-km amplifier span with one TOD compensator placed at the end of system.

C. 100-Gbit/s Data Transmission

We further investigate for the possibility of the transmission at higher data rate of 100 Gbit/s. Figure 4.8 shows the BER of the 100-Gbit/s signal at the output of the system where the amplifier is chosen at 50 km, and the TOD is not compensated. The BER is shown as a function of the bandwidth of OBPF with several input signal powers. The optimum input signal power, found from Fig. 4.8, is 1.0 mW. However, we cannot reach the BER below 10^{-9} with this input power.

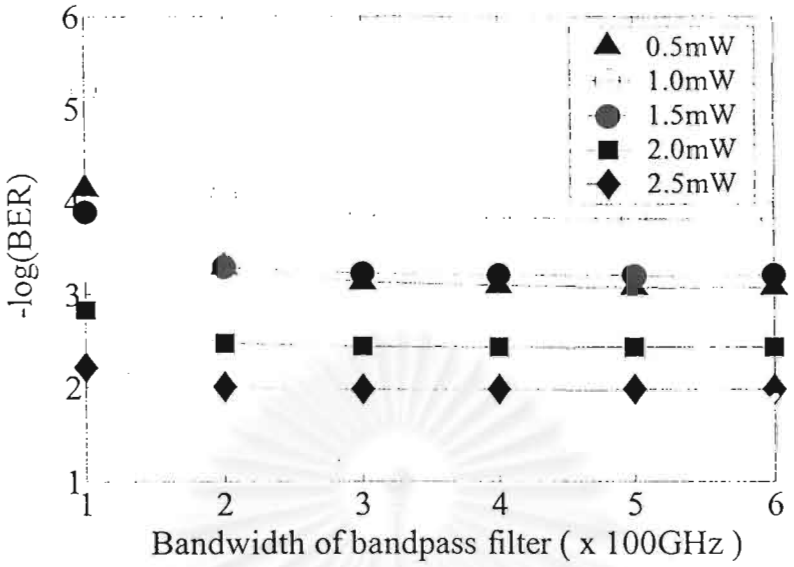

Figure 4.8: BER of the 100-Gbit/s signal at the output of the system as a function of the bandwidth of OBPF with several input signal powers. The amplifier is 50 km, and the TOD is not compensated.

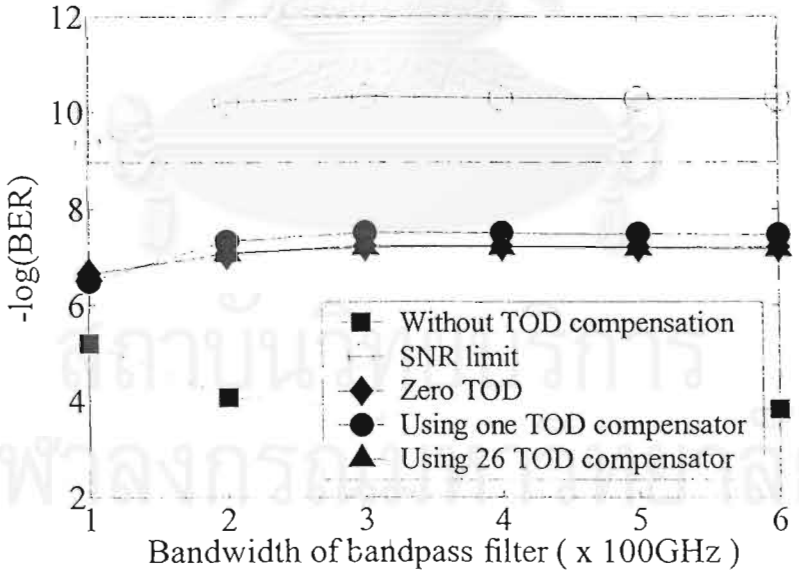

Figure 4.9: BER of the 100-Gbit/s signal using the optimum power of 1.0 mW, the TOD compensation in several schemes, and the span of 50 km as a function of OBPF bandwidth.

Next, we employ the TOD compensators to the system. Figure 4.9 shows the BER of the 100-Gbit/s signal using the optimum power of 1.0 mW, the TOD compensators, and the span of 50 km as a function of OBPF bandwidth. In Fig. 4.9, although the TOD compensators are employed, the minimum BER we achieved is about 10^{-7}, which is not a sufficient value for the optical data transmission we expected. The main problem that causes limitation on this ultra-high bit rate transmission is the degradation from the Kerr effect. To achieve such ultra-high bit rate transmission as well as to further increase in the bit rate of this system, some strategies for reducing the Kerr effect such as the dispersion management concept [5] should be employed.

5. DISPERSION MANAGEMENT: TRANSMISSION OF SIGNAL AT ZERO-DISPERSION ON AVERAGE AND PERFORMANCE IMPROVEMENT OF THAILAND-MALAYSIA SYSTEM USING OPTIMUM-DESIGNED DISPERSION-MANAGED TRANSMISSION

As discussed above, fiber systems whose operation wavelength is located directly at the zero dispersion wavelength (ZDWL) point encounter problems mainly induced by the nonlinearity of optical fibers. Since the second-order dispersion (SOD) length defined in [4] becomes infinity and no longer is compared to the nonlinear length at ZDWL point, the nonlinearity becomes stronger and pays important role in limiting the system performance. In order to avoid the nonlinear problems, a very slight displacement of a carrier wavelength from the ZDWL may be one way to alleviate the problems.

Furthermore, the more sufficient method is to arrange the various sections of fiber in such a way that none or only very few of them have ZDWL that coincide with the carrier wavelength while the total fiber exhibits zero dispersion on average. A method for construction a fiber system which consists of fiber sections that are arranged such that the dispersion of each amplifiers span is zero at the operation wavelength are generally called the dispersion management.

In this chapter, we numerically investigate the effectiveness of the optical amplification and the dispersion management in upgrading the electronic-repeated 1,318-long Thailand-Malaysia (T-M) system. By designing systems to work at optimum conditions, the possibility of increasing data rate in single-channel from 560 Mbit/s to 80 Gbit/s without reducing the amplifier span, or to 100 Gbit/s with reducing the span to be a half, and in wavelength division multiplexing (WDM) scheme to 6x10 Gbit/s, are demonstrated by computer simulations. This chapter is organized as follows. In section 5.1, we demonstrate that the dispersion management has several advantages in reducing the signal distortion induced from the Kerr effect, which has been shown to be very severe around ZDWL. Section 5.2 discusses about the optimum design rules for the dispersion management method including the concept of the transfer function analysis. In section 5.3, the

performance improvement results of employing the dispersion management to the T-M system are shown. In section 5.4, we further extend the dispersion management to the wavelength division multiplexed system. The numerical results for upgrading the T-M system with the use of dispersion-managed WDM are also shown in this section.

5.1 Dispersion Management: Transmission of Signal at Zero-Dispersion on Average

The idea of dispersion management comes from the completely cancellation of the frequency chirp resulting in the recovery of the pulse shape. If we consider the fiber section consisting of two pieces of fibers with the same value of SOD but different symbols (+ and -) shown in Fig. 2.10. This section of fiber exhibits the zero dispersion on average. An optical pulse launched to this fiber will be frequency-chirped induced by the SOD. The pulse will be broadened due to the SOD-induced pulse broadening. However, when the pulse is entered to the fiber which exhibits the opposite SOD symbol, the frequency chirp occurs in the opposite direction so that it will cancel the chirp induced by the first fiber resulting in pulse compression.

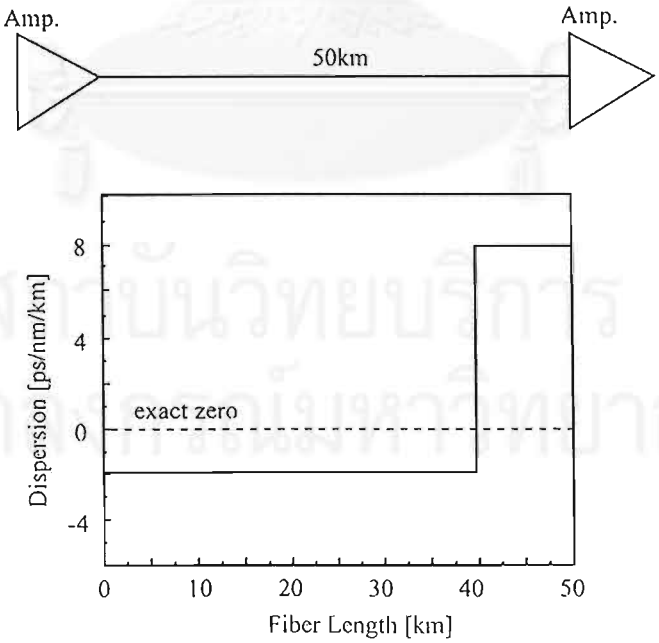

Figure 5.1: Dispersion management pattern.

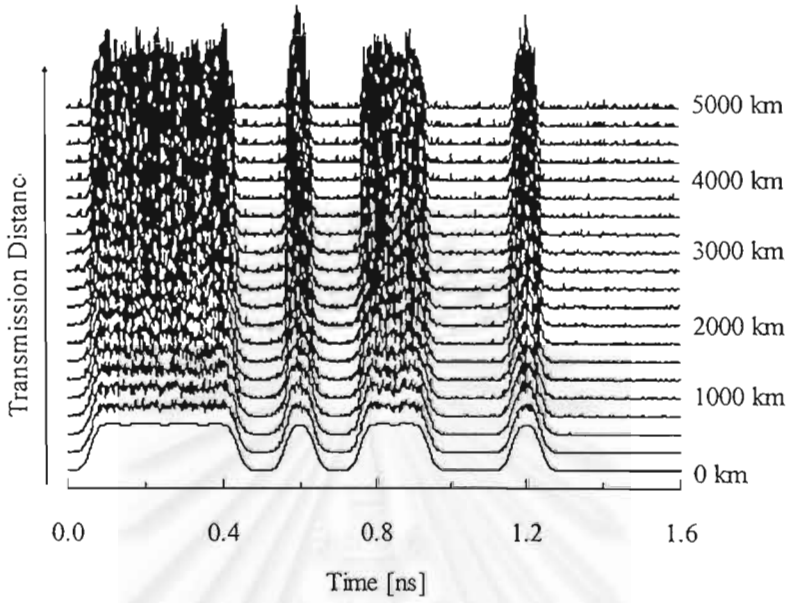

(a)

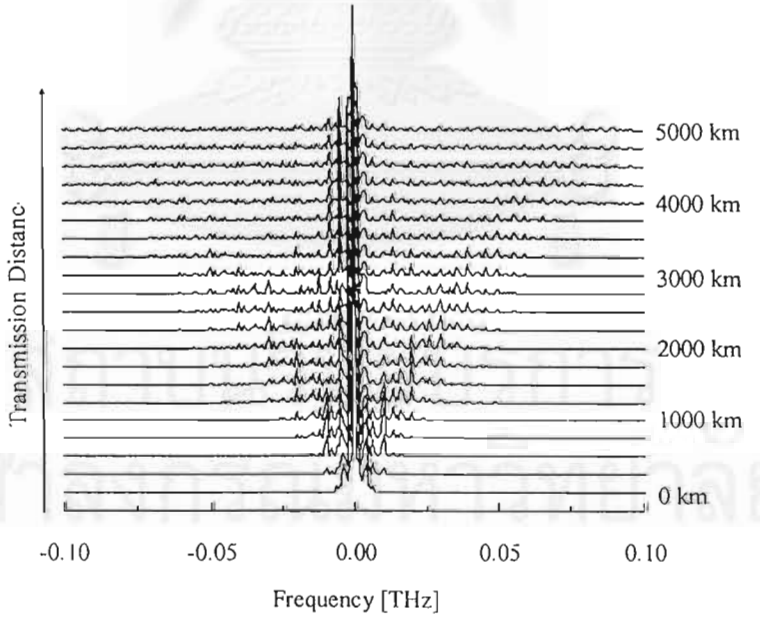

(b)

Figure 5.2: 16-bit NRZ signal and its spectrum evolution in the dispersion management system, (a) signal evolution, (b) spectral evolution.

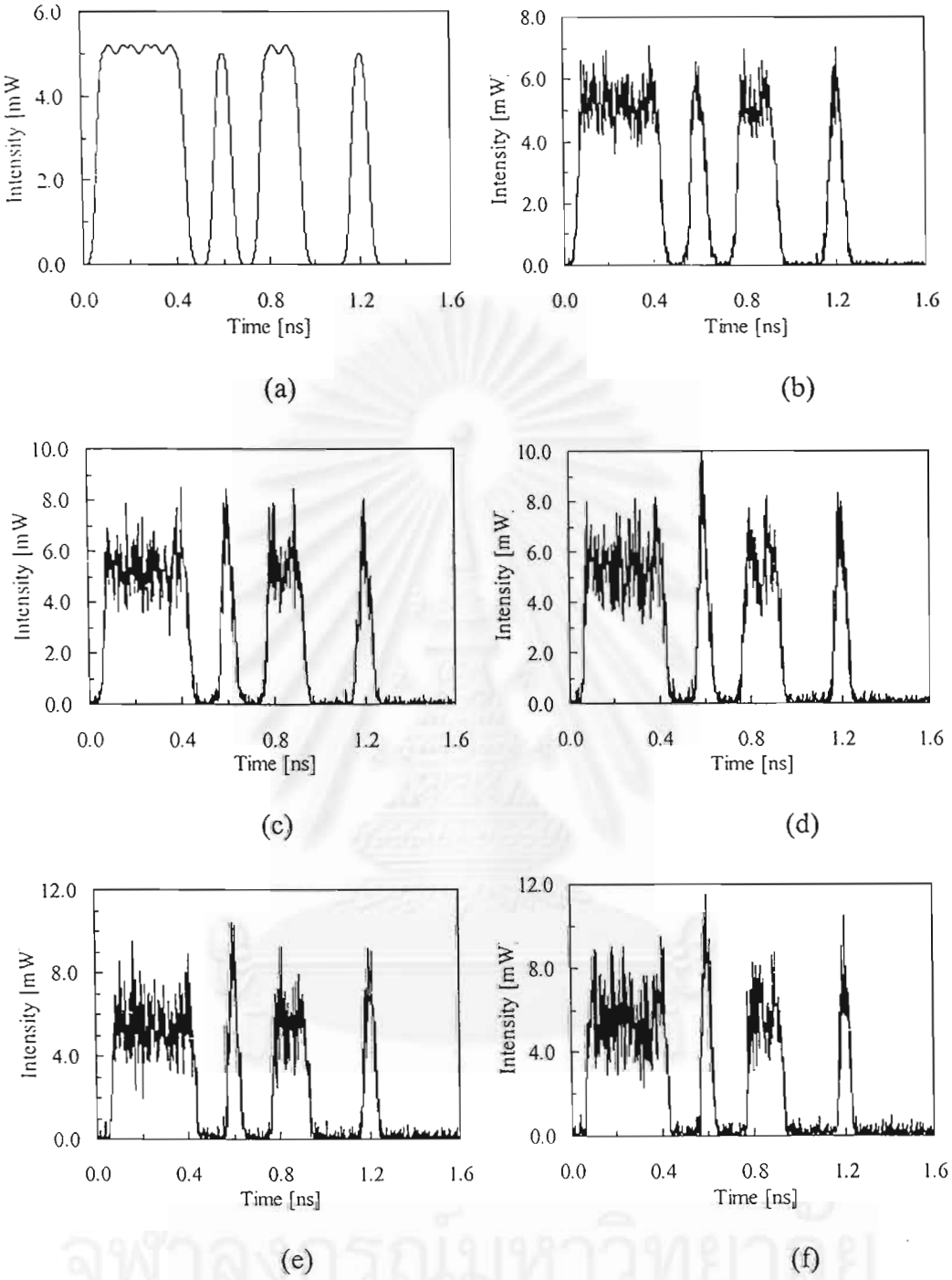

Figure 5.3: Optical signal shape at several distances according to Fig. 5.2, (a) initial pulse, (b) 1,000 km, (c) 2,000 km, (d) 3,000 km, (e) 4,000 km, (f) 5,000 km.

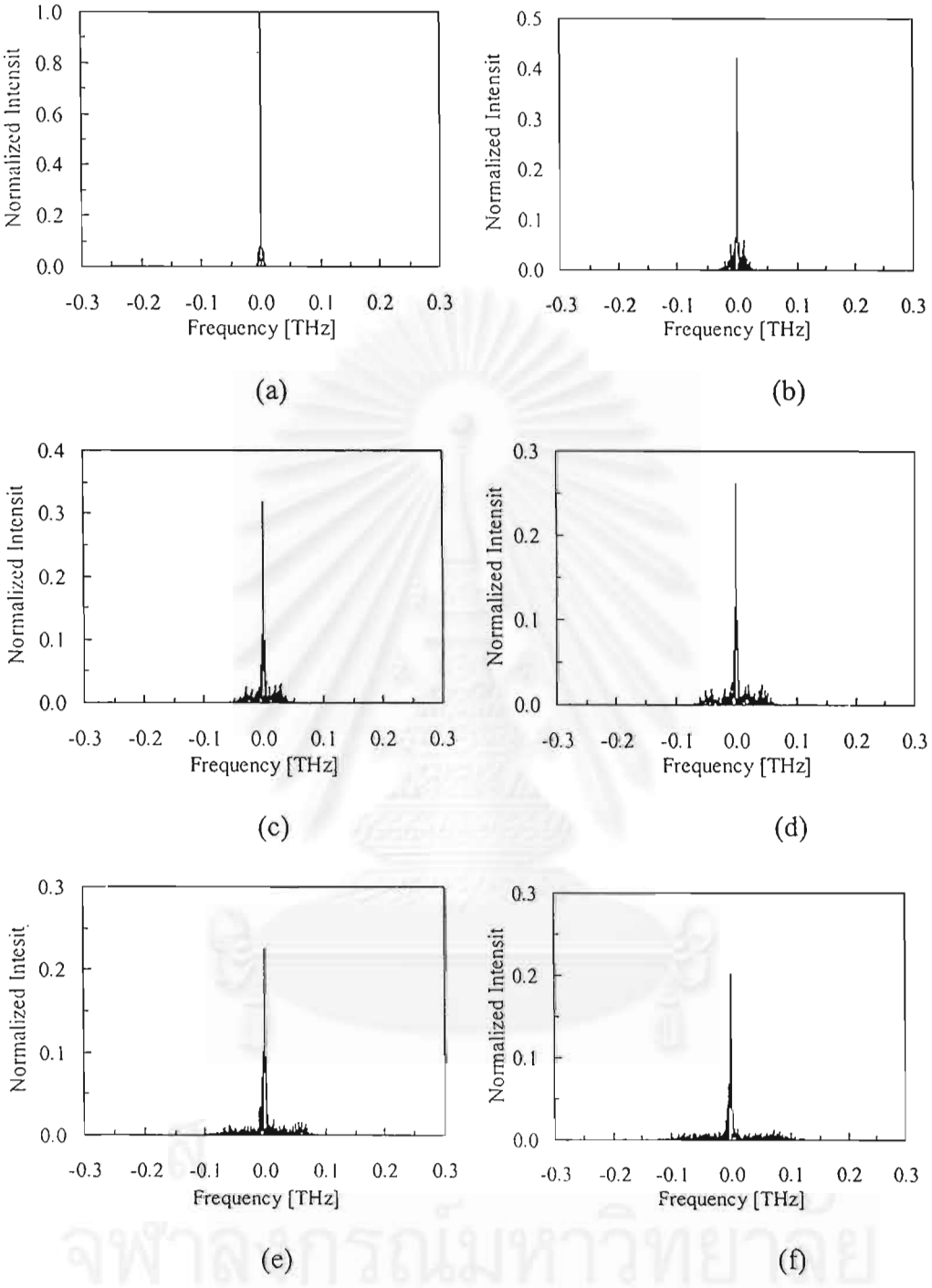

Figure 5.4: Optical spectrum at several distances according to Fig. 5.2, (a) initial spectrum, (b) 1,000 km, (c) 2,000 km, (d) 3,000 km, (e) 4,000 km, (f) 5,000 km.

To show the characteristics of pulse propagation in dispersion management systems and to compare to the exact-zero dispersion systems, we perform a numerical simulation based on a SOD distribution in each amplifier span as shown in Fig. 5.1. This can be realized by connecting the short piece of fiber which exhibits large value of anomalous dispersion to the longer fiber which exhibit normal dispersion in such a way that the total average SOD becomes zero. The shorter fiber is commonly called dispersion-compensated fiber (DCF). It should be noted that the first fiber is required to exhibit the normal dispersion since the power of the pulse is still intense so that if we use the anomalous dispersion fiber the nonlinear interaction between noise and signal will give rise to pulse distortion since the system is operating in modulation instability state. Therefore, it is favorable to use the normal dispersion region of the fiber.

The parameters set up for the simulation in this section are shown as follows. The signal is the 16-bit NRZ super Gaussian pulse train with data rate of 10 Gbit/s (1-bit time slot = 100 ps). The input power is 5 mW. Other parameters used for simulations are the same as used above. The optical bandpass filter is not applied. Figure 5.2 shows the results of the simulation by signal evolution and its spectrum evolution. The pulse shape and its spectrum at distance 0km (initial), 1000 km, 2000 km, 3000 km, 4000 km, and 5000 km are shown in Fig. 5.3 and Fig. 5.4, respectively.

As expected, the spectrum is narrower than the spectrum of exact-zero dispersion case. The increase of noise in signal evolution in Fig. 5.2 and signal waveform in Fig. 5.3 shows the linear accumulation and no pulse broadening is observed. The slight pulse compressing and the increase in peak of single pulse may be resulted from the incomplete cancellation of frequency chirping caused by nonlinear chirping.

Next, we simulate again by including the nonlinearity but ignoring the ASE noise. The signal waveform and its spectrum after 5000 km are shown in Fig. 5.5 (a) and (b). The pulse compression and increase in peak of single pulse are observed. This is clearly proved that the compression of pulse resulted from the incomplete compensation of frequency chirping. The optical spectrum in Fig. 5.5 (b) is almost the same as that of Fig. 5.4 (f) showing that the spectrum

broadening is mainly caused by the nonlinearity such as the SPM or the FWM rather than the nonlinear interaction between ASE noise and signal.

The SPM itself plays dominant role in spectrum broadening. The FWM may be the consequent effect of SPM occurs when the spectrum is broad enough to create the component which can satisfy the conditions of FWM. However, when the dispersion exists, the phase mismatch increases with β_2 [4] so that the spectrum spreading caused by FWM is not severe as that of exact-zero dispersion systems.

Since the spectrum of the signal transmitted in the dispersion management system is clearly narrower than that of exact-zero dispersion case, the application of narrower bandwidth optical band-pass filter becomes possible. For example, according to Fig. 5.3 we can use the optical filter whose bandwidth narrower than that of exact-zero dispersion system so that the noise which enters the receiver will decrease resulting in improvement SNR and consequently the BER. In Fig. 5.3, the bandwidth that matches to the spectrum may be 300 GHz so that we simulate the system again with this optical filter with 300-GHz bandwidth. The result, shown in Fig. 5.6 by the signal and its spectrum at the output end 5000-km fiber, confirms the possibility of filtering the signal. According to this result, for long-haul transmission, it is clear that the dispersion management system has greater performance than the exact-zero dispersion systems.

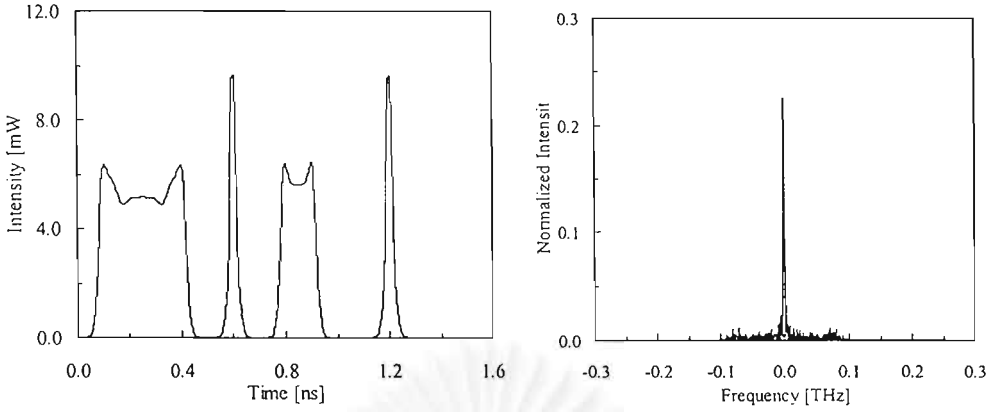

(a) (b)

Figure 5.5: 5000-km transmitted signal and its spectrum shape in the dispersion management system in the absence of ASE noise, (a) signal shape, (b) spectral shape.

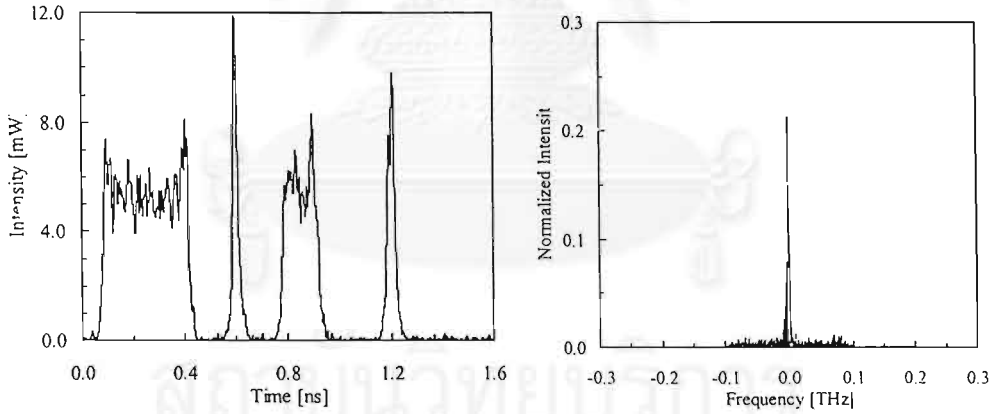

(a) (b)

Figure 5.6: 5000-km transmitted signal and its spectrum shape in dispersion management system with the employment of 300GHz optical band-pass filters, (a) signal shape, (b) spectral shape.

5.2 Design for Achieving Maximum Performance in Dispersion Managed Systems

When the electronic repeaters are replaced with optical amplifiers in long-haul high-speed system, efficient methods for compensating such signal distortion induced from fiber SOD and Kerr effect must be employed. The dispersion management is to arrange the various sections of fiber in such a way that none or only very few of them have ZDWL that coincide with the carrier wavelength while the total fiber exhibits zero SOD on average. Because the SOD exists along the transmission, we can achieve the compensation of the SOD and, at the same time, the reduction of fiber nonlinearity with this method. Not only in single-channel transmission, the dispersion management becomes a necessary method that is widely applied in practical WDM transmission systems. Since the signal distortion in WDM systems mainly causes from the cross-phase modulation (XPM) effect [4] and the four-wave mixing (FWM) effect, both originated by the Kerr effect, the use of dispersion management yields the possibility of increasing the difference in signal group velocity among channels, which consequently reduces these two effects.

The concept of dispersion management is to cancel the accumulated SOD by using negative value of SOD. This can be implemented by using the combination of various fibers or the combination of fibers with several SOD compensating devices.

The transfer function is a powerful method for roughly designing the dispersion management systems. The transfer function can be derived by using the small-signal approximation [28]. In this section, we calculate the transfer function of the T-M system when the dispersion management is employed. The T-M system has total length of 1,318 km. The transmission fiber is DSF. The electronic repeaters are periodically placed at span: L_a of 100 km with the last span of 118 km. The system operates in single channel with the data rate of only 560 Mbit/s.

In the calculation, we assume the typical parameter of DSF. The fiber loss coefficient and the nonlinear coefficient of DSF are 0.2 dB/km and 2.6 $W^{-1}km^{-1}$,

respectively. The SOD: D for transmission is -0.2 ps/km/nm. The DM period: l_d is the same as the amplifier span of 100 km. The dispersion management is done by reseting the accumulated SOD with a SOD compensator that is assumed to be a module installed in the optical amplifier. The path-averaged power within a 100-km amplifier span is 0.7 mW. We calculate the transfer function for only 12 amplifiers (1,200 km) because the last amplifier spacing is 118 km, which is not the period of 100 km.

Figure 5.7 shows the transfer functions for amplitude modulation components: T_a and phase modulation components: T_b, as a function of signal frequency shifted from carrier frequency. The ideal transmission is given by $T_a = 1$ and $T_b = 0$. In Fig. 5.7, T_a reduces to its minimum point below 1 at a specific frequency. We should define that point as the transmission window of the system. This is because the signal frequency exceeding this point cannot transmit without distortion. Within the transmission window, the signal will not suffer severe distortion except the enhancement of the phase noise because $T_b > 1$. For this system setting, the result from Fig. 5.7 indicates the possibility of about 40-Gbit/s data transmission on T-M system when the DM is employed.

The transmission window width obtained from Fig. 5.7 is very important parameter for evaluating the transmission performance of a DM system. Figure 5.8 shows how the window width varies with the changes in l_d and signal power. It should be noted that the minimum signal power required for signal transmission is determined by the SNR limit of the receiver. Figure 5.8 shows that the transmission window width greatly increases with the reduction in l_d, but slightly decreases with the increase in signal power. The use of smaller l_d yields wider window width. However, with very small l_d, the signal feels like propagating without the existance of SOD, therefore, the signal will suffer with high fiber nonlinearity. Thus, for design point of view, we should design the window width as small as the signal bandwidth to achieve the undistorted transmission and, at the same time, reduce the enhancement of phase noise and other signal distortions from fiber nonlinearity.

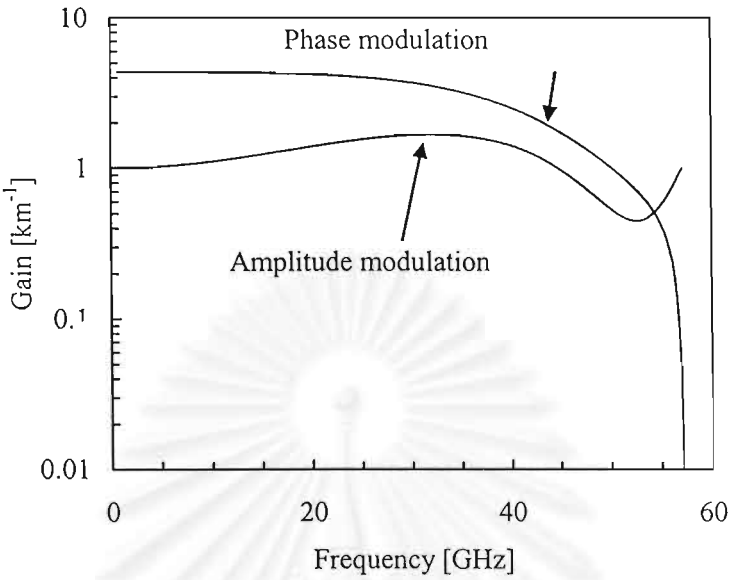

Figure 5.7: Transfer function characteristics of amplitude modulation components and phase modulation components in the T-M system employing dispersion management.

For long-haul, high-speed transmission, relatively low D is also required to increase the window width. This can be achieved by placing the carrier wavelength near ZDWL. In fact, the concept of transfer function does not account for the signal spectral broadening due to FWM and the random fluctuation of D, which turns to interplay with the Kerr effect when the carrier wavelength of the DM system is located near ZDWL. Thus, for detail design of dispersion management system, the optimum combination of three main operating parameters: l_a , D , and the signal power, should be obtained by computer simulations.

Also for computer simulation-based design, the bandwidth of OBPF placed at the end of fiber should be tuned at optimum value. Furthermore, for ultra-high data rate transmission, we have to investigate the necessary of the TOD compensation by calculating the TOD length: L_{d3} and the nonlinear length : L_{nl} [3] of the system. These lengths can be interpreted as the distance where those effects become significant. When L_{d3} is longer than system length, no TOD

compensator is needed. On the other hand, if L_{d3} is shorter than the system length, the TOD compensators have to be installed distributedly at the length shorter than L_{nl} to avoid the interplay between the TOD and the Kerr effect. To further increase the data rate, the span should be shortened in order to obtain good SNR with the use of low input signal power. The Kerr effect is then also reduced.

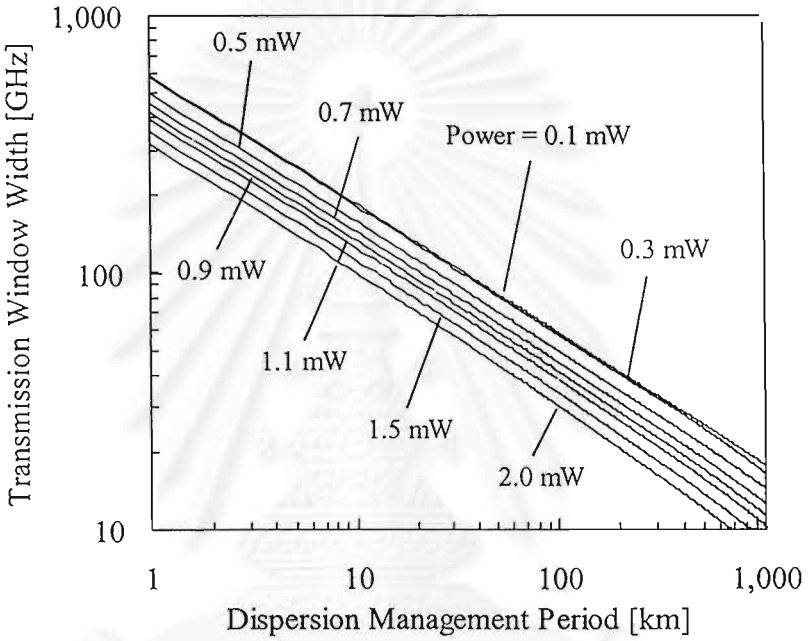

Figure 5.8: Dependence of the transmission window width on the dispersion management period and the path-average signal power of the T-M system employing dispersion management.

5.3 Computer Simulations

To demonstrate the efficiency of the dispersion management in upgrading the T-M system, we perform some of computer simulations. In the simulations, all system parameters are the same as those used for obtaining the transfer function. The optical signal is composed of a 32-bit pseudorandom RZ Gaussian pulse train with a duty cycle of 0.5. The TOD of DSF is assumed to be 0.06 ps/km/nm^2. D is assumed to randomly fluctuate around ZDWL every 2 km with variance of 0.5 ps/km/nm. The optical amplifier produces noise in process of amplification with a noise figure of 5.3 dB. At the end of system, the bandwidth adjustable OBPF is

placed. The bandwidth of the OBPF is always adjusted to obtain the minimum bit-error rate (BER). When the TOD compensation is required, the TOD compensator is an ideal device that multiplies the signal with negative amount of linearly accumulated phase shift caused by TOD. For all calculation, we consider l_d that is only equal or longer than L_a for practical. The propagation of the optical pulse is calculated by solving the nonlinear Schrodinger equation by the split-step Fourier method [4]. The integration step size of SSFM is always chosen at the value that gives a step size error less than 0.01 %. The receiver is modeled by a sixth-order Bessel-Thompson low-pass filter, followed by a BER detector. The system performance is evaluated in terms of the numerical BER. To calculate the numerical BER of the detected signal, the simulation is repeated 128 times for the pseudo-random pulse train. The numerical Q factor of every bit is then individually calculated at the maximum eye-opening point of the bit period. Based on the assumption of the Gaussian noise distribution, the numerical BER is computed from the bit numerical Q factor and is averaged over the entire bits [28]. The system limitation is defined by BER = 10^{-9}.

Figure 5.9 shows the BER of a 40-Gbit/s signal at the end of system, as a function of input signal power for several l_d. D is -0.2 ps/km/nm. L_{d3} for this data rate is about 4,400 km, therefore, the TOD compensation is not necessary. As discussed above, too short l_d will yield the result similar to the uniform D. On the other hand, too long l_d will shorten the transmission window. According to Fig. 5.9, the minimum BER about 10^{-11} is obtained with the optimum l_d of 400 km, and with the optimum input signal power of 4 mW. Excepting for l_d = 1,318 km, we achieve the BER lower than 10^{-9}, for all l_d used in our simulations.

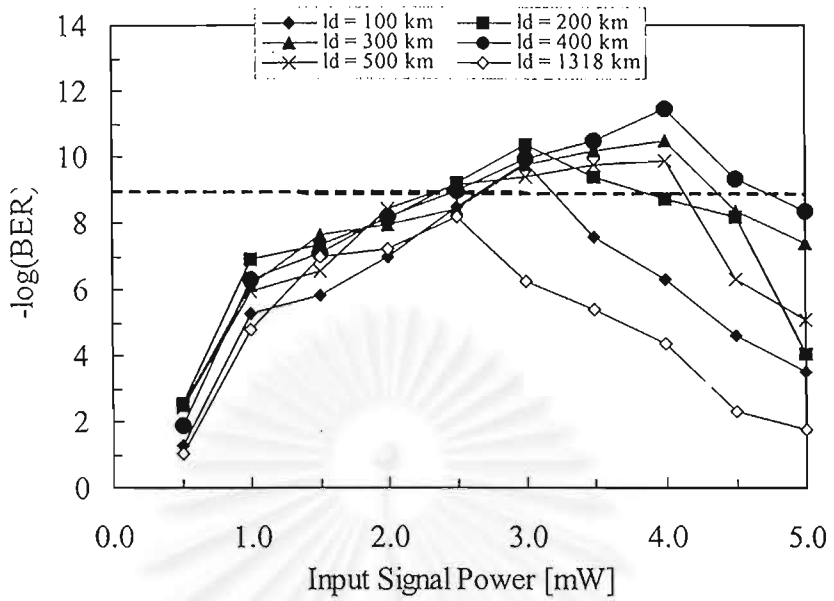

Figure 5.9: Numerical BER of the transmitted 40-Gbit/s signal as a function of input signal power, for several l_d.

For obtaining Fig. 5.9, since D (-0.2 ps/km/nm) is too small comparing to its variance (0.5 ps/km/nm), the increase in the operating SOD value should enhance the system performance. However, the transmission window becomes narrow when too large D is used. Figure 5.10 shows the BER of the 40-Gbit/s signal as a function of input signal power. Each BER curve is obtained at the optimum l_d for each operating D. The best BER is obtained from D = –1 ps/km/nm with the input signal power of 2 mW. On the other hand, the worst BER is resulted from D = –2 ps/km/nm, where we cannot obtain the BER lower than 10^{-9}.

Next we further explore the possibility of a 80-Gbit/s data transmission. For this data rate, the TOD also becomes a problem that causes signal waveform distortion because the TOD length is about 560 km. In fact, the TOD compensator should be periodically placed at the distance shorter than the nonlinear length. However, since the system length is not too long and the TOD length is relatively not too short comparing with the system length, we try to use only one TOD compensator install at the end of system to reduce the system cost. Figure 5.11 shows the BER of the 80-Gbit/s signal as a function of input signal power for

several D. Each BER curve is obtained at l_d = 100 km, which is the optimum value for this data rate. It is obvious that the higher data rate is, the shorter l_d is required for expanding the transmission window. From Fig. 5.11, we achieve the BER lower than 10^{-9} for the range of D from -0.5 to -1.5 ps/km/nm. The lowest BER is obtained by $D = -1$ ps/km/nm with the input signal power of 2 mW.

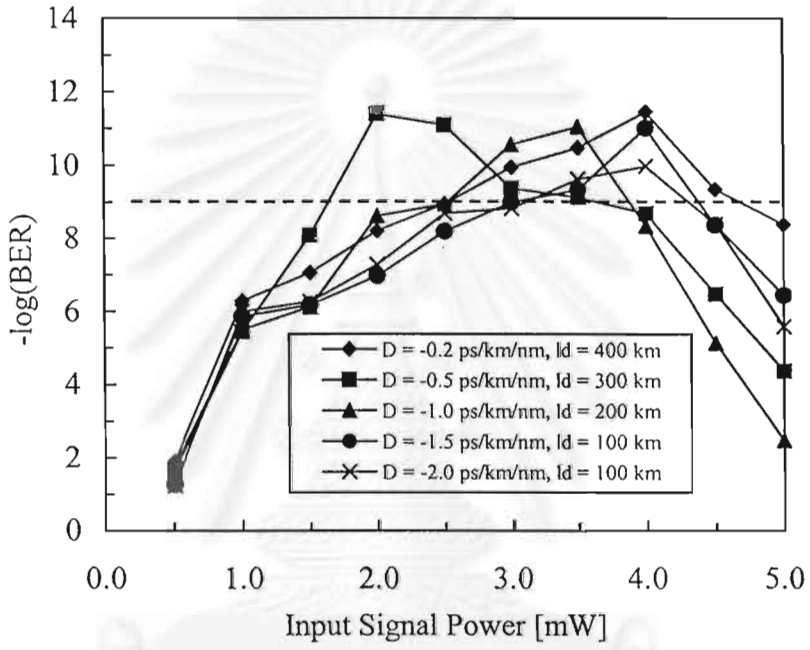

Figure 5.10: Numerical BER of the transmitted 40-Gbit/s signal as a function of input signal power, for several D with their corresponding optimum l_d.

To investigate whether the system is capable for higher transmission rate, we perform computer simulations based on the data rate of 100-Gbit/s. Since the TOD length of this data rate becomes as short as 280 km. This means that the TOD now becomes the significant problems. Moreover, the TOD will cause severe signal distortion through the interaction with the Kerr effect when the signal power becomes intense. Therefore, we perform the TOD compensation periodically at every amplifier span, which is shorter than L_{nl}. However, the BER less than 10^{-9} cannot be obtained for all possible parameters. This is due to large amount of amplifier noise is added to this broadband signal during the

amplification and then high signal power is required for maintaining a good OSNR. The high signal power will cause the nonlinear waveform distortion, and also shortens the transmission window. In order to achieve the BER less than 10^{-9} for this data rate, the first strategy is to reduce the amplifier span to 50 km with last span of 68 km. This is because the amount amplifier noise will reduce. Consequently, relatively low signal power is sufficient for good OSNR.

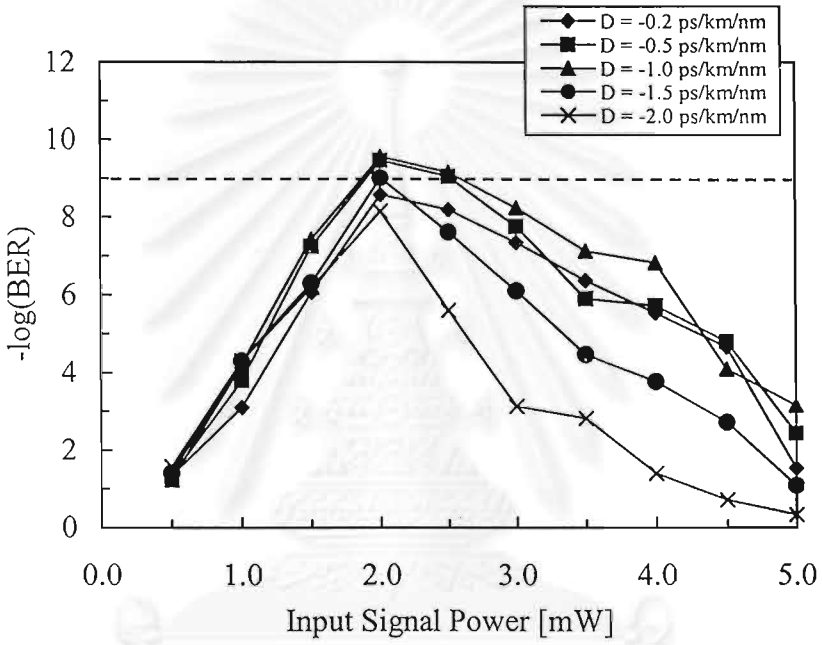

Figure 5.11: Numerical BER of the transmitted 80-Gbit/s signal as a function of input signal power, for several l_d.

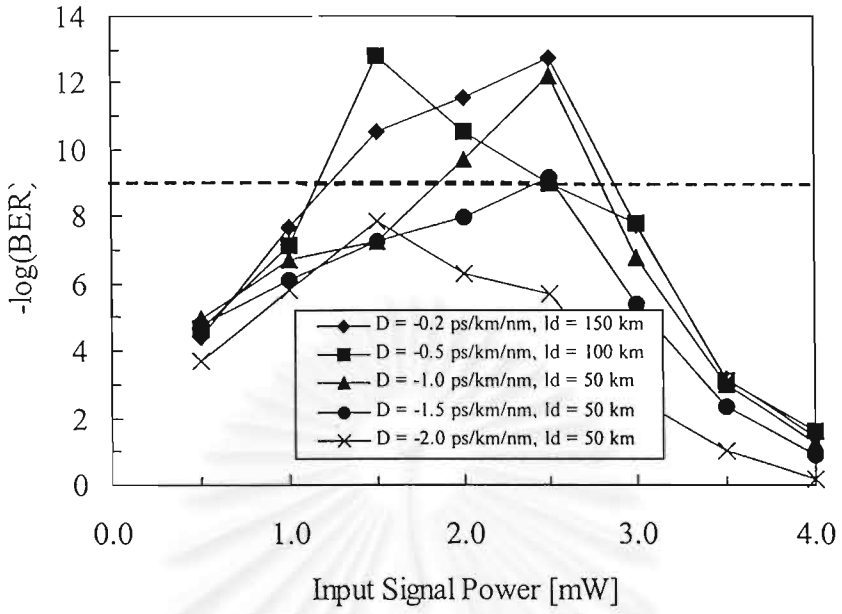

Figure 5.12: Numerical BER of the transmitted 100-Gbit/s signal as a function of input signal power, for several D, obtained by their optimum l_d. The amplifier span is 50 km.

Figure 5.12 shows the BER of the 100-Gbit/s signal as a function of input signal power for several D. Each BER curve is obtained at the optimum l_d indicated in the figure. The calculation results show that the transmission of 100-Gbit/s in T-M system becomes possible by using D = -0.5 ~ -1.5 ps/km/nm. For small D, the results from Fig. 5.9 ~ 5.12 mention that, the use of large l_d results in good BER. On the other hand, for large D, we have to use small l_d. This is because the effect of random D fluctuation, which interplays with the Kerr effect, can be reduced by using large D with sufficiently short l_d or smaller D with sufficiently long l_d.

5.4 Wavelength Division Multiplexing

An alternative way to increase the transmission data rate is the use of WDM scheme. The signal distortion in WDM system mainly originated from the XPM and the FWM. For the XPM, the signal phase in a channel is modulated by the

signal powers from other channels through the Kerr effect, resulting in a type of asymmetrical spectral broadening because signal in different channels travel with different group-velocity. The XPM will cause serious signal distortion when it interplays with dispersion. For the FWM, the signal distortion occurs because the FWM induces the power transfer among channels and power transfer to background noise.

The XPM and FWM can be reduced by increasing the channel spacing. However, if we design the WDM system following the ITU grid (channel spacing = 100 GHz in frequency unit or 0.8 nm in wavelength unit), the alternative way to avoid these two effects is the dispersion management. The use of dispersion management enables us to use relatively large SOD for WDM transmission. The difference in signal group velocity among channels, or the channel walk-off, is then increased. Therefore, it reduces the interaction time among channels, and at the same time, helps decreasing the signal peak power rapidly due to the SOD-induced signal pulse broadening. As a result, the effects of XPM and FWM are reduced. The optimum employment of dispersion management can be done by the optimum placement of center channel far from the ZDWL. An additional benefits should be noted for the shift of center wavelength from the ZDWL is the significant reduction of the gain bandwidth of FWM.

Other parameters to be designed are the optimum input power and the optimum bandwidth of OBPF for selecting each channel at the end of fiber. Noted that the optimum power is obtained at the balance between the improvement of OSNR and the degradation from the Kerr effect.

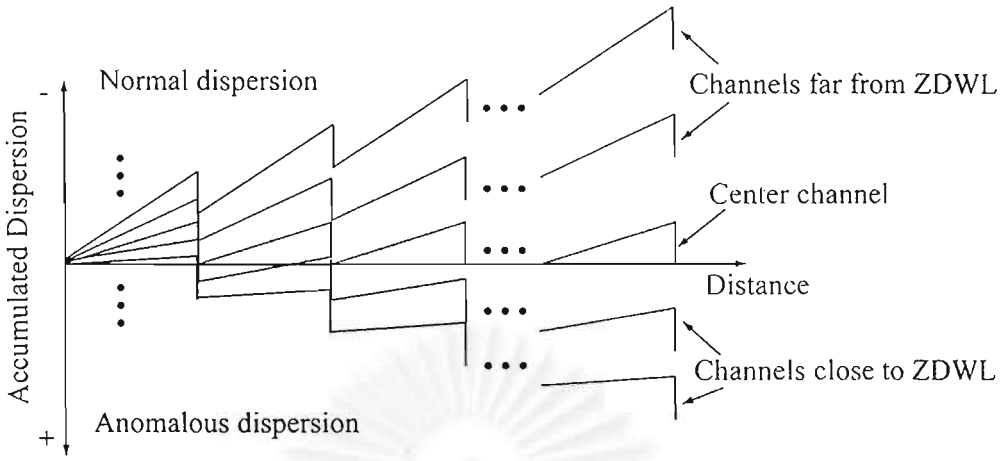

Figure 5.13: Dispersion management in WDM transmission.

In the presence of TOD, each channel experiences different SOD. Therefore, we cannot simultaneously compensate the accumulated SOD of all channels. As shown in Fig. 5.13, the dispersion management scheme is performed in such a way that the center wavelength will only have the perfect compensation, while all other channels around the center channel will have the over compensation or the under compensation depending on their wavelength. At the end of system after filtering the selected channel with OBPF, the amount of under-compensated or over-compensated SOD of that channel will be individually compensated. The amount of SOD D_i, which has to be compensated for channel i can be obtained by

$$D_i = -\frac{4\pi^2 c^2 \beta_3 N L_a}{\lambda_i^2}\left(\frac{1}{\lambda_i} - \frac{1}{\lambda_c}\right), \tag{5-1}$$

where λ_i denotes the wavelength of channel i, λ_c the center wavelength, L_a the amplifier span, N the number of amplifier, and c the velocity of light.

For computer simulations of WDM system, the parameters are the same as those used above. The channel bit rate is 10 Gbit/s. l_d is only set at 100 km, which is the same as L_a. The gain of each optical amplifier is equalized to match the fiber loss for each wavelength, giving flat signal peak power of every channel at the output of the optical amplifier.

Figure 5.14 shows the BER as a function of input signal power for 7-channel WDM case, when all of the channel wavelengths are set at the optimum value. The wavelengths of channel#1, #2, #3, #4, #5, #6, and #7 are 1,352.4, 1,351.6, 1,350.8, 1,350, 1,349.2, 1,348.4, and 1,347.6 nm, respectively. It should be noted the channel#1 is the nearest to ZDWL and the center channel is the channel#5. With defining BER = 10^{-9} as a limitation, the results from Fig. 5.14 indicates that we can achieve the WDM transmission for channel#2 to channel#7 for the input signal power from 0.9 mW to 2.6 mW, while channel#1 give the BER that is larger than 10^{-9} for this range of power.

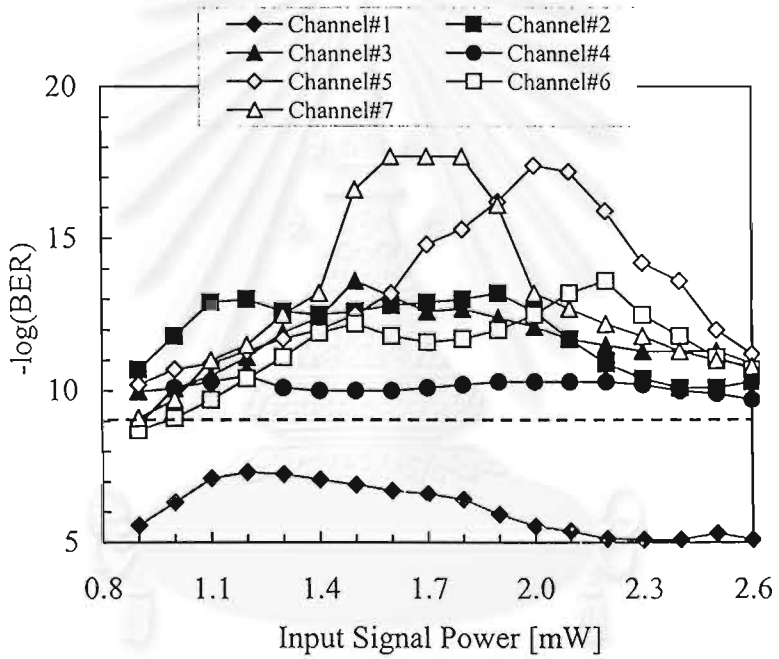

Figure 5.14: Numerical BER of the transmitted 7x10-Gbit/s WDM signal on the T-M system.

Figure 5.15 shows the signal and its spectral waveform of channel#5 with the input signal power of 2.1 mW, obtained at the output end of system. The signal waveform is in a very good shape which the bit "1" and "0" can be obviously distinguished. We also explore for the increase in the number of channel but the simulation results still inform the maximum channel number of 6. To expand to the number of channel, it may be first necessary to reduce the amplifier spacing.

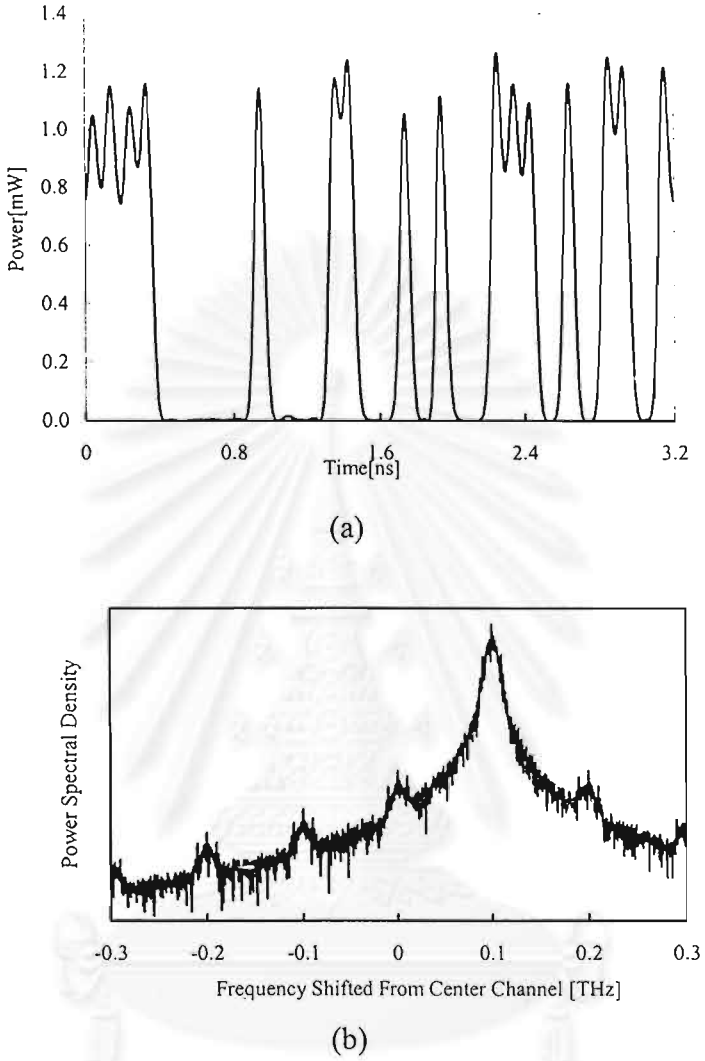

Figure 5.15: Signal and its spectral waveform of channel#5, obtained at the output end of system.

6. OPTICAL SOLITON TRANSMISSION IN UPGRADING THAILAND-MALAYSIA FIBER-OPTIC SYSTEM

Optical soliton is a special pulse that can maintain its shape during the propagation in lossless optical fiber because of the balance between the fiber second-order dispersion (SOD) and nonlinear effect called the self-phase modulation (SPM). The soliton is very suitable for signal transmission in all-optical transmission system, as well as for all-optical signal processing. However, for long-haul fiber link, the fiber loss causes the attenuation of soliton power resulting in the destruction of soliton waveform. Moreover, the collision between adjacent soliton pulse called the soliton interaction [45] also places a limit in both data rate and distance of the transmission system using soliton.

In order to transmit the soliton in long lossy fiber, the lumped optical amplifiers are necessary to be installed periodically to compensate the fiber attenuation. Then, the soliton is amplified in such a way that the average power in the amplifier span is equal to the value required for ideal soliton. This concept is well known as the guiding-centered soliton [42] or the average soliton [43]. The stability of the soliton in this scheme based on the ratio of the characteristic length called the soliton period and the amplifier span, which should be as large as possible [44]. This constraint brings a type of soliton distortion due to the dispersive wave [44] scattering out of soliton when we choose relatively large amplifier span. Moreover, the amplifier noise will cause the random modulation of soliton frequency, resulting in the random walk of among soliton pulses called the Gordon-Haus (GH) effect [46].

In this chapter, we numerically investigate the effectiveness of the optical amplification and the soliton method in upgrading the electronic-repeated 1,318-long Thailand-Malaysia (T-M) system. By designing systems to work at optimum conditions, the possibility of increasing data rate in single-channel from 560 Mbit/s to 10 Gbit/s without reducing the amplifier span, and to 20 Gbit/s with reducing the span to be a half, are demonstrated by computer simulations. Section 6.2 reviews about the generation of soliton in optical fiber and then describes about the system design strategies to achieve the maximum performance in the

system employing the optical amplification and the soliton technique. In section 6.3, we show the system modeling for single-channel T-M transmission system and the numerical simulation results, which indicates the performance upgrading.

6.2 Generation of Soliton Pulse in Optical Fiber and System Design Considerations

Soliton refers to special kind of waves that can propagate undistorted over long distances and remain unaffected after collision with each other. Optical soliton in optical fiber is conformed by balancing the SOD and the SPM in anomalous dispersion region. Quantitatively, this can be achieved by launching optical pulses with proper width and input power, which is given by Eq. (6-1), into the fiber.

$$P_0 = \frac{|\beta_2|}{\gamma T_0^2}, \tag{6-1}$$

where, P_0 is the input power required for forming the soliton pulse, β_2 the group-velocity dispersion (GVD) parameter, γ the nonlinear coefficient, and T_0 the soliton width. It should be noted that β_2 directly relates to the SOD: D, which is widely used in the context of fiber transmission, by

$$D = -\frac{2\pi c}{\lambda^2}, \tag{6-2}$$

where c and λ are the velocity of light and the carrier wavelength, respectively.

The most attractive characteristic of optical soliton is that they can propagate in optical fibers without distortion over a long distance if the fiber loss is negligible. There are several other reasons why soliton is attractive for optical communication systems and why they should be considered as a possible route for system upgrades. In particular, soliton is also compatible with all optical switching and routing technologies. The ability to optically process signal is essential if the bottleneck problems encountered at switching nodes are to be overcome for the high data rates.

The problems in soliton transmission systems are roughly classified into the following three problems; the fiber loss, the mutual interaction between adjacent solitons, and the GH effect. To transmit soliton pulses through actual

optical fibers, especially for a long distance, it is necessary to consider the fiber loss. The fiber loss results in exponentially increase of soliton width and decrease of soliton peak. It is necessary to amplify the soliton periodically to maintain its power. With the lump optical amplifier, the soliton power is amplified to have the power larger than P_0. Quanlitatively, P_0 will be multiplied by the power factor σ to be P_{av}, which is given by

$$P_{av} = P_0\sigma = \frac{P_0\alpha L_a}{1-\exp(-\alpha L_a)}, \tag{6-3}$$

where α is the loss coefficient of fiber and L_a is the amplfier span. Such a soliton called the guiding-center soliton or average soliton because, by incresing P_0 by the factor of σ, the average soliton power over L_a becomes equal to the soliton power in lossless fiber.

One of the important quantity in soliton system design is the ratio between the soliton period Z_0 [4] and L_a, where Z_0 can be obtained as

$$Z_0 = \frac{\pi T_0^2}{2|\beta_2|}. \tag{6-4}$$

It has been proved that the average soliton is stable during propagation when the ratio of Z_0 and L_a is much larger than unity [44]. Otherwise, serious soliton distortion is induced because large amount of the dispersive wave is generated and is emitted out of the soliton signal.

In addition to the stability requirement, there are two other effects limiting the capacity of soliton transmission. When the solitons are closely spaced, the mutual interaction changes the velocity of the solitons and causes the soliton to move out of the detection window. This effect is known as the soliton interaction. The collision between adjacent solitons is also induced from this effect. We can extend the distance where the collision occurs by increasing the time interval between adjacent solitons, i.e., by reducing the duty cycle of soliton pulse.

On the other hand, the GH effect is originated by the noise generated by the optical amplifiers. The amplifier noise randomly modulates the carrier frequency of the soliton, and then the group velocity varies. This effect leads to the timing jitter among soliton pulses. It should be noted that the soliton interaction and the

GH effect can be reduced by using relatively low D. However, using too small D, the soliton will suffer from low optical-signal-to-noise ratio (OSNR) at receiver because P_{av} will be at very low value according to Eq. (6-3).

In real system, D randomly changes along the transmission because of the temperature and the installed circumstance. The random variation of D also gives rise to the perturbation of soliton pulses resulting in large amount of dispersive wave that will disperse from the soliton pulse. The use of relatively large D can help reducing this signal distortion because the effect of D variation can then be treated as only small perturbation.

Taking into account all described problems, to design the soliton transmission system to achieve the maximum performance for a given fixed amplifier span, the following points should be concerned.

1. There should exist the optimum value of D that yields the trade off between the improvement of OSNR and the signal distortions.
2. The decrease in the duty cycle of the soliton pulse will increase all the nonlinear waveform distortion because relatively high P_{av} is required to form the soliton. On the other hand, the use of small duty cycle reduces the effect of soliton interaction. Therefore, the duty cycle should be set at the optimum value.
3. The bandwidth of the optical band-pass filter (OBPF) installed at the end of fiber should be adjusted to the optimum value, which selects only soliton spectrum and reject the accumulated noise.

6.3 Computer Simulations

To demonstrate the efficiency of the soliton in upgrading the electronic-repeated system, we perform some of computer simulations by taking the T-M system as the model. The T-M system starts from Petchburi, Thailand, ends at Chugai, Malaysia, with total length of 1,318 km. The transmission fiber is the dispersion-shifted fiber (DSF). The electronic repeaters are periodically placed at span (L_a) of 100 km with the last span of 118 km. The system operates in single channel with the data rate of only 560 Mbit/s.

In the calculation, we assume the typical parameter of DSF. The fiber loss coefficient and the nonlinear coefficient of DSF are 0.2 dB/km and 2.6 $W^{-1}km^{-1}$, respectively. The optical soliton signal is composed of a 32-bit pseudorandom return-to-zero pulse train with secant-hyperbolic shape. The SOD is assumed to randomly fluctuate around the operating D every 2 km with a variance of 0.5 ps/km/nm. The optical amplifier produces noise in process of amplification with a noise figure of 6.3 dB. At the end of system, the bandwidth adjustable OBPF is placed. The bandwidth of the OBPF is always adjusted to obtain the minimum bit-error rate (BER). The propagation of the soliton signal is calculated by solving the nonlinear Schrodinger equation by the split-step Fourier method (SSFM). The integration step size of the SSFM is always chosen at the value that gives a step size error less than 0.01 %. The receiver is modeled by a sixth-order Bessel-Thompson low-pass filter, followed by a BER detector. To calculate the numerical BER of the detected signal, the simulation is repeated 128 times for the pseudo-random pulse train. The numerical Q factor of every bit is then individually calculated at the maximum eye-opening point of the bit period. Based on the assumption of the Gaussian noise distribution, the numerical BER is computed from the bit numerical Q factor and is averaged over the entire bits. The system limitation is defined by BER = 10^{-9}.

Figure 6.1 shows the numerical BER, in logarithmic scale, of the soliton signal with data rate of 10 Gbit/s as a function of duty cycle for several D. We achieve BER < 10^{-9} by using D = 1.0 ps/km/nm with duty cycle of 0.2 and 0.6. For all D used in Fig. 1, the duty cycle of 0.2 and 0.5 yield better BER than other duty cycles. This can be interpreted that, by using the duty cycle of 0.5, although the soliton interaction becomes a serious problem, we can sufficiently reduce P_{av}. Therefore, the BER becomes relatively small because the signal distortion due to the GH effect and the emission of dispersive wave are simultaneously reduced. When we decrease the soliton duty cycle to 0.4 and 0.3, to reduce the effect of the soliton interaction, we have also unavoidably to increase P_{av}. Since the soliton interaction cannot be completely eliminated, at the same time, the GH effect and the emission of dispersive wave become more serious, the BER then slightly increases as appeared in Fig. 1. However, when we further reduce the duty cycle

to 0.2, the soliton interaction may be almost completely suppressed, and according to the fact that the GH effect and the emission of dispersive wave may be still not too strong, we can achieve the smallest BER at this duty cycle.

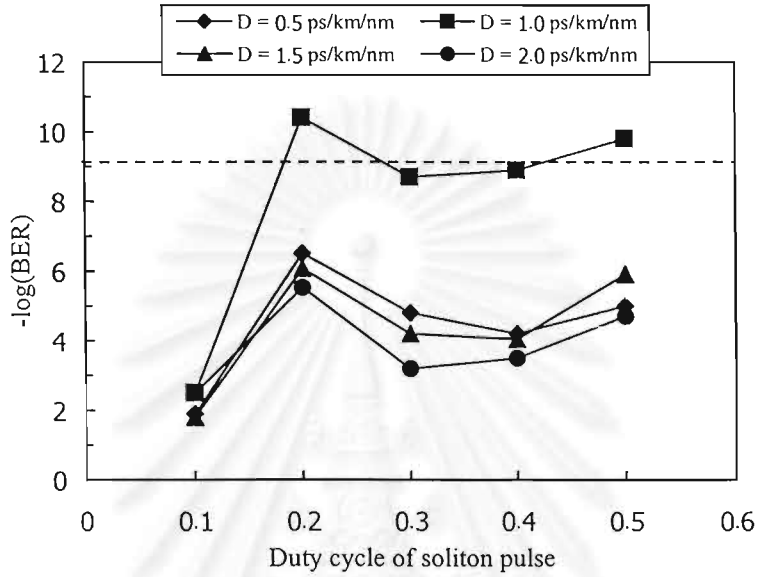

Figure 6.1: Numerical BER of the 10-Gbit/s soliton signal as a function of duty cycle for several D. L_a is 100 km. BER < 10^{-9} is obtained by using D = 1.0 ps/km/nm with duty cycle of 0.2 and 0.6.

As described above, the use of low operating D causes the signal distortion from the random fluctuation of SOD. However, the use of large D results in the enhancement of the GH effect and the emission of dispersive wave because very high P_{av} is required to be launched into the fiber to create optical soliton. As a result, in Fig. 1, D = 1.0 ps/km/nm is the optimum value that gives the balance among these problems. Figure 2 show the output eye pattern of the 32-bit soliton, obtained by using D = 1.0 ps/km/nm and duty cycle of 0.2. The soliton signal is in a very good shape, therefore, we can clearly distinguish the bit "1" and "0".

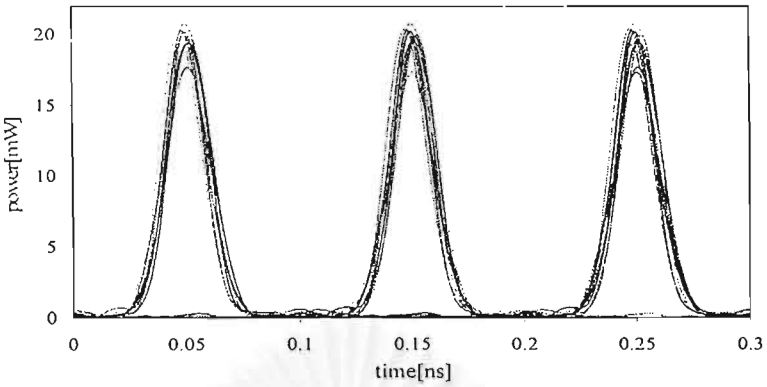

Figure 6.2: Eye pattern of the output 32-bit soliton waveform obtained by using D = 1.0 ps/km/nm and duty cycle of 0.2.

The easiest way to further increase the performance of this 10-Gbit/s soliton system is to reduce L_a. The GH effect and the amount of dispersion wave scattering from soliton will then be reduced because the ratio between Z_0 and L_a becomes large and also P_{av} is reduced. Figure 3 shows the numerical BER, in logarithmic scale, of the 10-Gbit/s soliton signal as a function of duty cycle for several D. L_a, in this case, is set at 50 km with the last span of 68 km. According to the numerical results, we can achieve BER < 10^{-9} for a wide range of duty cycle (> 0.1) by using D = 1.0 ps/km/nm, and for only a duty cycle of 0.2 with D = 1.5 ps/km/nm.

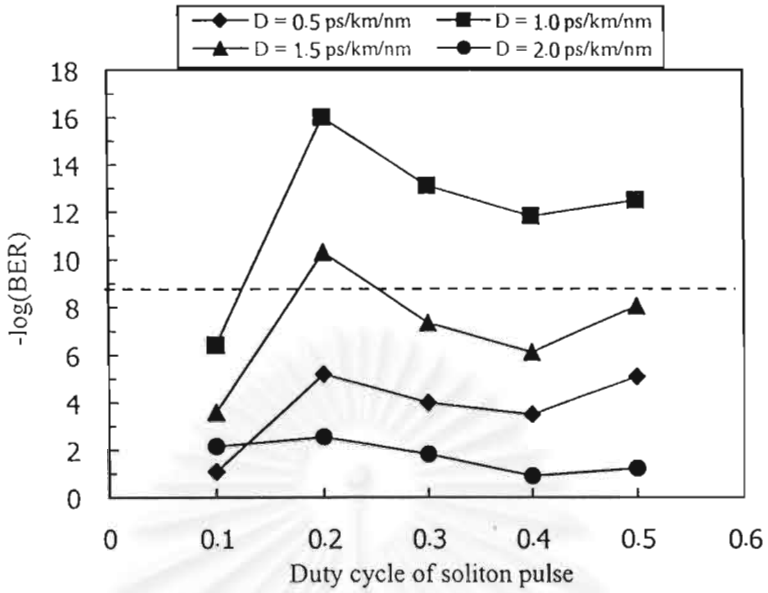

Figure 6.3: Numerical BER of the 10-Gbit/s soliton signal as a function of duty cycle for several D. L_a is 50 km. BER < 10^{-9} is achieved for a wide range of duty cycle by using D = 1.0 ps/km/nm, and for only a duty cycle of 0.2 with D = 1.5 ps/km/nm.

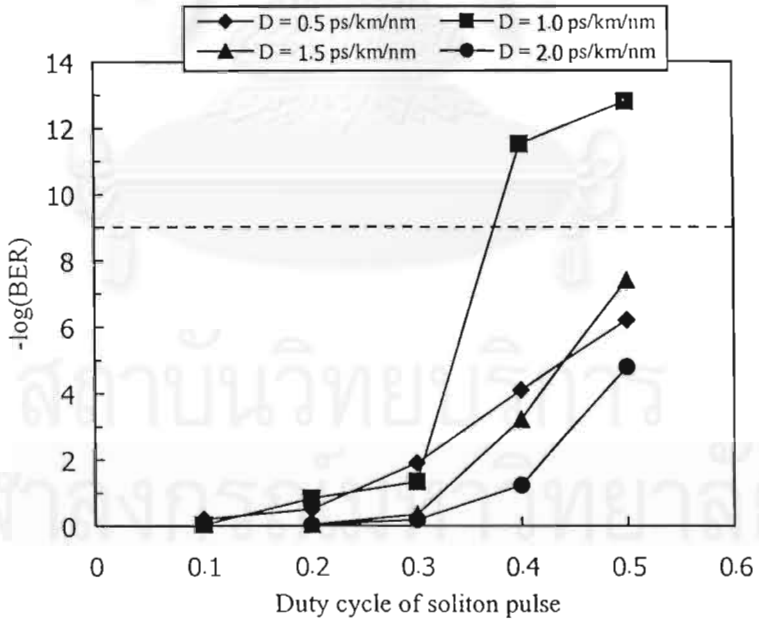

Figure 6.4: Numerical BER of the 20-Gbit/s soliton signal as a function of duty cycle for several D. L_a is 50 km. BER < 10^{-9} is obtained by using D = 1.0 ps/km/nm with duty cycle of 0.4 and 0.6.

Next we explore the possibility of higher data rate transmission using L_a = 50 km. Figure 6.4 shows the numerical BER for the case of a soliton signal with data rate of 20 Gbit/s, as a function of duty cycle for several D. Similar to the results from Fig. 6.1 and Fig. 6.3, the best BER is obtained by using D = 1.0 ps/km/nm. However, the transmitted soliton gives the BER less than 10^{-9} only for the duty cycle of 0.4 and 0.6. We can no longer achieve BER < 10^{-9} by using smaller duty cycle. This is because, in such high data rate, to generate the soliton with small duty cycle, P_{av} will be in an extremely high level. Therefore, the GH effect as well as the dispersive wave will play a dominant role in limiting the performance of this system. To improve the achievable BER in such system, L_a should be further reduced.

7. PERFORMANCE UPGRADING OF THAILAND-MALAYSIA SYSTEM USING OPTICAL AMPLICATION AND MIDWAY OPTICAL PHASE CONJUGATION

The midway optical phase conjugation (OPC) is very attractive method for upgrading performance of the installed systems because of its simplicity and practical implementation. By only placing an optical phase conjugator at the midpoint of system, the transmission data rate can be extremely increased. Our work also demonstrated the feasibility of a 200-Gbit data transmission over 10,000 km by a system using the OPC [67].

In this chapter, we investigate, by computer simulation, the results of upgrading the Thailand-Malaysia (T-M) submarine system using our optimum design scheme. Following our guidance, the possibility of increasing data rate in 1,318-km-long T-M submarine system from 560 Mbit/s to 200 Gbit/s is numerically shown. Section 7.1 reviews about the problems which limit the OPC system and describes the system design strategies which we introduces. Section 7.2 shows the computer simulation based on the T-M system where the OPC is performed to upgrade.

7.1 Design for maximum performance in systems upgraded by optical amplification and OPC

Figure 2.12 has shown schematically the midway OPC system. By performing the OPC at the midpoint of system, all signal distortions induced from the second-order dispersion (SOD) and the Kerr effect can be compensated if all of the system characteristics in the first half is symmetrical to the second half. The optical phase conjugator is placed at the midpoint of the system. However, in real transmission, two problems occur and limit a performance of the OPC systems.

First, since the transmission fiber of the second half cannot have negative third-order dispersion (TOD) while its SOD still keeps the same sign as that of first half, similar to other systems, the TOD in OPC systems cannot be compensated by OPC but it just accumulates along the system length and will also cause the signal waveform distortion. Second, because we cannot generate a

distributed gain that exhibit the reverse sign of the fiber attenuation constant through the second half, in real system with long distance transmission, a periodic lumped amplification forms a periodic signal power distribution along the system length and at the same time produces a periodic variation of fiber refractive index through the nonlinear Kerr effect of an optical fiber. By this process, it seems like a grating is virtually constructed in the transmission fiber. As has been shown in Fig. 2.13, a resonance between the virtual grating and the signal will occur at the signal sideband component whose wave vector matches the wave vector of this virtual grating resulting in exponential growth of that component with transmission length. This phenomenon is known as the sideband instability (SI), which causes signal waveform distortion if SI arises at frequency inside the signal bandwidth, which cannot be eliminated by using optical bandpass filter [51], [52], [58]. The sideband angular frequency ω_n shifted from the carrier frequency, at which SI arises is obtained as

$$\omega_n = \pm\sqrt{\frac{1}{|\beta_2|}\left(k_f n - 2\,\mathrm{sgn}(\beta_2)\overline{P}\right)}. \tag{6-1}$$

where $\overline{P}$ is the path-averaged signal power, β_2 the group-velocity dispersion parameter, and k_f the wave number of the virtual grating which is given as

$$k_f = \frac{2\pi n}{l_f}, \tag{6-2}$$

where $n = 0,\pm1,\pm2,...,$ and l_f is the amplifier spacing.

In order to avoid the signal distortion due to the SI, Fig. 7.1 shows the magnitude of signal degradation in OPC system as a function of the SOD in the absence of the TOD. In Fig. 7.1, two transmission windows are observed at relatively large anomalous dispersion region and at relatively low normal dispersion. The SI causes the serious signal distortion when the operation SOD becomes larger because the SI will occur at inner signal bandwidth according to Eq. (6-1). Therefore, the use of relatively low SOD is preferred. However, the lowest SOD that can be used is limited by the effect of the SOD fluctuation around zero-dispersion point. In anomalous dispersion region, the use of low SOD induces the modulation instability effect, which will result in much signal

degradation. Thus, for anomalous dispersion region, the optimum operation SOD is located at relatively large value.

As alternative method for reducing the effect of SI, Watanabe and Shirasaki have given a condition for perfect SI compensation [68] as shown below.

$$\frac{\beta_2(-z_1')}{\gamma(-z_1')P(-z_1')} = \frac{\beta_2(z_2')}{\gamma(z_2')P(z_2')}, \tag{7-3}$$

where the nonlinear coefficient γ, and the signal power P are the function of distance z.

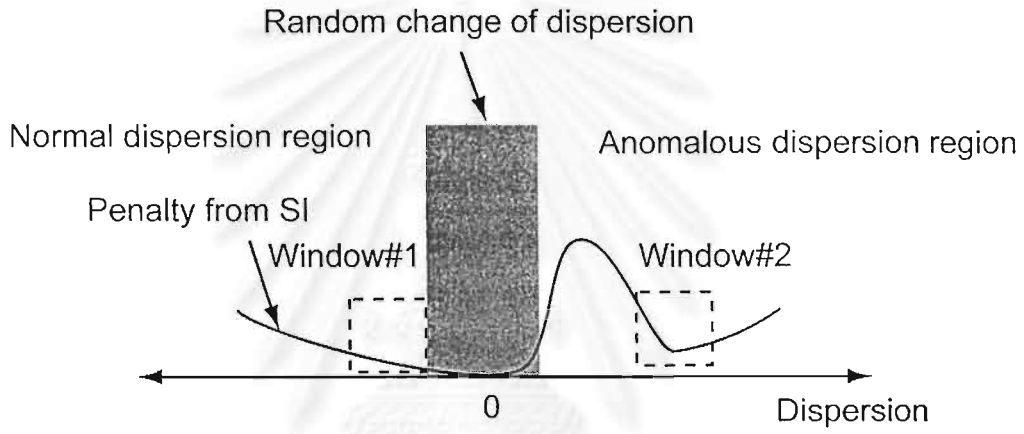

Figure 7.1: Operation windows for OPC systems.

Equation (7-3) indicates that the perfect suppression of SI is achieved when the cumulative SOD-induced chirp and the cumulative Kerr effect-induced chirp integrated from the OPC position at $z' = 0$ to $-z_1'$ and z_2' are equal. This relation means that providing the equal ratio of the SOD and the nonlinearity at the corresponding position symmetrical from the system midpoint, perfect distortion compensation can be obtained. This relation gives us the following freedoms for the OPC system design.

1) The OPC needs not be placed at the midway of the system. Assuming that the SOD value, the signal power, and the system length of the first half are D_A, P_A, and L_A, respectively, and those of the second section are D_B, P_B, and L_B, respectively. We find that Eq. (7-3) holds provided that $D_A = kD_B$, $P_A = kP_B$, and $kL_A = L_B$.

2) The power distribution needs not to be uniform. Equation (7-3) holds when the SOD value is properly tailored to follow attenuation of the signal power.

In order to satisfy the condition, a SOD-decreasing fiber (DDF), whose SOD-decreasing coefficient is proportional to a fiber loss coefficient, must be installed throughout the entire OPC system length. A good transmission result of 20 Gbit/s over 3,000 km [68] was demonstrated by using a quasi-DDF in which short fibers with different dispersion values were concatenated to form the dispersion-decreasing profile. However, such the approach sounds too impractical to be employed in real systems. Moreover, for both two proposed schemes the uncompensated TOD will show up to affect the long-haul transmission with the bit rate higher than 40 Gbit/s.

For simplicity of design, we will not use the scheme that Watanabe has introduced. We will design system such as the OPC system can operate at condition where the signal distortion from SI is as small as possible. After replacing the electronic repeaters with optical amplifiers, first, we should place the optical phase conjugator (wavelength-shift-free type) closed to the system midpoint as much as possible. The deviation from the midpoint causes the signal distortion from the SOD and the Kerr effect induced from the unbalance section. To reduce this kind of distortion, the SOD of the unbalance section must be compensated.

The increase in signal power gives rise to the improvement of the optical-signal-to-noise ratio (OSNR). At the same time, for long-haul system, the use of high signal power results in the nonlinear waveform distortion induced from the fiber loss and the periodic amplification called the SI, and the nonlinear waveform distortion induced from the random dispersion fluctuation through the Kerr effect [52], [69]. The optimum signal power will be found at the balance of this improvement and the degradation.

The operating SOD value is also the important parameter to be designed. We should place the signal wavelength in the normal dispersion region to avoid the distortion from the MI. The use of low SOD value enhances the effect of random dispersion fluctuation. However, high SOD value causes the SI to occur

closed to the signal carrier. The optimum dispersion value is also needed to be set at the optimum value.

The next step is to investigate the necessary of the TOD compensation. This can be done by calculating the TOD length (L_{d3}) [4] of the system. When L_{d3} is longer than system length, no TOD compensator is needed. On the other hand, if L_{d3} is shorter than the system length, The TOD compensation is needed. However, since we have proved that the accumulation of the TOD in OPC system is linear [49], we can achieve the perfect compensation of the TOD by placing only one TOD compensator at any point in the system.

The system performance may be further improved by reducing the amplifier spacing. The short amplifier span gives better OSNR at low signal power, and makes the SI occur more outside signal bandwidth than the long span.

7.2 Computer simulations

To demonstrate the efficiency of the upgrading scheme, we consider the T-M submarine system as the simulation model. The system starts from Petchburi, Thailand, ends at Chugai, Malaysia, with total length of 1,318 km. The fiber is dispersion-shifted fiber (DSF). The electronic repeaters are periodically placed at span of 100 km with the last span 118 km. The system operates with single channel with the data rate of only 560 Mbit/s.

In the simulations, the optical signal is 32-bit pseudorandom Gaussian RZ pulses. The fiber loss coefficient, the TOD, and the fiber nonlinear coefficient of DSF are 0.2 dB, 0.06 ps/km/nm, and 2.6 $W^{-1}km^{-1}$, respectively. The dispersion is assumed to randomly fluctuate around the operating dispersion value at every 2 km with standard deviation of 0.5 ps/km/nm. The optical amplifier produces noise in process of amplification with noise figure of 5.3 dB. At the end of system, the bandwidth adjustable optical bandpass filter is placed. The TOD compensator, placed at the end of system, is an ideal device that multiplies the signal with negative amount of linearly accumulated phase shift caused by TOD. The wavelength-shift-free optical phase conjugator is placed at the end of the 6^{th} span for 100-km amplifier spacing or at the end of the 13^{th} span for 50-km amplifier spacing. The conversion efficiency of the optical phase conjugator is assumed to

be -14.7 dB. The amount of the unbalance accumulated dispersion of the first half and the second half, as well as the accumulated random dispersion are compensated by the adjustable dispersion compensator placed before the receiver. The propagation of the optical pulse is calculated by solving the nonlinear Schrodinger equation by the split-step Fourier method (SSFM). The integration step of the SSFM is always chosen to give the step error less than 0.01%. The system performance is evaluated in terms of bit-error rate (BER) calculated by repeating 128 times the transmission of the same signal and assuming the Gaussian distribution of amplifier noise. The receiver is modeled by electronic low-pass filter followed by a BER detector.

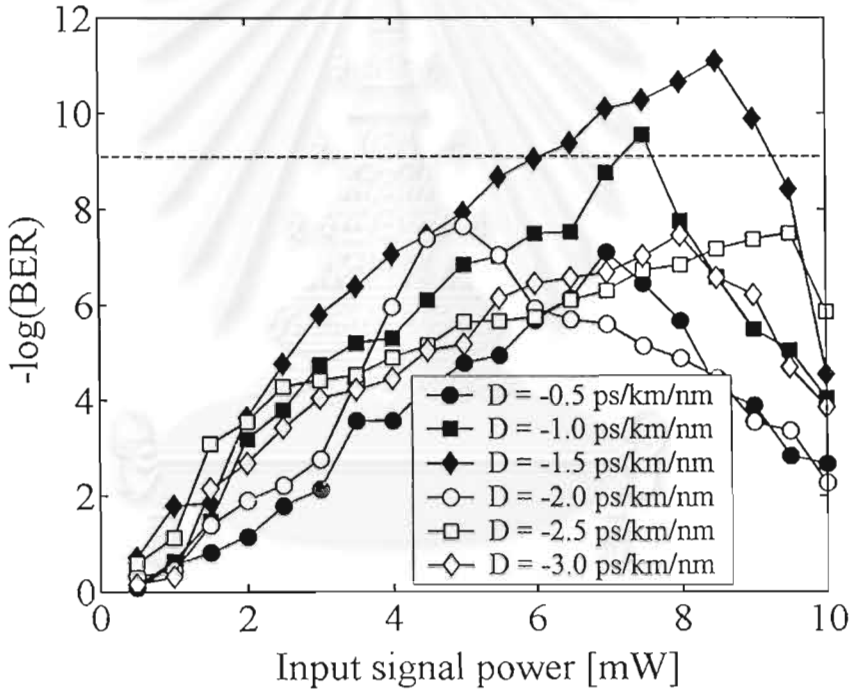

Figure 7.2: BER of transmitted 160-Gbit/s signal in OPC system using 100-km amplifier spacing, as a function of input signal powers for several operating SOD values.

Figure 7.2 shows the BER of the transmitted 160-Gbit/s signal, as a function of input signal power for several operating dispersion values. For given SOD value, the minimum BER for given SOD is obtained at the signal power that

yields the balance between the improvement of SNR and the degradation from the nonlinear waveform distortion. With this optimum power, the overall minimum BER is obtained by using the optimum SOD that yields the balance between the avoidance from the effect of random SOD fluctuation and the signal distortion from SI effect. From Fig. 7.2, with defining BER = 10^{-9} as system limitation, the T-M system can be upgraded for 160-Gbit/s transmission by using the OPC scheme with the signal power of 7.5 mW and the operating dispersion value of –1 ps/km/nm or the signal power of 6.5-9.0 mW and the operating SOD value of –1.5 ps/km/nm.

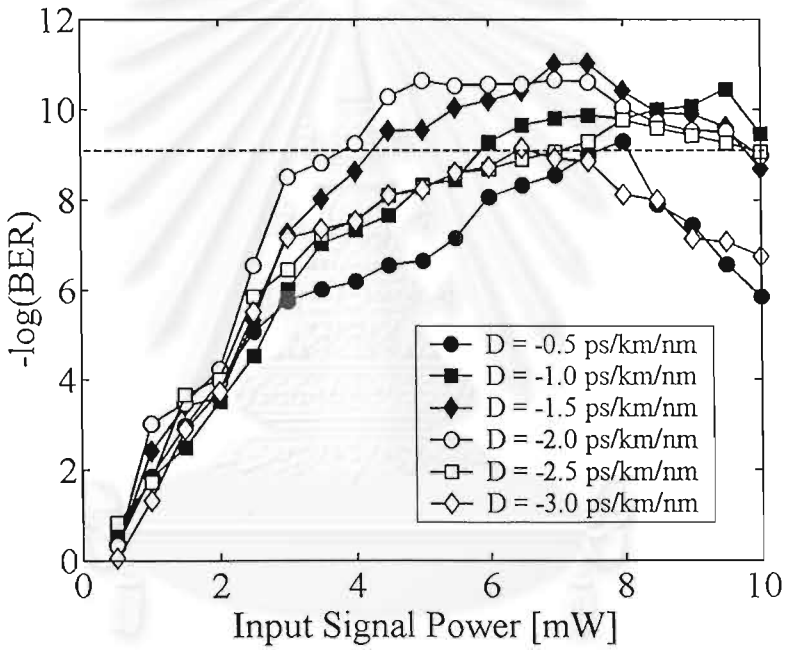

Figure 7.3: BER of transmitted 200-Gbit/s signal in OPC system using 50-km amplifier spacing, as a function of input signal powers for several operating SOD values.

We have explored the data rate of 200 Gbit/s. However, we cannot achieve this data rate with the amplifier span of 100 km. Therefore, we reduce amplifier span to be 50 km with the last span of 68 km. Figure 7.3 shows the results of the 200-Gbit/s data transmission using 50-km span, as a function of input signal power for several operating dispersion values. The results show the possibility of the transmission at this data rate with wide range of input signal powers (4 ~ 10 mW) incorporated with the dispersion of –1.0 ~ -2.5 ps/km/nm. We also investigate the

transmission of lower data rates and summarize the optimum power and dispersion in Table 7.1.

Table 7.1: Optimum signal powers and SOD values for 40, 80, and 100 Gbit/s data transmission for achieving BER < 10^{-9}.

Bit rate [Gbit/s]	40	80	100
Input power [mW]	1.5-12.5	3.0-8.0	6.0-10.5
SOD [ps/km/nm]	-0.5	-1.0	-1.5

8. CONCLUSIONS

8.1 Summary of this Report

In this report, we have explored the optimum system design strategies for four second-order dispersion (SOD) compensation schemes: the zero-dispersion wavelength (ZDWL) transmission, the dispersion management (DM), the optical soliton, and the midway optical phase conjugation (OPC) system. Then we have numerically studied the efficiency of these four schemes in upgrading the installed electronic-repeated system to optically amplified system. The system used for model in this study was the Thailand-Malaysia (T-M) submarine fiber-optic system as the simulation model. The system starts from Petchburi, Thailand, ends at Chugai, Malaysia, with total length of 1,318 km. The fiber is dispersion-shifted fiber (DSF). The electronic repeaters are periodically placed at span of 100 km with the last span 118 km. The system operates with single channel with the data rate of only 560 Mbit/s.

When the electronic repeaters are replaced with the optical amplifiers, we have described that the main problems which cause the signal waveform distortion are the fiber dispersion and the fiber nonlinearity, especially the Kerr effect. The fiber second-order dispersion (SOD) results in pulse broadening, for ultra-high data rate, the third-order dispersion (SOD) generates subpulses at the tailing edge of the signal, while the Kerr effect affects the signal spectrum to be broadened. The signal distortion becomes more serious when the dispersive effect and the nonlinear effect interplay with each other on some conditions, which can be estimated by using the characteristic lengths that we have introduced.

The ZDWL transmission was the simplest type. By only placing the carrier at ZDWL of the transmission fiber, the signal pulse broadening induced from the SOD can be overcome. However, our computer simulations demonstrated that such transmission scheme suffers from the Kerr effect through the self-phase modulation (SPM) and the four-wave mixing (FWM). The SPM and the FWM causes the rapid spectral broadening in ZDWL region. Moreover, the effect of TOD is also very significant at ZDWL. The interplay among the

SPM, the FWM and the TOD results in more rapid spectral broadening, as well as signal waveform distortion.

Nevertheless, when we employed the ZDWL scheme to upgrade the T-M system, which has a relative long-haul length, the ZDWL showed sufficient potention in improving system performance. Our design guidelines for achieving maximum performance in the ZDWL transmission were, first for a given data rate, to find the optimum combination between the optimum signal power, which balances the improvement in optical signal-to-noise ratio (OSNR) and the degradation from fiber nonlinearity, and the optimum bandwidth of the optical bandpass filter (OBPF), that can collect the necessary spectral components, which had been broadened during propagation. We also showed the effectiveness of the TOD compensation for ultra-high bit rate. The TOD compensator placement was demonstrated by installing these devices at the length smaller than the nonlinear length of the system. According to the simulation results, by only replacing the electronic-repeaters with the optical amplifiers, we demonstrated that the transmission bit rate can be increased from 560 Mbit/s to 40 Gbit/s. Moreover, with reducing the amplifier span to be 50 km and employing only one TOD compensator at the end of the system, we also demonstrated the possibility of the optical data transmission at a data rate as high as 80 Gbit/s.

To overcome the problems occurring around ZDWL is to use the concept of dispersion management. This method is to arrange the various sections of fiber in such a way that none or only very few of them have ZDWL that coincide with the carrier wavelength while the total fiber exhibits zero dispersion on average. We have demonstrated that the dispersion management has several advantages in reducing the signal distortion induced from the Kerr effect near ZDWL. We introduced the optimum design rules for the dispersion management method including the concept of the transfer function analysis. For given data rate and system length, the design guidelines bases on finding the optimum signal power in combination with the dispersion management period, and the operating SOD value. By designing systems to work at optimum conditions, our numerical simulation results demonstrated the possibility of increasing data rate in single-channel from 560 Mbit/s to 80 Gbit/s without reducing the amplifier span, or to

100 Gbit/s with reducing the span to be a half, and in wavelength division multiplexing (WDM) scheme to 6x10 Gbit/s.

Optical soliton is a special pulse that can maintain its shape during the propagation in lossless optical fiber because of the balance between the fiber SOD and the SPM. However, for long-haul transmission, the fiber loss causes the attenuation of soliton power resulting in the destruction of soliton waveform. Therefore, the lumped optical amplifiers are necessary to be installed periodically to compensate the fiber attenuation. This soliton then is considered as the average soliton, and the system is limited by the constraint that the amplifier spacing must be very shorter than the characteristic length called the soliton period. Moreover, the collision between adjacent soliton pulse called the soliton interaction, as well as the random walk of among soliton pulses due to amplifier noise called the Gordon-Haus effect, also place a limit in both data rate and distance of the transmission system using soliton. We described that the design issue for avoiding these problems is to find the optimum operating SOD value and the duty cycle of soliton pulses. We have numerically investigated the effectiveness of the optical amplification and the soliton method in upgrading the T-M system. By designing systems to work at optimum conditions, the possibility of increasing data rate in single-channel from 560 Mbit/s to 10 Gbit/s without reducing the amplifier span, and to 20 Gbit/s with reducing the span to be a half, are demonstrated by computer simulations.

The last system upgrading method is the use of OPC at the midpoint of a given system. By performing the OPC at the midpoint of system, all signal distortions induced from the SOD and the Kerr effect can be compensated if all of the system characteristics in the first half is symmetrical to the second half. The optical phase conjugator is placed at the midpoint of the system. However, in real transmission, the TOD, and the nonlinear resonance called the sideband instability (SI) induced from the fiber loss and periodic signal amplification through the Kerr effect causes the signal distortion in OPC systems.

We have discussed about the design concept for this OPC system. The SOD should be chosen at an optimum value, which is in the normal dispersion region. Similarly, the signal power should be also in an optimum value. For the

TOD compensation issue, after investigating the necessary of the TOD compensation by calculating the TOD length, we can achieve the perfect compensation of the TOD by placing only one TOD compensator at any point in the system. The deviation from the midpoint of the OPC causes the signal distortion from the SOD and the Kerr effect induced from the unbalance section. To reduce this kind of distortion, the SOD of the unbalance section must be compensated.

By computer simulation, we demonstrated that the T-M system can be upgraded from 560 Mbit/s to 160 Gbit/s by only employing the optical phase conjugator and following our design guidelines. When we reduced the amplifier span to be a half, the T-M system has been shown to be capable for 200 Gbit/s data transmission.

8.2 Comparison among Dispersion Compensating Schemes

Table 8.1 shows the comparison in several aspects among four SOD compensation methods which we have studied in this project. For the reduction of fiber nonlinearity, the ZDWL transmission faces the most serious problems because the SOD completely vanishes along the transmission. Therefore, the nonlinearity becomes the main factor that limits the system performance. The advantage of the ZDWL transmission is originated from its simplicity in system structure and it is very easy and practical to upgrade any install systems with out reinstall new transmission fibers. For extending to WDM scheme, however, the center channel can only experience the zero SOD, therefore, the accumulated SOD in other channels must be compensated. T

The dispersion management method realizes the transmission under the effect of SOD, while the accumulated SOD is reset at given interval. Although this method cannot compensate the fiber nonlinearity, however, the reduction of signal distortion due to the fiber nonlinearity is significantly less severe than the case of ZDWL. For upgrading the installed systems, the disadvantage is that we have to install additional dispersion compensating devices or reinstall new fibers if the dispersion compensating fibers are required to use. Therefore, it is however, not a cost-performance scheme for system length that is relatively short. To apply

for WDM scheme, this method is one of the most suitable scheme because the different in the accumulated SOD among channels can be reset by this method as discussed in Chapter 5.

Table 8.1: Comparison in several aspects among four SOD compensation methods

Upgrading Schemes	**Fiber nonlinearity**	**System configuration**	**Upgrading installed systems**	**To WDM**
ZDWL transmission	Very serious	Very simple	OK for relatively short length	Must be incorporated with dispersion managment
Dispersion management	Reduced	Not so complicated	Install additional devices or install new fibers	Practical
Optical soliton	Compensated	Complicated	Complicated design theories and required much system cost	Must be incorporated with dispersion management
Midway OPC	Compensated	Relatively simple	OK for long-haul point-to-point link because the signal cannot monitored at intermediate node	Depending on the bandwidth of optical phase conjugator

The soliton system looks beautiful in its pure nature. The soliton is very tolerance to fiber nonlinearity because the soliton itself utilizes the SPM to be generated. However, for implementation, it will face several problems both in system cost and technologies. The very high laser source together with relatively short amplifier span will significantly raise up the system cost, while the data rate cannot be too much improved. In order to extend the soliton to WDM scheme, the dispersion management has to be incorporated with the soliton, otherwise, the soliton in each channel will has different power due to the different in channel SOD. Therefore, the soliton system configuration becomes more complicated for WDM application. As a consequence, the design theories also become very complicated and hard to understand.

One of the simplest technologies to upgrade an install system is to perform OPC closed to the midpoint of the system as much as possible. This scheme offers the simultaneous compensation of both SOD and the Kerr effect. The system using the OPC has very simple structure. For WDM transmission, it is dependent on the supported bandwidth of the optical phase conjugator. The disadvantage of this scheme is that we cannot monitor the transmission signal at any intermediate node because the SOD exists for entire system length. Therefore, this scheme may be suitable for upgrading such long-haul point-to-point link. Another disadvantage is that there is no optical phase conjugator that yields high conversion efficiency available nowadays.

Table 8.2: Comparison in difficulty of upgrading and investment cost among four SOD compensation methods.

Upgrading Schemes	**Difficulty of upgrading**	**Investment cost**
ZDWL transmission	Only replace all electronic repeaters with optical amplifiers For ultra-high bit rate, additionally optimize the number of TOD compensator	Only depend on the number of optical amplifiers For ultra-high bit rate, additional cost of TOD compensators

Dispersion management	Replace all electronic repeaters with optical amplifiers and installed dispersion compensating fibers or dispersion compensating devices For ultra-high bit rate, additionally optimize the number of TOD compensator	Depend on the number of optical amplifiers and the number of installed dispersion compensating fibers or dispersion compensating devices For ultra-high bit rate, additional cost of TOD compensators
Optical soliton	Replace all electronic repeaters with optical amplifiers and using high intensity signal source	Depend on the number of optical amplifiers and the high intensity signal source
Midway OPC	Replace all electronic repeaters with optical amplifiers, construct the optical phase conjugator, install the optical phase conjugator, install tunable dispersion compensating device and tune accumulated dispersion For ultra-high bit rate, additionally install only one TOD compensator	Depend on the number of optical amplifiers, the optical phase conjugator, and the tunable dispersion compensating device For ultra-high bit rate, additional cost of one TOD compensator

Table 8.2 shows the comparison about the difficulty of upgrading and the investment cost among four SOD compensation methods. For the ZDWL transmission, the upgrading is only to replace all the electronic repeaters with the all optical amplifiers. Since the investment cost of common lightwave transmission system depends on the cost of the electronic components in the system as well as the signal light source, receiver, and the optical amplifiers. Therefore, the cost of the ZDWL is then almost increased proportional to the number of optical amplifier because no other additional devices is required. Since for ultra-high data rate transmission, the TOD compensators are additionally

needed. We then have to optimize the number of the TOD compensators in order to reduce the cost. The system cost for such ultra-high data rate transmission has to include the total cost of the employed TOD compensators.

For the DM, not only to replace all electronic repeaters with optical amplifiers, we have to installed dispersion compensating fibers or dispersion compensating devices at suitable period. As a result, the system cost depends on the number of optical amplifiers and the number of installed dispersion compensating fibers or dispersion compensating devices used in the system. Similar to the ZDWL transmission, for ultra-high bit rate transmission, it is also necessary to optimize the number of TOD compensators. Therefore, the additional cost is increased proportional to the number of the TOD compensator.

For optical soliton scheme, since the high intensity signal source is required to form the soliton signal, this will yield significant increase in system cost because the high power laser source is very expensive. Therefore, the system cost using soliton is then mainly caused by this high power soliton source and the optical amplifiers. According to the calculation results shown previously, the soliton scheme may not give a good result for ultra-high data rate transmission. Therefore, the TOD compensation can be ignored because using the soliton we cannot reach the transmission data rate where the TOD becomes a significant problem.

Since the transmission scheme using midway OPC is under developed. Therefore, the optical phase conjugator is still not available in telecommunication market. To employ this scheme in real system, first, we have to construct the optical phase conjugator by ourselves. The wavelength-shift-free optical phase conjugator [56], [57] is commonly consisted of highly-nonlinear dispersion-shifted fiber, optical isolators, optical WDM couplers, wavelength tunable high-power lasers, and OBPFs. Others stability control methods such as the temperature control unit are also necessary in the same package. The main issue is that we have to design the optical phase conjugator to have both high conversion efficiency and broad bandwidth. Assuming that we have sufficiently good optical phase conjugator, for upgrading, we have to replace all electronic repeaters with optical amplifiers, install the optical phase conjugator at the amplifier that is

closed to the system midpoint as much as possible, install tunable dispersion compensating device, and tune this device to compensate for the accumulated dispersion from the unbalance section. For ultra-high bit rate transmission, the advantage of this OPC scheme is that we can only install only one TOD compensator for perfect compensation of the TOD. The investment cost mainly comes from the number of optical amplifiers installed in the system, the development cost and the devices for constructing the optical phase conjugator, and the tunable dispersion compensating device. For upgrading the system for ultra-high bit rate transmission, additional cost of one TOD compensator has to be included.

Table 8.3: Comparison of achievable transmission data rates, obtained from all four upgrading schemes.

Amplifier span	**ZDWL**	**Dispersion management**	**Optical soliton**	**Midway OPC**
100 km	40 Gbit/s	80 Gbit/s	10 Gbit/s	160 Gbit/s
50 km	80 Gbit/s	100 Gbit/s	20 Gbit/s	200 Gbit/s

According to all of our simulation results, Table 8.3 summarizes the achievable transmission data rate for all four upgrading schemes. The midway OPC scheme yields the best results for both 100-km span and 50-km span, with data rate as high as 160 Gbit/s and 200 Gbit/s, respectively, while the soliton yields the achievable data rate of 10 Gbit/s and 20 Gbit/s, respectively. Since the length of T-M system is not too long, the ZDWL transmission can result sufficiently high data rates. This is due to the Kerr effect becomes not too much significant in such system length. However, the use of dispersion management instead of ZDWL transmission gives the obvious improvement in data rate because the Kerr effect is reduced. For soliton transmission, the reason, why the achievable data rate is very small comparing to other schemes, originates from the constraint of amplification period. On the other hand, in midway OPC system, the SOD can exist along the transmission length without intermediate compensation, therefore, the nonlinearity in such system is not so significant comparing to the

SOD. Moreover, the OPC itself can compensate for the Kerr effect. These reasons make the OPC scheme give the best results for upgrading the T-M system. Al though the OPC scheme shows the most attractive data rate, we should emphasize that we cannot monitor the signal quality or performing data add-drop process at any intermediate point in the system without additional SOD compensation. This is because, in OPC scheme, the SOD exists for the entire transmission line.

Lastly, since all of the results shown in our work are obtained from computer simulation, one should doubt the accuracy or the reliability when the T-M system is upgraded in the real world. In fact, we have taken into account as much as possible for all possible problems occurring in the real system, as well as the simulation method: the split-step Fourier, is the method that has been recognized in its accuracy and it has been widely used in the field of optical fiber transmission. Therefore, we expect that the actual results will not differ from our simulated results too much.

REFERENCES

[1] T. Naito, N, Shimojoh, T. Tanaka, H. Nakamoto, M. Doi, T. Ueki, and M. Suyama. 1 Terabit/s WDM transmission over 10,000km. Proc. European Conf. on Opt. Commun. (ECOC'99), PD2-1, Nice France, Sept. 26-30, 1999: pp. 24-25.

[2] S. Walker, L. C. Blank, L. Bicker, and R. Garnham. Transmission and signal precessing techniques for gigabit lightwave systems. J. Lightwave Technol., vol. LT-4, 1986: pp. 759-766.

[3] A. F. Elrefaie, R. E. Wagner, D. A. Atlas, and D. G. Daut. Chromatic dispersion limitations in coherent lightwave transmission systems. J. Lightwave Technol., vol. 6, 1988: pp. 704-709.

[4] G. P. Agrawal. Nonlinear Fiber Optics. 3rd Ed.: New York, Academic Press, 2001.

[5] G. P. Agrawal. Fiber-optic communication systems. 2nd Ed.: New York, Academic Press, 1997.

[6] R. Chraplyvy. Limitations on lightwave communications imposed optical-fiber nonlinearities. J. Lightwave Technol., vol. 8, 1990: pp. 1548-1557.

[7] D. Marcuse, A. R. Chraplyvy, and R. W. Tkach. Effect of fiber nonlinearity on long-distance transmission. J. Lightwave Technol., vol. 9, 1991.

[8] J. P. Hamaide, Ph. Emplit, J. M. Gabriagues. Limitations in long haul IM/DD optical fibre systems caused by chromatic dispersion and nonlinear Kerr effect. Electron. Lett., vol. 26, 1990: pp. 1451-1452.

[9] K. Kikuchi. Enhancement of optical-amplifier noise by nonlinear refractive index and group-velocity dispersion of optical fibers. IEEE Photon. Technol. Lett., vol. 5, 1993: pp. 221-223.

[10] C. Lorattanasane and K. Kikuchi. Parametric instability of optical amplifier noise in long-distance optical transmission systems. IEEE J. Quantum Electron., vol. 33, 1997: pp. 1068-1074.

[11] S. Bigo, O. Leclerc, E. Desurvire. All-optical fiber signal processing and regeneration for soliton communications. IEEE J. on Selected Topics in Quantum Electron. vol. 3, no. 5, 1997: pp. 1208-1223.

REFERENCES (Continued)

[12] C. R. Giles and E. Desurvire. Propagation of signal and noise in concatenated Erbium-doped fiber optical amplifiers. J. Lightwave Technol., vol. 9, 1991: pp. 147-154.

[13] B. J. Ainslie. A review of the fabrication and properties of Erbium-doped fibers for optical amplifiers. J. Lightwave Technol. vol. 9, 1991: pp. 220-227.

[14] C. R. Giles and E. Desurvire. Modeling Erbium-doped fiber amplifiers. J. Lightwave Technol., vol. 9, 1991: pp. 271-283.

[15] M. Potenza. Optical fiber amplifiers for telecommunication systems. IEEE Communication Magazine. August, 1996: pp. 96-102.

[16] R. S. Tucker, G. Eisenstein, and S. K. Corotky. Optical time-division multiplexing for very high bit-rate transmission. J. Lightwave Technol., vol. 6, 1988: pp. 1737-1749.

[17] G. P. Agrawal. Nonlinear pulse distortion in single-mode optical fibers at the zero-dispersion wavelength. Phys. Rev. A, vol. 33, 1986: pp. 1765-1776.

[18] D. Marcuse. Single-channel operation in very long nonlinear fibers with optical amplifiers at zero dispersion. J. Lightwave Technol., vol. 9, 1991: pp. 356-361.

[19] T. Matsuda, A. Naka and S. Saito. 10Gbit/s, 6000km NRZ and 4400km RZ signal transmission experiments at zero-dispersion wavelength. Electron. Lett., vol. 32, 1996: pp. 229-231.

[20] D. Marcuse. Bit-error rate of lightwave systems at the zero dispersion wavelength. J. Lightwave Technol., vol. 9, 1991: pp. 1330-1334.

[21] N. Kikuchi and S.Sasaki. Fiber nonlinearity in dispersion-compensated conventional fiber transmission. Electron. Lett., vol. 32, 1996: pp. 570-572.

[22] R. J. Nuyts, Y. K. Park, and P. Gallion. Dispersion equalization of a 10Gbit/s repeatered transmission system using dispersion compensating fibers. J. Lightwave Technol., vol. 15, 1997: pp. 31-41.

[23] M. Murakami, T. Matsuda, H. Maeda, and T. Imai. Long-haul WDM transmission using higher order fiber dispersion management. J. Lightwave Technol., vol. 18, no. 9, 2000: pp. 1197-1204.

REFERENCES (Continued)

[24] M. Murakami, K. Suzuki, H. Maeda, T. Takahashi, A. Naka, N. Ohkawa, and M. Aiki. High speed TDM-WDM techniques for long-haul submarine optical amplifier systems. Optic. Fiber Technol., vol. 3, no. 4, 1997: pp. 320-338.

[25] X. Wang, K. Kikuchi, and Y. Takushima. Analysis of dispersion-managed optical fiber transmission system using non-return-to-zero pulse format and performance restriction from third-order dispersion. IEICE Trans. Electron., vol.E82-C, no.8, 1999: pp.1407-1413.

[26] K. Mukasa, R. Sugizaki, S. Hayami, and S. Ise. Dispersion-managed transmission lines with reverse-dispersion fiber. Furukawa Review, no. 19, 2000: pp. 5-9.

[27] C. Lin, H. Kogelnik, and L. G. Cohen. Optical-pulse equalization of low-dispersion transmission in single-mode fibers in the 1.3-1.7 μm spectral region. Opt. Lett., vol. 5, 1980: pp. 476-478.

[28] H. Izadpanah, C. Lin, J. L. Gimlett, A. J. Antos, D. W. Hall, and D. K. Smith. Dispersion compensation in 1310nm-optimized SMFs using optical equalizer fiber, EDFA's and 1310/1550nm WDM. Electron. Lett., vol. 28, 1992: pp. 1469-1471.

[29] H. Izadpanah, E. Goldstein, and C. Lin. Broadband multiwavelength simultaneous dispersion compensation near 1550nm through single-mode fiber optimized for 1310nm. Electron. Lett., vol. 29, 1993: pp. 364-365.

[30] A. R. Chraplyvy, A. H. Gnauck, R. W. Tkach, R. M. Derosier, C. R. Giles, B. M. Nyman, G. A. Ferguson, J. W. Sulhoff, and J. L. Zyskind. One-third terabit/s transmission through 150km of dispersion 150km of dispersion-managed fiber. IEEE Photon. Technol. Lett., vol. 7, 1995: pp. 98-100.

[31] S. Kawanishi, H. Takara, O. Kamatani, T. Morioka, and M. Saruwatari. 100Gbit/s 560km optical transmission experiment with 80km amplifier spacing employing dispersion management. Electron. Lett., vol. 32, 1996: pp. 470-471.

[32] N. Kikuchi and S.Sasaki. Fiber nonlinearity in dispersion-compensated conventional fiber transmission. Electron. Lett., vol. 32, 1996: pp. 570-572.

REFERENCES (Continued)

[33] R. J. Nuyts, Y. K. Park, and P. Gallion. Dispersion equalization of a 10Gbit/s repeatered transmission system using dispersion compensating fibers. J. Lightwave Technol., vol. 15, 1997: pp. 31-41.

[34] Stern, J. P. Heritage, R. N. Thurston, and S. Tu. Self-phase modulation and dispersion in high data rate fiber-optic transmission systems. J. Lightwave Technol., vol. 8, 1991: pp. 1009-1016.

[35] C. Kurtzke. Suppression of fiber nonlinearities by appropriate dispersion management. IEEE Photon. Technol. Lett., vol. 5, no. 10, 1993: pp. 1250–1253.

[36] A. Hasegawa and F. Tappert, " Transmission of stationary nonlinear optical pulses in dispersive dielectric fibers, " Appl. Phys. Lett., vol. 23, pp. 142-144, 1973.

[37] L. F. Mollenauer, R. H. Stolen, and J. P. Gordon. Experimental observation of picosecond pulse narrowing and soliton in optical fibers. Phys. Rev. Lett., vol. 45, 1980: pp. 1095-1098.

[38] N. J. Doran, and K. J. Blow. Solitons in optical communications. IEEE J. Quantum Electron., vol. QE-19, 1983: pp-1883-1888.

[39] M. Nakazawa, Y. Kimura, K. Suzuki. Soliton transmission at 20Gbit/s over 2000km in Tokyo metropolitan optical network. Electron. Lett., vol. 31, 1995: pp. 1478-1479.

[40] Y. Takushima, X. Wang, and K. Kikuchi. Transmission of 3ps dispersion-managed soliton pulses over 80km distance under influence of third-order dispersion. Electron. Lett., vol. 35, no. 9, 1999: pp.739-740.

[41] I. Morita, K. Tanaka, N. Edagawa, and M. Suzuki. 40Gbit/s single-channel soliton transmission over 10,200km without active inline transmission control. Proc. of 24th European Conference on Optical Communication (ECOC'98), Postdeadline paper, Madrid, Spain, Sept. 20-24, 1998: pp.49-51,

[42] A. Hasegawa and Y. Kodama. Guiding-center soliton in optical fibers. Opt. Lett., vol. 15, 1990: pp. 1443-1445.

REFERENCES (Continued)

[43] K. J. Blow and N. J. Doran. Average soliton dynamics and the operation of soliton systems with lumped amplifiers. IEEE Photon. Technol. Lett., vol. 3, 1991, pp. 369-371.

[44] L. F. Mollenauer, S. G. Evangelides, and H. A. Haus. Long-distance soliton propagation using lumped amplifiers and dispersion-shifted fiber. J. Lightwave Technol., vol. LT-9, 1991: pp. 194-197.

[45] Y. Kodama and K. Nozaki. Soliton interaction in optical fibers. Opt. Lett., vol. 12, 1987: pp. 1038-1040.

[46] J. P. Gordon and H. A. Haus. Random walk of coherently amplified solitons in optical fiber transmission. Opt. Lett., vol. 11, 1986: pp. 665-667.

[47] D. Marcuse. An alternative derivation of the Gordon-Haus effect. J. Lightwave Technol., vol. 10, 1992: pp. 273-278.

[48] C. Lorattanasane and K. Kikuchi. Design theory of long-distance optical transmission systems using midway optical phase conjugation. J. Lightwave Technol., vol. 15, 1997: pp. 948-955.

[49] K. Pasu, A. Tuptim, and K. Kikuchi. Feasibility of 100-Gb/s 10000-km single-channel optical transmission by midway optical phase conjugation in corporated with third-order dispersion compensation. IEEE Photon. Technol. Lett., vol. 13, no. 4, 2001: pp. 293–295.

[50] F. Matera, A. Mecozzi, M. Romagnoli and M. Settembre. Sideband instability induced by periodic power variation in long distance fiber links. Opt. Lett., 18, 1993: pp. 1499-1501.

[51] K. Pasu and A. Tuptim. Sideband instability in the presence of periodic power variation and periodic dispersion management. Proc. Opt. Fiber Comm. (OFC'2001), Anaheim, CA, Mar. 17-22, 2001: paper WDD32.

[52] K. Pasu, A. Tuptim, and K. Kikuchi. Complete analysis of sideband instability in chain of periodic dispersion-managed fiber link and its effect on higher-order dispersion-managed long-haul wavelength division multiplexed systems. OSA/IEEE J. Lightwave Technol., vol. 20, no. 11, 2002: pp. 1895-1907.

REFERENCES (Continued)

[53] Y. Takushima, X. Wang, and K. Kikuchi. Transmission of 3ps dispersion-managed soliton pulses over 80km distance under influence of third-order dispersion. Electron. Lett., vol.35, no.9, 1999: pp.739-740.

[54] I. Morita, K. Tanaka, N. Edagawa, and M. Suzuki. 40Gbit/s single-channel soliton transmission over 10,200km without active inline transmission control. Proc. 24th European Conference on Optical Communication (ECOC'98), Postdeadline paper, Madrid, Spain, Sept. 20-24, 1998: pp.49-51.

[55] C. Lorattanasane and K. Kikuchi. Design theory of long-distance optical transmission systems using midway optical phase conjugation. J. Lightwave Technol., vol. 15, 1997: pp. 948-955.

[56] H. C. Lim, F. Futami, K. Taira, and K. Kikuchi. Broad-band mid-span spectral inversion without wavelength-shift of 1.7-ps optical pulses using a highly-nonlinear fiber Sagnac interferometer. IEEE Photon. Technol. Lett., vol. 11, 1999: pp. 1405-1407.

[57] H. C. Lim and K. Kikuchi. A filter-free scheme for orthogonally-pumped, polarization-insensitive optical phase conjugation of broad-band optical signals. IEEE Photon. Technol. Lett., vol. 13, no. 5, 2001: pp. 481-483.

[58] F. Matera, A. Mecozzi, M. Romagnoli and M. Settembre. Sideband instability induced by periodic power variation in long distance fiber links. Opt. Lett., 18, 1993: pp. 1499-1501.

[59] J. P. Gordon and L. F. Mollenauer. Phase noise in photonic communications systems using linear amplifiers. Opt. Lett., 15, 1990: pp. 1351-1353.

[60] S. Ryu. Signal linewidth broadening due to fiber nonlinearities in long-haul coherent optical fiber communication systems. Electron. Lett., 27, 1991: pp. 1527-1529.

[61] S. Ryu. Signal linewidth broadening due to nonlinear Kerr effect in long-haul coherent systems using cascaded optical amplifiers. J. Lightwave Technol., 1992: pp. 1450-1457.

[62] D. Marcuse. Bit-error rate of lightwave systems at the zero dispersion wavelength. J. Lightwave Technol., 9, 1991: pp. 1330-1334.

REFERENCES (Continued)

[63] D. Marcuse. Single-channel operation in very long nonlinear fibers with optical amplifiers at zero dispersion. J. Lightwave Technol., 9, 1991: pp. 356-361.

[64] S. Ryu. Change of field spectrum of signal light due to fiber nonlinearities and chromatic dispersion in long-haul coherent systems using in-line optical amplifiers. Electron. Lett., 28, 1992: pp. 2212-2213.

[65] K. Kikuchi. Enhancement of optical-amplifier noise by nonlinear refractive index and group-velocity dispersion of optical fibers. IEEE Photon. Technol. Lett., 5, 1993: pp. 221-223.

[66] C. Lorattanasane and K. Kikuchi. Parametric instability of optical amplifier noise in long-distance optical transmission systems. IEEE J. Quantum Electron., 33, 1997: pp. 1068-1074.

[67] P. Kaewplung, T. Angkaew, and K. Kikuchi. Simultaneous suppression of third-Order dispersion and sideband instability in single-channel optical fiber transmission by midway optical phase conjugation systems employing higher-order dispersion management. IEEE/OSA J. Lightwave Technol., vol. 21, no. 6, 2003: pp. 1465-1473.

[68] S. Watanabe and M. Shirasaki. Exact compensation for both chromatic dispersion and Kerr effect in a transmission fiber using optical phase conjugation. J. Lightwave Technol., vol. 14, 1996: pp. 243-248.

[69] N. J. Smith and N. J. Doran. Modulation instability in fibers with periodic dispersion management. Opt. Lett., vol. 21, 1996: pp. 570-572.

PUBLICATIONS

International Periodical Journals

- **P. Kaewplung**, W. Kasantikul, P. Jarupoom, E. Tangdamrongtham, T. Ratanasopitkul, and N. Raopattananon, " Numerical comparison among dispersion compensating schemes in upgrading installed long-haul electronic-repeated optical fiber transmission system to optically amplified system: Case study of Thailand-Malaysia submarine fiber-optic line," *Submitted to IEICE transaction on communications.*

International Conferences

- **P. Kaewplung** and W. Kasantikul, "Performance Upgrading of Thailand-Malaysia Submarine Fiber-Optic System Using Optically Amplification and Optimized Zero-dispersion Transmission Scheme, " *in Proc. IEEE Asia-Pacific Communication Conference (APCC'2003)*, Penang, Malaysia, September 21-24, 2003.
- **P. Kaewplung** and W. Kasantikul, " Simple and practical approaches for upgrading installed electronic-repeater-based fiber systems to optically amplified systems, " *in Proc. Opto-Electronic Communication Conference (OECC'2003)*, Shianghai, China, October 13-16, 2003.
- **P. Kaewplung**, and N. Raopattananon, " Performance upgrading of single-channel electronic-repeated fiber-optic system using optical amplification and midway optical phase conjugation, " *in Proc. 2004 Opto-Electronic Communication Conference (OECC'2004)*, Yokohama, Japan, July 12-16, 2004, paper 13P39.
- **P. Kaewplung**, and P. Jarupoom, " Performance improvement of electronic-repeated fiber-optic transmission system using optical amplification and dispersion Management, " *To be presented in 2004 IEEE 10th Region Analog and Digital Techniques in Electrical Engineering Conference (TENCON'2004)*, Chiang Mai, Thailand, November 21-24, 2004.

PUBLICATIONS (Continued)

Domestic Conferences

- **P. Kaewplung**, and T. Ratanasopitkul, "Optical soliton transmission in upgrading electronic-repeated single-channel long-haul system, "*in Proc. 27th Electrical engineering conference (EECON'27)*, Khon Kaen, Thailand, November 11-12, 2004, paper CM01.

Performance Upgrading of Thailand-Malaysia Submarine Fiber-Optic System Using Optically Amplification and Optimized Zero-dispersion Transmission Scheme

Pasu Kaewplung and Wadis Kasantikul.
Department of Electrical Engineering, Faculty of Engineering, Chulalongkorn University,
Payathai Rd., Pathumwan, Bangkok 10330, Thailand
Phone (66-2)218-6907, Fax (66-2)218-6912, E-mail : pasu@ee.eng.chula.ac.th

Abstract— **We propose simple and practical approaches to upgrade electronic-repeated systems by using optical amplifiers and zero-dispersion wavelength transmission. Possibility of increasing data rate from 560 Mbit/s to 80 Gbit/s in 1,318-km-long Thai-Malaysia system is demonstrated.**

Keywords-optical fiber transmission, fiber nonlinearity, dispersion, zero dispersion wavelength, third-order dispersion, dispersion compensation

I. INTRODUCTION

Rapid growth on both transmission bit rate and distance in this decade is very remarkable. Transmission of data rate as high as 1 Tbit/s over 10,000 km has been demonstrated [1]. However, at presence, there exists many installed fiber systems which still operate with electronic repeaters at very low bit rate. Such systems need to be upgraded to response the demand for increasing the transmission capacity in the future.

In this paper, we present simple and practical approaches, together with design schemes for achieving the maximum performance, for upgrading such systems using the zero-dispersion wavelength (ZDWL) transmission and the optical amplification. To our knowledge, this is the first time that the design guideline for the ZDWL transmission is presented. Following our guidance, the possibility of increasing data rate in the 1,318-km-long Thai-Malaysia submarine system from 560 Mbit/s to 80 Gbit/s is numerically shown.

II. DESIGN FOR ACHIEVING MAXIMUM PERFORMANCE IN ZERO-DISPERSION WAVELENGTH TRANSMISSION

The advantage of the zero-dispersion system to other types of systems mainly originates from its simplicity of system configuration. By only placing the carrier wavelength at ZDWL of optical fiber, the limitation of the system performance due to the fiber dispersion is easily overcome. However, for long-haul high-speed transmission, strong self-phase modulation (SPM) effect, as well as the third-order dispersion (TOD) at ZDWL cause serious problems to the signal transmission [2]-[4], resulting in poorer performance compared to other nonzero-dispersion systems. Nevertheless, we present here that the ZDWL transmission using optical amplifiers with optimum design is very simple and very cost-performance scheme for sufficiently increasing the data rate of the installed fiber systems.

In order to break through the electronic bottle-neck, the first step of upgrading is to replace the electronic repeaters with the optical amplifiers. Then, the second step is to find the optimum input signal power and the optimum bandwidth of an optical bandpass filter (OBPF) which give the maximum performance of the system. The increase in input signal power improves the signal-to-noise-ratio (SNR) at a receiver, at the same time, results in the system penalty due to the SPM. The optimum power will exist at the balance point of these improvement and degradation. On the other hand, since the SPM causes rapid spectrum broadening at ZDWL, the maximum system performance will be reached when we use the OBPF with an appropriate bandwidth that collects all signal spectra with the least amount of noise.

For overcoming the signal distortion induced from the TOD, the third step is to calculate the TOD length (L_{d3}) and the nonlinear length of the system (L_{nl}), which are defined in [3]. These characteristic lengths can be interpreted as the distance where those effects become significant. When L_{d3} is longer than system length, no TOD compensator is needed. On the other hand, if L_{d3} is shorter than the system length, we have to install the TOD compensators distributedly at the length shorter than L_{nl} to avoid the interplay between the TOD and the SPM. To further increase the data rate, the span should be shortened in order to obtain good SNR with the use of low input signal power. Then, the SPM effect is consequently reduced.

III. COMPUTER SIMULATIONS

To demonstrate the efficiency of our proposed upgrading scheme, we consider the Thai-Malaysia submarine system as the simulation model. The system starts from Petchburi, Thailand, ends at Chugai, Malaysia, with total length of 1,318

0-7803-8114-9/03/$17.00 ©2003 IEEE.

km. The fiber is the dispersion-shifted fiber (DSF). The electronic repeaters are periodically placed at a span of 100 km with the last span of 118 km. The system operates with single channel with the data rate of only 560 Mbit/s.

In the simulations, the optical signal is composed of a 32-bit pseudorandom RZ Gaussian pulse train with a duty cycle of 0.5. The fiber loss coefficient, the TOD, and the fiber nonlinear coefficient of DSF, respectively, are typical values of 0.2 dB, 0.06 ps/km/nm, and 2.6 $W^{-1}km^{-1}$. The dispersion is assumed to randomly fluctuate around ZDWL point every 2 km with a standard deviation of 0.5 ps/km/nm. The optical amplifier produces noise in process of amplification with a noise figure of 5.3 dB. At the end of system, the bandwidth adjustable OBPF is placed. The TOD compensator is an ideal device that multiplies the signal with negative amount of linearly accumulated phase shift caused by TOD.

The propagation of the optical pulse is calculated by solving the nonlinear Schrodinger (NLS) equation by the split-step Fourier method (SSFM) [14]. The integration step size of SSFM is always chosen at the value that gives a step size error less than 0.01 % [17]. The receiver is modeled by a sixth-order Bessel-Thompson low-pass filter, followed by a BER detector. The system performance is evaluated in terms of the numerical bit-error rate (BER). The bandwidth of the OBPF is always adjusted to obtain the minimum BER. To calculate the numerical BER of the detected signal, the simulation is repeated 128 times for the same pseudo-random pulse train. The numerical Q factor of every bit is then individually calculated at the maximum eye-opening point of the bit period. Based on the assumption of the Gaussian noise distribution, the numerical BER is computed from the bit numerical Q factor and is averaged over the entire bits [18].

A. 40-Gbit/s Data Ttransmission

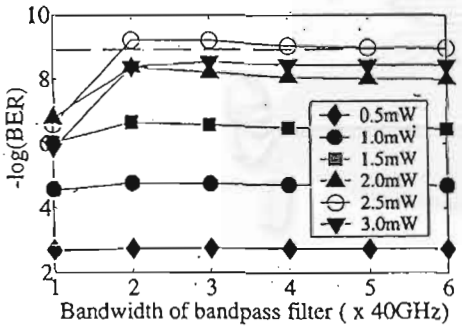

Figure 1. Numerical BER of the transmitted 40-Gbit/s signal as a function of OBPF bandwidth for several input signal powers.

We start the simulation with the data rate of 40 Gbit/s, which is the bottle-neck speed of the electronic repeaters. Figure 1 shows the numerical BER of the transmitted 40-Gbit/s signal as a function of OBPF bandwidth for several input signal powers. The minimum BER is obtained with the optimum power of 2.5 mW (shown by spaced circles) and the OBPF bandwidth of 80 GHz. In Figure 1, the BER are obtained without using TOD compensator. With defining BER = 10^{-9}, which is commonly used for the limitation in lightwave systems, as the system limitation, the Thai-Malaysia system can be upgraded for 40-Gbit/s data transmission by only using ZDWL and replacing electronic repeaters with optical amplifiers.

Figure 2(b) shows the 40-Gbit/s signal using the input power of 2.5 mW and the bandwidth of the OBPF of 80 GHz, compared with its input waveform shown in Fig. 2(a). The signal which is composed of a 32-bit pseudorandom RZ Gaussian pulse train with a full-width at the half maximum (FWHM) of 12.5 ps (duty cycle = 0.5). From Fig. 2, sufficiently good output signal waveform is observed.

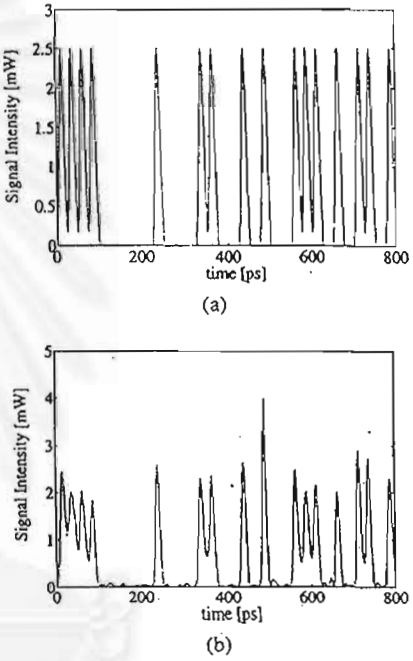

Figure 2. (b) Output waveform of this 40-Gbit/s signal using the input power of 2.5 mW and the bandwidth of the OBPF of 80 GHz, compared with (a) its input waveform. The signal is composed of a 32-bit pseudorandom RZ Gaussian pulse train with a full-width at the half maximum (FWHM) of 12.5 ps (duty cycle = 0.5)

For this 40 Gbit/s data transmission, the employment of TOD compensator may not give significant improvement of the BER since L_{d3} (= 4,430 km) is much longer than the system length. Therefore, in this case, the TOD still does not appear to affect the signal propagation. Figure 3 shows the BER of the transmitted 40-Gbit/s signal with the input power of 2.5 mW, as a function of OBPF bandwidth when the TOD compensators are used in several schemes, compared with the SNR-limited BER (shown by spaced circles), the BER where the TOD is neglected (shown by squares), and the BER

without the TOD compensation (shown by reversed triangles). It should be noted that the SNR-limited BER is calculated by neglecting the nonlinear coefficient of the DSF and performing the TOD compensation at the end of the system. As predicted, the use of 13 TOD compensators placed distributedly at the output of every amplifier (shown by diamonds) or the use of only one TOD compensator at the end of the system (shown by triangles) can only slightly improve BER. This result mentions that the TOD compensation is still not necessary at this speed of data transmission.

When the TOD is completely neglected (shown by squares), the BER becomes the worst because the TOD intrinsically causes the decrease of optical signal peak power and the asymmetrical broadening of optical signal pulse, therefore, the existance of TOD along the transmission can help reducing the nonlinear waveform distortion caused by the SPM effect which is very strong in the ZDWL transmission scheme. Also, the difference in BER between the SNR-limited BER and the TOD-compensated BER originates from the signal waveform distortion induced by the SPM effect

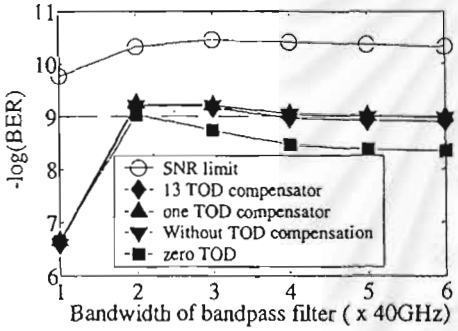

Figure 3. BER of the transmitted 40-Gbit/s signal with the input power of 2.5 mW, as a function of OBPF bandwidth when the TOD compensators are used in several schemes, compared with the SNR-limited BER, the BER where the TOD is neglected, and the BER without TOD compensation.

B. 80-Gbit/s Data Ttransmission

To explore whether the system is capable for higher transmission rate, we perform the computer simulation based on the signal with a data rate of 80 Gbit/s. Figure 4 shows the numerical BER of the 80-Gbit/s signal after transmission, as a function of OBPF bandwidth for several input signal powers. The BER less than 10^{-9} cannot be obtained for all input powers and all OBPF bandwidth values. This is due to large amount of noise is generated through the very high amplifier gain in order to compensate the fiber loss in relatively long amplifier spacing (100 km). The noise will be strongly enhanced by the SPM effect induced the conversion of amplitude, noise components to phase noise components along the transmission in ZDWL [2]-[4]. This results in rapid signal spectral broadening and consequently brings large amount of noise entering the receiver.

In order to achieve the BER less than 10^{-9} for the transmission of this data rate, the first strategy is to reduce the amplifier span to 50 km with last span of 68 km. This will require the use of the optical amplifiers double in number. Figure 5 shows the results of the 80-Gbit/s data transmission using the 50-km span for several input signal power as a function of the bandwidth of the OBPF. From Fig. 5, the optimum power is 1 mW and the optimum OBPF bandwidth is 80 GHz. It should be noted that the optimum power of this data rate is lower than that of the data rate of 40 Gbit/s because the improvement in the SNR due to the use of shorter span. However we cannot achieve BER < 10^{-9} with these optimum parameters. This is mainly resulted from the TOD because L_{d3} (= 554 km) becomes shorter than the system length.

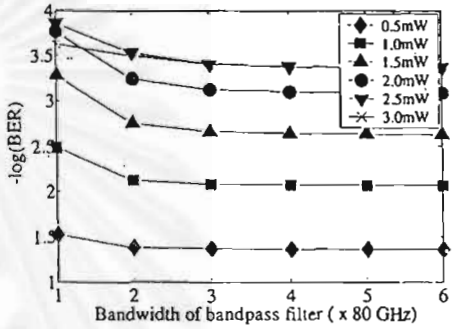

Figure 4. Numerical BER of the 80-Gbit/s signal after transmission, as a function of OBPF bandwidth for several input signal powers.

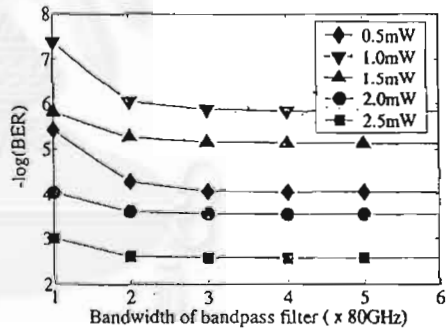

Figure 5. Numerical BER of the 80-Gbit/s signal after transmission with the amplifier span is reduced to 50 km, as a function of OBPF bandwidth for several input signal powers.

In order to improve the BER characteristic of the data transmission at bit rate of 80 Gbit/s, we investigate the transmission performance of the system when the TOD is compensated. Figure 6 shows the BER of the transmitted 80-Gbit/s signal with the input power of 1.0 mW and the span of 50 km as a function of OBPF bandwidth when the TOD compensators are used in several schemes, compared with the SNR-limited BER (shown by reversed triangles), the BER

where the TOD is neglected (shown by circles), and the BER without the TOD compensation (shown by diamonds).

From the results in Fig. 6, the use of only one TOD compensator placed at the end of system (shown by squares) can significantly improve the BER to be lower than 10^{-9}. The minimum BER for this case obtained by setting the bandwidth of the OBPF at 240 GHz. Since L_{nl} for the 1-mW input power is 980 km, the placement of TOD compensators at the output end of each amplifier (shown by triangles) yields better BER because the accumulated the TOD is reset before turning to interplay with the SPM. However, when the use of only one TOD compensator gives the BER less than 10^{-9}, we should use only one TOD compensator in order to help reducing the system cost. The output of the signal with the data rate of 80 Gbit/s using the input power of 1 mW, the bandwidth of OBPF of 240 GHz, the 50-km amplifier span with one TOD compensator placed at the end of system is shown in Fig. 7

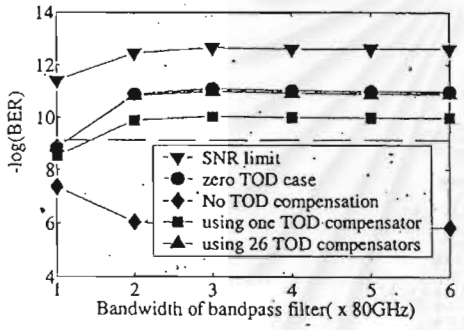

Figure 6. BER of the transmitted 80-Gbit/s signal with the input power of 1.0 mW and the amplifier span of 50 km, as a function of OBPF bandwidth when the TOD compensators are used in several schemes, compared with the SNR-limited BER, the BER where the TOD is neglected, and the BER without TOD compensation.

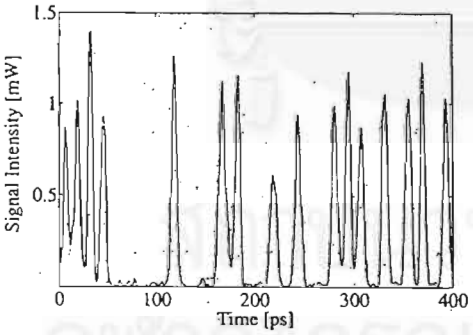

Figure 7. Output of the signal with data rate of 80 Gbit/s using the input power of 1 mW, the bandwidht of OBPF of 240 GHz, the 50-km amplifier span with one TOD compensator placed at the end of system.

C. 100-Gbit/s Data Transmission

We further investigate for the possibility of the transmission at higher data rate of 100 Gbit/s. Figure 8 shows the BER of the 100-Gbit/s signal at the output of the system where the amplifier is chosen at 50 km, and the TOD is not compensated. The BER is shown as a function of the bandwidth of OBPF with several input signal powers. The optimum input signal power, found from Fig. 8, is 1.0 mW. However, we cannot reach the BER below 10^{-9} with this input power.

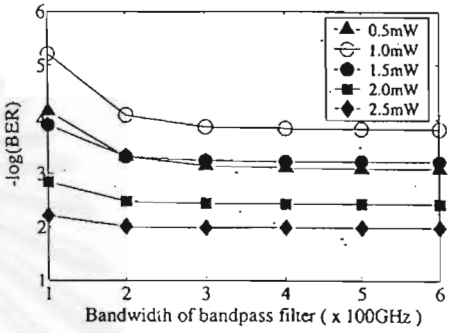

Figure 8. BER of the 100-Gbit/s signal at the output of the system as a function of the bandwidth of OBPF with several input signal powers. The amplifier is 50 km, and the TOD is not compensated.

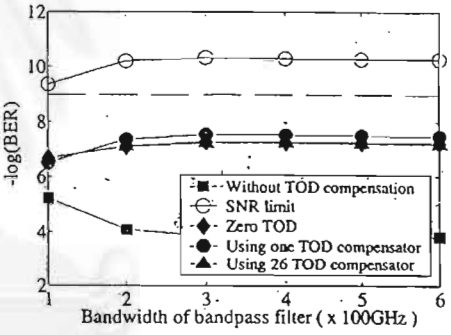

Figure 9. BER of the 100-Gbit/s signal using the optimum power of 1.0 mW, the TOD compensation in several schemes, and the span of 50 km as a function of OBPF bandwidth.

Next, we employ the TOD compensators to the system. Figure 9 shows the BER of the 100-Gbit/s signal using the optimum power of 1.0 mW, the TOD compensators, and the span of 50 km as a function of OBPF bandwidth. In Fig. 9, although the TOD compensators are employed, the minimum BER we achieved is about 10^{-7}, which is not a sufficient value for the optical data transmission we expected. The main problem that causes limitation on this ultra-high bit rate transmission is the degradation from the SPM effect. To achieve such ultra-high bit rate transmission as well as to further increase in the bit rate of this system, some strategies

for reducing the SPM such as the dispersion management concept [5] should be employed.

IV. Conclusion

Performance improvement of electronic-repeated fiber systems by using optical amplifiers and optimum-designed ZDWL transmission is investigated by computer numerical simulation. We took into account the Thai-Malasia submarine fiber-optic line, which has a length of 1,318 km and a 100-km repeater span, for system model. By only replacing the electronic-repeaters with the optical amplifiers, we demonstrated that the transmission bit rate can be increased from 560 Mbit/s to 40 Gbit/s. Moreover, with reducing the amplifier span to be 50 km and employing only one TOD compensator at the end of the system, we also demonstrated the possibility of the optical data transmission at a data rate as high as 80 Gbit/s.

References

[1] T. Naito, N, Shimojoh, T. Tanaka, H. Nakamoto, M. Doi, T. Ueki, and M. Suyama, " 1 Terabit/s WDM transmission over 10,000km, " in Proc. European Conf. on Opt. Commun. (ECOC'99), Nice France, Sept. 26-30, PD2-1, pp. 24-25, 1999.

[2] D. Marcuse, " Single-channel operation in very long nonlinear fibers with optical amplifiers at zero dispersion , " J. Lightwave Technol., vol. 9, pp. 356-361, 1991.

[3] G. P. Agrawal, Nonlinear Fiber Optics (New York, Academic Press, 3rd edition, 2001).

[4] C. Lorattanasane and K. Kikuchi, " Parametric instability of optical amplifier noise in long-distance optical transmission systems, " J. Quantum Electron., vol. 33, pp. 1068-1074, 1997.

[5] X. Wang, K. Kikuchi and Y. Takushima, "Analysis of Dispersion-Managed Optical Fiber Transmission System Using Non-Return-to-Zero Pulse Format and Performance Restriction from Third-Order Dispersion," IEICE Trans. Electron. , Vol.E82-C, No.8, 1999.

Simple and Practical Approaches for Upgrading Installed Electronic-Repeater-Based Fiber Systems to Optically Amplified Systems

Pasu Kaewplung and Wadis Kasantikul

Department of Electrical Engineering, Faculty of Engineering, Chulalongkorn University,

Phayathai Rd., Pathumwan, Bangkok 10330, Thailand.

Phone: (66-2)218-6907, Fax: (66-2)218-6912, E-mail : pasu@ee.eng.chula.ac.th

Abstract

We propose simple and practical approaches to upgrade electronic-repeated systems by using optical amplifiers and zero-dispersion wavelength transmission. Possibility of increasing data rate from 560 Mbit/s to 80 Gbit/s in 1,318-km-long Thai-Malaysia system is demonstrated.

1 Introduction

Rapid growth on both transmission bit rate and distance in this decade is very remarkable. Transmission of data rate as high as 1 Tbit/s over 10,000 km has been demonstrated [1]. However, at present, there exists many installed fiber systems which still operate with electronic repeaters at very low bit rate. Such systems need to be upgraded to response the demand for increasing transmission capacity in the future. In this paper, we present simple and practical approaches, together with design schemes for achieving maximum performance, for upgrading such systems using zero-dispersion wavelength (ZDWL) transmission and optical amplification. To our knowledge, this is the first time that the design guideline for ZDWL transmission is presented. Following our guidance, the possibility of increasing data rate in 1,318-km-long Thai-Malaysia submarine system from 560 Mbit/s to 80 Gbit/s is numerically shown.

2 Design for achieving maximum performance in Zero-dispersion wavelength transmission

The advantage of the zero-dispersion system to other types of systems mainly originates from its simplicity of system configuration. By only placing carrier wavelength at ZDWL of optical fiber, the limitation of system performance due to fiber dispersion is easily overcome. However, for long-haul transmission, strong self-phase modulation (SPM) effect, as well as the third-order dispersion (TOD) at ZDWL cause serious problems to signal transmission [2], [3], resulting poorer performance compared to other nonzero-dispersion systems. Nevertheless, we present here that the ZDWL transmission using optical amplifiers with optimum design is the most cost-performance scheme for sufficiently increasing data rate of installed fiber systems.

In order to break through the electronic bottle-neck, the first step of upgrading is to replace electronic repeaters with optical amplifiers. Then, the second step is to find the optimum input signal power and the optimum bandwidth of optical bandpass filter (OBPF) which give maximum performance of system. The increase in input signal power improves the signal-to-noise-ratio (SNR) at receiver, at the same time, results in system penalty due to the SPM. The optimum power exists at the balance point of these improvement and degradation. On the other hand, since the SPM causes rapid spectrum broadening at ZDWL, the maximum system performance will be reached when we use the OBPF with appropriate bandwidth that collects all signal spectra with the least noise. The third step is to calculate the TOD length (L_{d3}) and the nonlinear length of the system (L_{nl}), defined in [3]. These characteristic lengths can be interpreted as the distance where those effects become significant. When L_{d3} is longer than system length, no TOD compensator is needed. On the other hand, if L_{d3} is shorter than the system length, we have to install the TOD compensators distributedly at the length shorter than L_{nl} to avoid the interplay between TOD and SPM. To further increase the data rate, the span should be shortened to obtain good SNR with the use of low input power. Then, the SPM effect is consequently reduced.

3 Computer simulations

To demonstrate the efficiency of our proposed upgrading scheme, we consider the Thai-Malaysia submarine system as the simulation model. The system starts from Petchburi, Thailand, ends at Zugaai, Malaysia, with total length of 1,318 km. The fiber is dispersion-shifted fiber (DSF). The electronic repeaters are periodically placed at span of 100 km with the last span 118 km. The system operates with single channel with the data rate of only 560 Mbit/s. In the simulations, the optical signal is 32-bit pseudorandom Gaussian RZ pulses. The fiber loss coefficient, the TOD, and the fiber nonlinear coefficient of DSF are 0.2 dB, 0.06 ps/km/nm, and 2.6 $W^{-1}km^{-1}$, respectively. The dispersion is assumed to randomly fluctuate around ZDWL point every 2 km with standard deviation of 0.5 ps/km/nm. The optical amplifier produces noise in process of amplification with noise figure of 5.3 dB. At the end of system, the bandwidth adjustable OBPF is placed. The TOD compensator is an ideal device that multiplies the signal with negative amount of linearly accumulated phase shift caused by TOD. The propagation of the optical pulse is calculated by solving the nonlinear Schrodinger equation by the split-step Fourier method [3]. The receiver is modeled by electronic low-pass filter followed by a BER detector. The system performance is evaluated in terms of bit-error rate (BER) calculated by repeating 128 times the transmission of the same signal and assuming Gaussian distribution of noise.

Figure 1 shows the BER of transmitted 40-Gbit/s signal as a function of OBPF bandwidth for several cases. Without TOD compensator, the minimum BER is obtained with the optimum power 2.5 mW and the OBPF bandwidth 80 GHz. Since L_{d3} (= 4,430 km) is longer than the system length, the use of TOD compensator can only slightly improve BER. With defining BER = 10^{-9} as system limitation, the Thai-Malaysia system can be upgraded for 40-Gbit/s data transmission by only using ZDWL and replacing electronic repeaters with optical amplifiers.

To further increase data rate, we reduce amplifier span to be 50 km with last span of 68 km. Figure 2 shows the results of the 80-Gbit/s data transmission using 50-km span for several cases. The optimum power is 1 mW and the optimum OBPF bandwidth is 240 GHz. However we cannot achieve BER < 10^{-9} with these optimum parameters. This is mainly resulted from the TOD because L_{d3} (= 554 km) becomes shorter than the system length. The use of only one TOD compensator placed at the end of system can significantly improve BER to be lower than 10^{-9}. However, since L_{nl} for 1-mW input power is 980 km, the placement of TOD compensators at each span yields better BER because the accumulated the TOD is reset before turning to interplay with the SPM. We also explore the data rate of 100 Gbit/s, however, the best BER we obtain is about 10^{-7}.

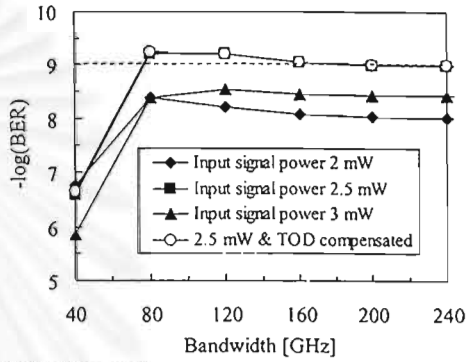

Fig. 1: BER of transmitted 40-Gbit/s signal as a function of bandwidth of OBPF for several cases.

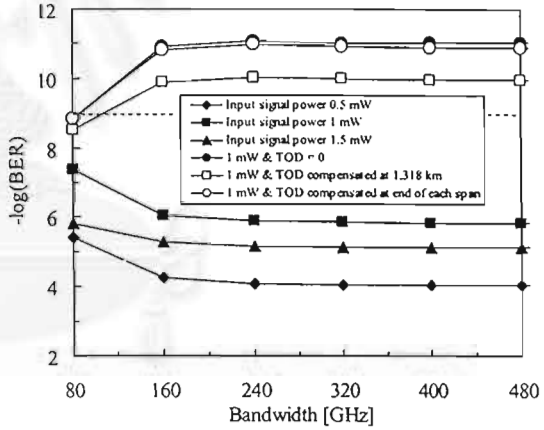

Fig. 2: BER of transmitted 80-Gbit/s signal as a function of bandwidth of OBPF for several cases.

4 Conclusion

Performance improvement of electronic-repeated fiber systems by using optical amplifiers and ZDWL transmission has been discussed. We have numerically demonstrated that the data rate of the 1,318-km-long Thai-Malaysia submarine system can be easily increased from 560 Mbit/s to 80 Gbit/s.

5 References

[1] T. Naito, et al., Proc. ECOC'99, PD2-1, pp. 24-25, 1999.

[2] D. Marcuse, J. Lightwave Technol., pp. 356-361, 1991.

[3] G. P. Agrawal, Nonlinear Fiber Optics, Academic Press, 2001.

PERFORMANCE IMPROVEMENT OF ELECTRONIC-REPEATED FIBER-OPTIC TRANSMISSION SYSTEM USING OPTICAL AMPLIFICATION AND DISPERSION MANAGEMENT

Pasu Kaewplung and Preeda Jarupoom

Department of Electrical Engineering, Faculty of Engineering, Chulalongkorn University,
Payathai Rd., Pathumwan, Bangkok 10330, Thailand
Phone (66-2)218-6907, Fax (66-2)218-6912, E-mail : Pasu.K@Chula.ac.th

ABSTRACT

We numerically study the use of optical amplification and dispersion management for upgrading single-channel electronic-repeated optical fiber system. The increase in data rate from 560 Mbit/s to 100 Gbit/s in 1,318-km-long Thailand-Malaysia system becomes feasible when the system is optimally designed.

1. INTRODUCTION

Rapid growth on both transmission bit rate and distance in this decade is very remarkable. Transmission of data rate as high as 1 Tbit/s over 10,000 km has been demonstrated [1]. However, at presence, there exists many installed fiber systems, which still operate with electronic repeaters at very low bit rate. Such systems need to be upgraded to response the demand for increasing the transmission capacity in the future.

When the electronic repeaters are replaced with optical amplifiers in long-haul high-speed system, the waveform distortion induced from fiber dispersion and nonlinearity cannot be removed from the signal because the optical amplifiers can only amplify the signal. As a result, when we upgrade the electronic-repeated to the optically-amplified system, efficient methods for compensating such signal distortions must be employed.

The zero-dispersion wavelength (ZDWL) transmission scheme [2], [3] is to set an operation wavelength of the system at zero-second-order dispersion (SOD) wavelength of the transmission fiber, so that the pulses can propagate without broadening. However, in the absence of the SOD, the fiber nonlinearity, especially the Kerr effect [3], becomes a serious problem that limits the system performance. The spectra of the signal transmission zero-dispersion wavelength will be rapidly broadened by the self-phase modulation (SPM) [3] and four-wave mixing (FWM) [3], both induced from the Kerr effect.

The dispersion management (DM) [4] is to arrange the various sections of fiber in such a way that none or only very few of them have zero SOD wavelengths that coincide with the carrier wavelength while the total fiber exhibits zero SOD on average. Because the SOD exists along the transmission, we can achieve the compensation of the SOD and, at the same time, the reduction of fiber nonlinearity with this method.

0-7803-8560-8/04/$20.00©2004IEEE

In this paper, we numerically investigate the effectiveness of the optical amplification and the DM in upgrading the electronic-repeated 1,318-long Thailand-Malaysia (T-M) system. By designing systems to work at optimum conditions, the possibility of increasing data rate in single-channel transmission from 560 Mbit/s to 80 Gbit/s without reducing the amplifier span, or to 100 Gbit/s with reducing the span to be a half, are demonstrated by computer simulations.

2. DESIGN FOR ACHIEVING MAXIMUM PERFORMANCE IN DM TRANSMISSION

The concept of DM is to cancel the accumulated positive value of dispersion by using negative value of dispersion. This can be implemented by using the combination of the transmission fibers and the dispersion compensating fibers or devices.

The transfer function is a powerful method for roughly designing the DM systems. The transfer function can be derived by using the small-signal approximation [4]. In this paper, since we consider the T-M system as the simulation model for demonstrating the efficiency of the upgrading scheme, in this section, we calculate the transfer function of the T-M system when the DM is employed using the T-M system parameters.

The T-M system starts from Petchburi, Thailand, ends at Zugaai, Malaysia, with total length of 1,318 km. The transmission fiber is the dispersion-shifted fiber (DSF). The electronic repeaters are periodically placed at span: L_a of 100 km with the last span of 118 km. The system operates in single channel with the data rate of only 560 Mbit/s.

In the calculation, we assume the typical parameter of DSF. The fiber loss coefficient and the nonlinear coefficient of DSF are 0.2 dB/km and 2.6 $W^{-1}km^{-1}$, respectively. The SOD: D for transmission is -0.2 ps/km/nm. The DM period: l_d is the same as the amplifier span of 100 km. The DM is done by reseting the accumulated SOD with the SOD compensator that is assumed to be a module installed in the optical amplifier. The path-averaged power within a 100-km amplifier span is 0.7 mW. We calculate the transfer function for

only 12 amplifiers (1,200 km) because the last amplifier spacing is 118 km, which is not the period of 100 km.

Figure 1 shows the transfer functions for amplitude modulation components: T_a and phase modulation components: T_b, as a function of signal frequency. The ideal transmission is given by $T_a = 1$ and $T_b = 0$, where the signal distortion as well as the enhancement of noise do not appear. In Fig. 1, T_a reduces to its minimum point below 1 at a specific frequency. We should define that point as the transmission window of the system. This is because the signal frequency exceeding this point cannot transmit without distortion. If we assume that the modulation bandwidth of the signal does not exceed this window and the receiver can accept all the optical power within the window, the demodulated signal will not suffer severe distortion except the enhancement of the phase noise because $T_b > 1$ in the transmission window. However, similar to the case of the ZDWL transmission, within the transmission window, the exchange between the amplitude modulation components and the phase modulation components will not occur. For the system setting, the result from Fig. 1 indicates the possibility of about 40-Gbit/s data transmission on T-M system when the DM is employed.

The transmission window width obtained from Fig. 1 is very important parameter for evaluating the transmission performance of a DM system. Figure 2 shows how the window width varies with the changes in l_d and signal power. To obtain this figure, all parameters are the same as those used in Fig. 1. The signal power shown in Fig. 2 is the path-averaged power for amplifier spacing of 100 km. It should be noted that the minimum signal power required for signal transmission is determined by the signal-to-noise ratio (SNR) limit of the receiver.

Furthermore, figure 2 shows that the transmission window width greatly increases with the reduction in l_d, but slightly decreases with the increase in signal power. The use of smaller l_d yields wider window width. However, with very small l_d, the signal feels like propagating at exact ZDWL, therefore, all the problems occuring in ZDWL transmission will also cause the signal distortion in DM system. Thus, for design point of view, we should design the window width as small as the signal bandwidth to achieve the undistorted transmission and, at the same time, reduce the enhancement of noise and other signal distortions from fiber nonlinearity.

For long-haul, high-speed transmission, relatively low D is also required to increase the window width. This can be achieved by placing the carrier wavelength near ZDWL. In fact, the concept of transfer function does not account for the signal spectral broadening due to FWM through the enhancement of phase noise and the random fluctuation of D, which turns to interplay with the Kerr effect when the carrier wavelength of the DM system is located near ZDWL. Thus, for detail design of DM system, the optimum combination of three main operating parameters: l_d, D, and the signal power, should be obtained by computer simulations.

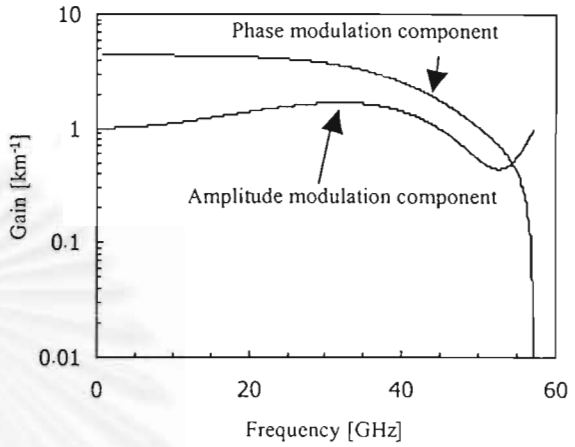

Figure 1: Transfer function characteristics of amplitude modulation components and phase modulation components in the T-M system employing DM.

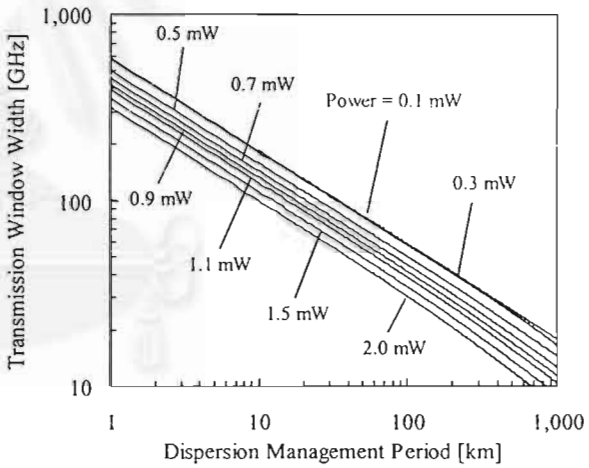

Figure 2: Dependence of the transmission window width on the DM period and the path-average signal power of the T-M system employing DM.

Also for computer simulation-based design, the bandwidth of an optical bandpass filter (OBPF) placed at the end of fiber should be tuned at optimum value. For ultra-high data rate transmission, we have to investigate the necessary of the third-order dispersion (TOD) compensation by calculating the TOD length: L_{d3} and the nonlinear length: L_{nl} [3] of the system. These characteristic lengths can be interpreted as the distance where those effects become significant. When L_{d3} is longer than system length, no TOD compensator is

needed. On the other hand, if L_{d3} is shorter than the system length, we have to install the TOD compensators distributedly at the length shorter than L_{nl} to avoid the interplay between the TOD and the SPM. To further increase the data rate, the span should be shortened in order to obtain good SNR with the use of low input signal power. Then, the SPM effect is consequently reduced.

3. COMPUTER SIMULATIONS

To demonstrate the efficiency of the DM in upgrading the T-M system, we perform some of computer simulations. In the simulations, all system parameters are the same as those used for obtaining the transfer function. The optical signal is composed of a 128-bit pseudorandom return-to-zero (RZ) Gaussian pulse train with a duty cycle of 0.5. The TOD of DSF is assumed to be 0.06 ps/km/nm^2. D is assumed to randomly fluctuate around ZDWL every 2 km with variance of 0.5 ps/km/nm. The optical amplifier produces noise in process of amplification with a noise figure of 5.3 dB. At the end of system, the bandwidth adjustable OBPF is placed. The bandwidth of the OBPF is always adjusted to obtain the minimum bit-error rate (BER). When the TOD compensation is required, the TOD compensator is an ideal device that multiplies the signal with negative amount of linearly accumulated phase shift caused by TOD. For all calculation, we consider l_d that is only equal or longer than L_a for practical.

The propagation of the optical pulse is calculated by solving the nonlinear Schrodinger equation by the split-step Fourier method [3]. The integration step size of SSFM is always chosen at the value that gives a step size error less than 0.01 %. The receiver is modeled by a sixth-order Bessel-Thompson low-pass filter, followed by a BER detector. The system performance is evaluated in terms of the numerical BER. To calculate the numerical BER of the detected signal, the simulation is repeated 32 times for the pseudo-random pulse train. The numerical Q factor of every bit is then individually calculated at the maximum eye-opening point of the bit period. Based on the assumption of the Gaussian noise distribution, the numerical BER is computed from the bit numerical Q factor and is averaged over the entire bits [4]. The system limitation is defined by BER = 10^{-9}.

First, we calculate the BER of a 40-Gbit/s signal at the end of system using D is -0.2 ps/km/nm and l_d is varied to find the optimum value. As discussed above, too short l_d will yield the result similar to the uniform D. On the other hand, too long l_d will shorten the transmission window. The minimum BER about 10^{-11} is obtained with the optimum l_d of 400 km, incorporated with the optimum input signal power of 4 mW. Excepting for l_d = 1,318 km, we also achieve the BER lower than 10^{-9}, for l_d = 100, 200, 300, and 500 km. Since D = -0.2 ps/km/nm is too small comparing to its variance (0.5 ps/km/nm), the increase in the operating SOD value should enhance the system performance. However, the transmission window becomes narrow when too large D is used. Figure 3 shows the BER of the 40-Gbit/s signal as a function of input signal power. Each BER curve is obtained at the optimum l_d for each operating D. The best BER is obtained from D = –1 ps/km/nm with the input signal power of 2 mW. On the other hand, the worst BER is resulted from D = –2 ps/km/nm, where we cannot obtain the BER lower than 10^{-9}.

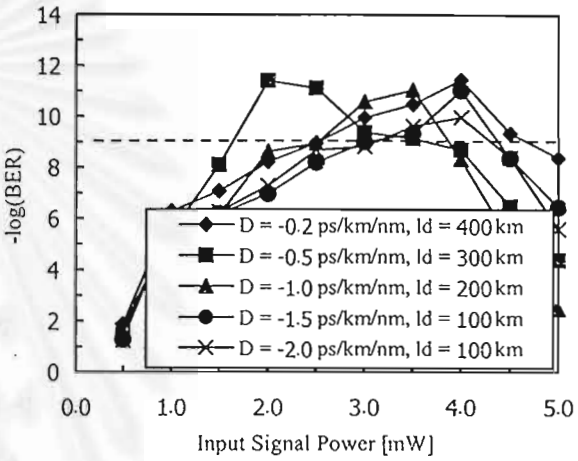

Figure 3: Numerical BER of the transmitted 40-Gbit/s signal as a function of input signal power, for several D with their corresponding optimum l_d.

Next we further explore the possibility of a 80-Gbit/s data transmission. For this data rate, the TOD also becomes a problem that causes signal waveform distortion because L_{d3} is about 560 km. In fact, the TOD compensator should be periodically placed at the distance shorter than L_{nl}. However, since the system length is not too long and L_{d3} is relatively not too short comparing with the system length, we try to use only one TOD compensator install at the end of system to reduce the system cost. Figure 4 shows the BER of the 40-Gbit/s signal as a function of input signal power for several D. Each BER curve is obtained at l_d = 100 km, which is the optimum value for this data rate. It is obvious that the higher data rate is, the shorter l_d is required for expanding the transmission window. From Fig. 4, we achieve the BER lower than 10^{-9} for the range of D from -0.5 to -1.5 ps/km/nm. The lowest BER is obtained by D = –1 ps/km/nm with the input signal power of 2 mW.

For higher data rate, we perform computer simulations based on the data rate of 100-Gbit/s. Since L_{d3} of this data rate becomes as short as 280 km. This means that the TOD now becomes the significant problems. Moreover, the TOD will cause severe signal distortion through the interaction with the Kerr effect when the signal power becomes intense. Therefore, we perform the TOD compensation periodically at every amplifier span, which is shorter than L_{nl}. However, the BER less than 10^{-9} cannot be obtained for all possible parameters. This is due to large amount of amplifier noise is added to this broadband signal during the amplification and then high signal power is required for maintaining a good SNR. The high signal power will cause the nonlinear waveform distortion, and also shortens the transmission window. In order to achieve the BER less than 10^{-9} for this data rate, the first strategy is to reduce L_a to 50 km with last span of 68 km. This is because the amount amplifier noise will reduce. Consequently, relatively low signal power is sufficient for good SNR.

Figure 5 shows the BER of the 100-Gbit/s signal as a function of input signal power for several D. Each BER curve is obtained at the optimum l_d indicated in the figure. The calculation results show that the transmission of 100-Gbit/s in T-M system becomes possible by using D = -0.5 ~ -1.5 ps/km/nm.

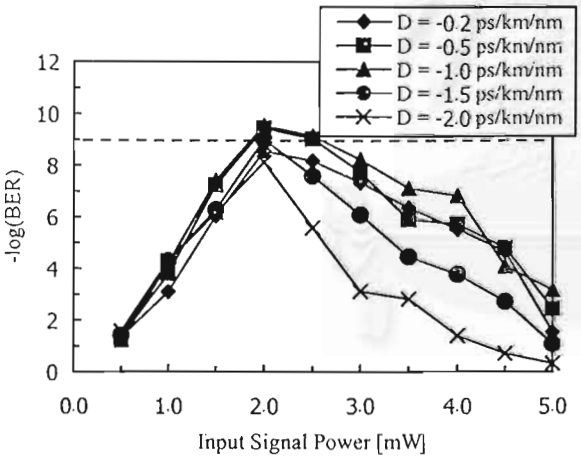

Figure 4: Numerical BER of the transmitted 80-Gbit/s signal as a function of input signal power, for several D with the optimum l_d = 100 km.

For small D, the results from Fig. 3 ~ 5 mention that, the use of large l_d results in good BER. On the other hand, for large D, we have to use small l_d. This is because the effect of random D fluctuation, which interplays with the Kerr effect, can be reduced by using large D with sufficiently short l_d or smaller D with sufficiently long l_d.

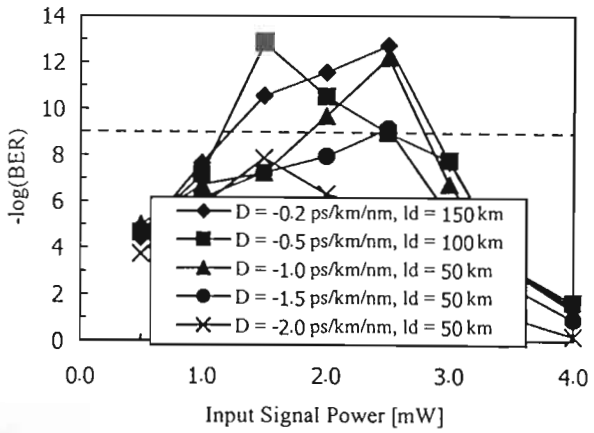

Figure 5: Numerical BER of the transmitted 100-Gbit/s signal as a function of input signal power, for several D, obtained by their optimum l_d and L_a = 50 km.

4. CONCLUSIONS

Performance improvement of single-channel electronic-repeated fiber systems by using the optimum-designed DM method was investigated by numerical simulations. We took into account the T-M submarine fiber-optic line, which has a length of 1,318 km and a 100-km repeater span, for system model. By designing the system to operate with optimum parameters, we numerically demonstrated that the transmission data rate can be increased from 560 Mbit/s to 80 Gbit/s. Moreover, with reducing the amplifier span to 50 km, we also demonstrated the possibility of the transmission at a data rate as high as 100 Gbit/s.

5. ACKNOWLEDGMENTS

This work was supported by Chulalongkorn University, Bangkok, Thailand, under the Ratchadapisek Somphot Endowment.

REFERENCES

[1] T. Naito, N, Shimojoh, T. Tanaka, H. Nakamoto, M. Doi, T. Ueki, and M. Suyama, " 1 Terabit/s WDM transmission over 10,000km, " in *Proc. European Conf. on Opt. Commun. (ECOC'99)*, Nice France, Sept. 26-30, PD2-1, pp. 24-25, 1999.

[2] D. Marcuse, " Single-channel operation in very long nonlinear fibers with optical amplifiers at zero dispersion , " *J. Lightwave Technol.*, vol. 9, pp. 356-361, 1991.

[3] G. P. Agrawal, *Nonlinear Fiber Optics* (New York, Academic Press, 3rd edition, 2001).

[4] X. Wang, K. Kikuchi and Y. Takushima, "Analysis of Dispersion-Managed Optical Fiber Transmission System Using Non-Return-to-Zero Pulse Format and Performance Restriction from Third-Order Dispersion," *IEICE Trans. Electron.* , Vol.E82-C, No.8, 1999.

Optical Soliton Transmission in Upgrading Electronic-Repeated Single-Channel Long-Haul System

Pasu Kaewplung and Thanakorn Ratanasopitkul
Department of Electrical Engineering, Faculty of Engineering, Chulalongkorn University,
Phayathai Rd., Pathumwan, Bangkok 10330, Thailand
Phone (66-2)218-6907, Fax (66-2)218-6912, E-mail : Pasu.K@Chula.ac.th

Abstract

We numerically investigate the performance improvement of electronic-repeated fiber system by using optical soliton transmission The Thailand-Malaysia submarine line is used for system model. Following our optimum soliton system design strategies, by only replacing the electronic-repeaters with the optical amplifiers, we demonstrated that the transmission bit rate can be improved from 560 Mbit/s to 10 Gbit/s. Moreover, when the amplifier span is reduced to 50 km, we succeed the transmission at a data rate as high as 20 Gbit/s.

Keywords: optical fiber transmission, fiber nonlinearity, dispersion, dispersion compensation, optical soliton, optical amplification

1. Introduction

Rapid growth on both transmission bit rate and distance in this decade is very remarkable. Transmission of data rate as high as 1 Tbit/s over 10,000 km has been demonstrated [1]. However, at presence, there exists many installed fiber systems which still operate with electronic repeaters at very low bit rate. Such systems need to be upgraded to response the demand for increasing the transmission capacity in the future.

Electronic repeaters in optical fiber transmission systems are the main bottle-neck that limits the increase of information data rate. To overcome this bottle-neck, optical signal must transmit transparently only in optical domain from a transmitter to a destination without converting to electronic signal. To realize such transparent optical transmission, firstly, the electronic repeaters must be replaced by the optical amplifiers. However, since the optical amplifier can only amplify the signal, for long-haul-high-speed systems, all-optical method for compensating the signal waveform distortion due to fiber dispersion and fiber nonlinearity, is the key technology that must be also employed.

Optical soliton [2] is a special pulse that can maintain its shape during the propagation in lossless optical fiber because of the balance between the fiber second-order dispersion (SOD) and nonlinear effect called the self-phase modulation (SPM) [2]. The soliton is very suitable for signal transmission in all-optical transmission system, as well as for all-optical signal processing [3]. However, for long-haul fiber link, the fiber loss causes the attenuation of soliton power resulting in the destruction of soliton waveform. Moreover, the collision between adjacent soliton pulse called the soliton interaction [2] also places a limit in both data rate and distance of the transmission system using soliton.

In order to transmit the soliton in long lossy fiber, the lumped optical amplifiers are necessary to be installed periodically to compensate the fiber attenuation. Then, the soliton is amplified in such a way that the average power in the amplifier span is equal to the value required for ideal soliton. This concept is well known as the guiding-centered soliton [4] or the average soliton [5]. The stability of the soliton in this scheme based on the ratio of the characteristic length called the soliton period and the amplifier span, which should be as large as possible [6], [7]. This constraint brings a type of soliton distortion due to the dispersive wave [6], [7] scattering out of soliton when we choose relatively large amplifier span. Moreover, the amplifier noise will cause the random modulation of soliton frequency, resulting in the random walk of among soliton pulses called the Gordon-Haus (GH) effect [8].

In this paper, we numerically investigate the effectiveness of the optical amplification and the soliton method in upgrading the electronic-repeated 1,318-long Thailand-Malaysia (T-M) system. By designing systems to work at optimum conditions, the possibility of increasing data rate in single-channel from 560 Mbit/s to 10 Gbit/s without reducing the amplifier span, and to 20 Gbit/s with reducing the span to be a half, are demonstrated by computer simulations. Section 2 reviews about the generation of soliton in optical fiber and then describes about the system design strategies to achieve the maximum performance in the system employing the optical amplification and the soliton technique. In section 3, we show the system modeling for single-channel T-M transmission system and the numerical simulation results, which indicates the performance upgrading. Finally, the conclusion of this paper is made at section 4.

2. Generation of Soliton Pulse in Optical Fiber

Soliton refers to special kind of waves that can propagate undistorted over long distances and remain unaffected after collision with each other. Optical soliton in optical fiber is conformed by balancing the SOD and the SPM in anomalous dispersion region [2]. Quantitatively, this can be achieved by launching optical pulses with proper width and input power, which is given by Eq. (1), into the fiber.

$$P_0 = \frac{|\beta_2|}{\gamma T_0^2}, \qquad (1)$$

CM01

where, P_0 is the input power required for forming the soliton pulse, β_2 the second-order group-velocity parameter, γ the nonlinear coefficient, and T_0 the soliton width. It should be noted that β_2 directly relates to the SOD [2]: D , which is widely used in the context of fiber transmission, by

$$D = -\frac{2\pi c}{\lambda^2}, \qquad (2)$$

where c and λ are the velocity of light and the carrier wavelength, respectively.

The most attractive characteristic of optical soliton is that they can propagate in optical fibers without distortion over a long distance if the fiber loss is negligible. There are several other reasons why soliton is attractive for optical communication systems and why they should be considered as a possible route for system upgrades. In particular, soliton is also compatible with all optical switching and routing technologies [3]. The ability to optically process signal is essential if the bottleneck problems encountered at switching nodes are to be overcome for the high data rates.

The problems in soliton transmission systems are roughly classified into the following three problems; the fiber loss, [2], [4], [5] the mutual interaction between adjacent solitons [2], [9], and the GH effect [8]. To transmit soliton pulses through actual optical fibers, especially for a long distance, it is necessary to consider the fiber loss. The fiber loss results in exponentially increase of soliton width and decrease of soliton peak. It is necessary to amplify the soliton periodically to maintain its power. With the lump optical amplifier, the soliton power is amplified to have the power larger than P_0. Quanlitatively, P_0 will be multiplied by the power factor σ to be P_{av}, which is given by

$$P_{av} = P_0\sigma = \frac{P_0\alpha L_a}{1-\exp(-\alpha L_a)}, \qquad (3)$$

where α is the loss coefficient of fiber and L_a is the amplfier span. Such a soliton called the guiding-center soliton [4] or average soliton [5] because, by incresing P_0 by the factor of σ, the average soliton power over L_a becomes equal to the soliton power in lossless fiber.

One of the important quantity in soliton system design is the ratio between the soliton period Z_0 [2] and L_a, where Z_0 can be obtained as

$$Z_0 = \frac{\pi T_0^2}{2|\beta_2|}. \qquad (4)$$

It has been proved that the average soliton is stable during propagation when the ratio of Z_0 and L_a is much larger than unity [6], [7]. Otherwise, serious soliton distortion is induced because large amount of the dispersive wave is generated and is emitted out of the soliton signal.

In addition to the stability requirement, there are two other effects limiting the capacity of soliton transmission. When the solitons are closely spaced, the mutual interaction changes the velocity of the solitons and causes the soliton to move out of the detection window. This effect is known as the soliton interaction [2], [9]. The collision between adjacent solitons is also induced from this effect. We can extend the distance where the collision occurs by increasing the time interval between adjacent solitons, i.e., by reducing the duty cycle of soliton pulse.

On the other hand, the GH effect is originated by the noise generated by the optical amplifiers. The amplifier noise randomly modulates the carrier frequency of the soliton, and then the group velocity varies. This effect leads to the timing jitter among soliton pulses [8]. It should be noted that the soliton interaction and the GH effect can be reduced by using relatively low D. However, using too small D, the soliton will suffer from low optical-signal-to-noise ratio (OSNR) at receiver because P_{av} will be at very low value according to Eq. (3).

In real system, D randomly changes along the transmission because of the temperature and the installed circumstance. The random variation of D also gives rise to the perturbation of soliton pulses resulting in large amount of dispersive wave that will disperse from the soliton pulse. The use of relatively large D can help reducing this signal distortion because the effect of D variation can then be treated as only small perturbation.

Taking into account all described problems, to design the soliton transmission system to achieve the maximum performance for a given fixed amplifier span, the following points should be concerned.

1. There should exist the optimum value of D that yields the trade off between the improvement of OSNR and the signal distortions.
2. The decrease in the duty cycle of the soliton pulse will increase all the nonlinear waveform distortion because relatively high P_{av} is required to form the soliton. On the other hand, the use of small duty cycle reduces the effect of soliton interaction. Therefore, the duty cycle should be set at the optimum value.
3. The bandwidth of the optical band-pass filter (OBPF) installed at the end of fiber should be adjusted to the optimum value, which selects only soliton spectrum and reject the accumulated noise.

3. Computer Simulations

To demonstrate the efficiency of the soliton in upgrading the electronic-repeated system, we perform some of computer simulations by taking the T-M system

as the model. The T-M system starts from Petchburi, Thailand, ends at Chugai, Malaysia, with total length of 1,318 km. The transmission fiber is the dispersion-shifted fiber (DSF). The electronic repeaters are periodically placed at span (L_a) of 100 km with the last span of 118 km. The system operates in single channel with the data rate of only 560 Mbit/s.

In the calculation, we assume the typical parameter of DSF. The fiber loss coefficient and the nonlinear coefficient of DSF are 0.2 dB/km and 2.6 $W^{-1}km^{-1}$, respectively. The optical soliton signal is composed of a 128-bit pseudorandom return-to-zero pulse train with secant-hyperbolic shape. The SOD is assumed to randomly fluctuate around the operating D every 2 km with a variance of 0.5 ps/km/nm. The optical amplifier produces noise in process of amplification with a noise figure of 5.3 dB. At the end of system, the bandwidth adjustable OBPF is placed. The bandwidth of the OBPF is always adjusted to obtain the minimum bit-error rate (BER). The propagation of the soliton signal is calculated by solving the nonlinear Schrodinger equation by the split-step Fourier method (SSFM) [2]. The integration step size of the SSFM is always chosen at the value that gives a step size error less than 0.01 %. The receiver is modeled by a sixth-order Bessel-Thompson low-pass filter, followed by a BER detector. To calculate the numerical BER of the detected signal, the simulation is repeated 32 times for the pseudo-random pulse train. The numerical Q factor of every bit is then individually calculated at the maximum eye-opening point of the bit period. Based on the assumption of the Gaussian noise distribution, the numerical BER is computed from the bit numerical Q factor and is averaged over the entire bits [10]. The system limitation is defined by BER = 10^{-9}.

Figure 1 shows the numerical BER, in logarithmic scale, of the soliton signal with data rate of 10 Gbit/s as a function of duty cycle for several D. We achieve BER < 10^{-9} by using D = 1.0 ps/km/nm with duty cycle of 0.2 and 0.5. For all D used in Fig. 1, the duty cycle of 0.2 and 0.5 yield better BER than other duty cycles. This can be interpreted that, by using the duty cycle of 0.5, although the soliton interaction becomes a serious problem, we can sufficiently reduce P_{av}. Therefore, the BER becomes relatively small because the signal distortion due to the GH effect and the emission of dispersive wave are simultaneously reduced. When we decrease the soliton duty cycle to 0.4 and 0.3, to reduce the effect of the soliton interaction, we have also unavoidably to increase P_{av}. Since the soliton interaction cannot be completely eliminated, at the same time, the GH effect and the emission of dispersive wave become more serious, the BER then slightly increases as appeared in Fig. 1. However, when we further reduce the duty cycle to 0.2, the soliton interaction may be almost completely suppressed, and according to the fact that the GH effect and the emission of dispersive wave may be still not too strong, we can achieve the smallest BER at this duty cycle.

As described above, the use of low operating D causes the signal distortion from the random fluctuation of SOD. However, the use of large D results in the enhancement of the GH effect and the emission of dispersive wave because very high P_{av} is required to be launched into the fiber to create optical soliton. As a result, in Fig. 1, D = 1.0 ps/km/nm is the optimum value that gives the balance among these problems. Figure 2 show the output eye pattern of the 32-bit soliton, obtained by using D = 1.0 ps/km/nm and duty cycle of 0.2. The soliton signal is in a very good shape, therefore, we can clearly distinguish the bit "1" and "0".

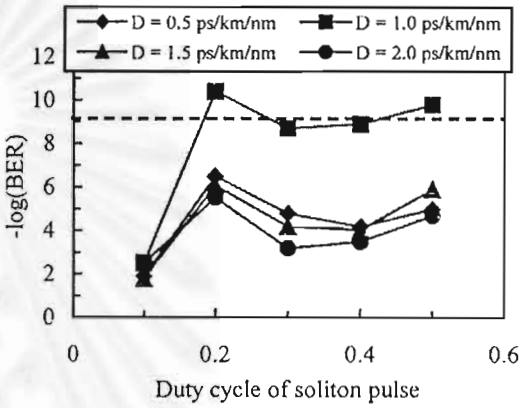

Fig. 1: Numerical BER of the 10-Gbit/s soliton signal as a function of duty cycle for several D. L_a is 100 km. BER < 10^{-9} is obtained by using D = 1.0 ps/km/nm with duty cycle of 0.2 and 0.5.

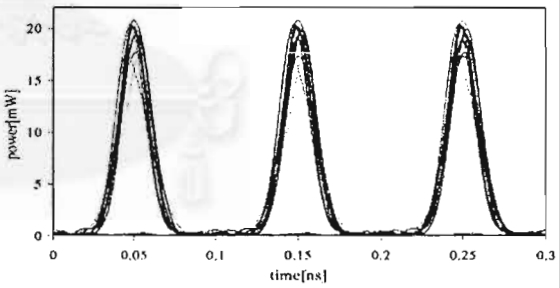

Fig. 2: Eye pattern of the output 32-bit soliton waveform obtained by using D = 1.0 ps/km/nm and duty cycle of 0.2.

The easiest way to further increase the performance of this 10-Gbit/s soliton system is to reduce L_a. The GH effect and the amount of dispersion wave scattering from soliton will then be reduced because the ratio between Z_0 and L_a becomes large and also P_{av} is reduced. Figure 3 shows the numerical BER, in logarithmic scale, of the 10-Gbit/s soliton signal as a function of duty cycle for several D. L_a, in this case, is set at 50 km with the last span of 68 km. According to the numerical results, we can achieve BER < 10^{-9} for a wide

CM01

range of duty cycle (> 0.1) by using D = 1.0 ps/km/nm, and for only a duty cycle of 0.2 with D = 1.5 ps/km/nm.

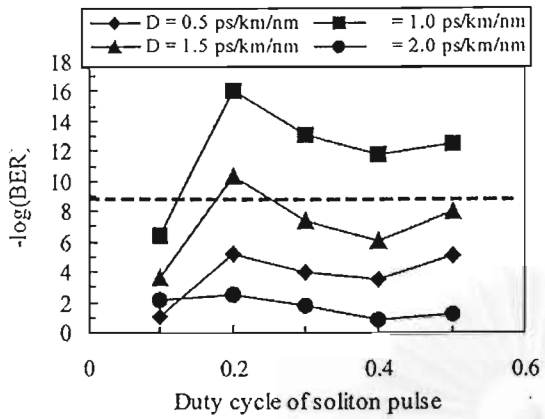

Fig. 3: Numerical BER of the 10-Gbit/s soliton signal as a function of duty cycle for several D. L_a is 50 km. BER < 10^{-9} is achieved for a wide range of duty cycle by using D = 1.0 ps/km/nm, and for only a duty cycle of 0.2 with D = 1.5 ps/km/nm.

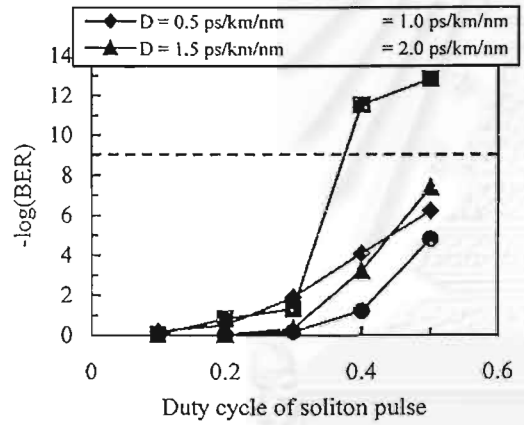

Fig. 4: Numerical BER of the 20-Gbit/s soliton signal as a function of duty cycle for several D. L_a is 50 km. BER < 10^{-9} is obtained by using D = 1.0 ps/km/nm with duty cycle of 0.4 and 0.5.

Next we explore the possibility of higher data rate transmission using L_a = 50 km. Figure 4 shows the numerical BER for the case of a soliton signal with data rate of 20 Gbit/s, as a function of duty cycle for several D. Similar to the results from Fig. 1 and Fig. 3, the best BER is obtained by using D = 1.0 ps/km/nm. However, the transmitted soliton gives the BER less than 10^{-9} only for the duty cycle of 0.4 and 0.5. We can no longer achieve BER < 10^{-9} by using smaller duty cycle. This is because, in such high data rate, to generate the soliton with small duty cycle, P_{av} will be in an extremely high level. Therefore, the GH effect as well as the dispersive wave will play a dominant role in limiting the performance of this system. To improve the achievable BER in such system, L_a should be further reduced.

4. Conclusion

In this paper, we have studied the performance improvement of the electronic-repeated fiber system by using the optical amplification and the soliton transmission is investigated by computer numerical simulations. We took into account the Thai-Malaysia submarine fiber-optic line, which has a length of 1,318 km and a 100-km repeater span, for system model. With our optimum soliton system design strategies, by only replacing the electronic-repeaters with the optical amplifiers, we demonstrated that the transmission bit rate can be increased from 560 Mbit/s to 10 Gbit/s. Moreover, with reducing the amplifier span to be 50 km, we also demonstrated the possibility of the optical data transmission at a data rate as high as 20 Gbit/s. Further improvement of the system may be based on the reduction of amplifier span.

5. Acknowledgement

This work was supported by Chulalongkorn University, under the Ratchadapisek Somphot Endowment.

References

[1] T. Naito, N, Shimojoh, T. Tanaka, H. Nakamoto, M. Doi, T. Ueki, and M. Suyama, " 1 Terabit/s WDM transmission over 10,000km, " in Proc. European Conf. on Opt. Commun. (ECOC'99), Nice France, Sept. 26-30, PD2-1, pp. 24-25, 1999.

[2] G. P. Agrawal, *Nonlinear fiber optics*, New york: Academic Press, 3rd edition, 2001.

[3] S. Bigo, O. Leclerc, E. Desurvire, " All-optical fiber signal processing and regeneration for soliton communications, " *IEEE J. on Selected Topics in Quantum Electron.*, vol. 3, no. 5 , pp. 1208-1223, 1997.

[4] A. Hasegawa and Y. Kodama, " Guiding-center soliton in optical fibers, " *Opt. Lett.*, vol. 15, pp. 1443-1445, 1990.

[5] K. J. Blow and N. J. Doran, " Average soliton dynamics and the operation of soliton systems with lumped amplifiers, " *IEEE Photon. Technol. Lett.*, vol. 3, pp. 369-371, 1991.

[6] L. F. Mollenauer, J. P. Gordon, and M. N. Islam, " Soliton propagation in long fibers with periodically compensated loss, " *IEEE J. Quantum Electron.*, vol. QE-22, no. 1, pp. 157-173, 1986.

[7] L. F. Mollenauer, S. G. Evangelides Jr., and H. A. Haus, " Long-distance soliton propagation using lumped amplifiers and dispersion shifted fiber, " *J. Lightwave Technol.*, vol. 9, no. 2, pp. 194-196, 1991.

[8] J. P. Gordon and H. A. Haus, " Random walk of coherently amplified solitons in optical fiber transmission, " *Opt. Lett.*, vol. 11, pp. 665-667, 1986.

[9] Y. Kodama and K. Nozaki, " Soliton interaction in optical fibers, " *Opt. Lett.*, vol. 12, pp. 1038-1040, 1987.

[10] X. Wang, K. Kikuchi, and Y. Takushima, " Analysis of dispersion-managed optical fiber transmission system using non-return-to-zero pulse format and performance restriction from third-order dispersion, " *IEICE Trans. Electron.*, vol. E82-C, no. 8, pp. 1407-1413, 1999.